INTERNATIONAL COMMITTEE FOR COAL AND ORGANIC PETROLOGY • ICCP

U.PORTO

FACULDADE DE CIÊNCIAS
UNIVERSIDADE DO PORTO

ICT
Instituto de Ciências da Terra
Institute of Earth Sciences

77th ANNUAL ICCP MEETING

BOOK OF ABSTRACTS

Organic Petrology for a Changing World

13–18 SEPTEMBER 2026 | PORTO & LISBOA, PORTUGAL

77th Annual ICCP Meeting

Book of Abstracts

Organic Petrology for a Changing World

Title: Book of Abstracts - Organic Petrology for a Changing World – 77th Annual ICCP Meeting
Editor: Universidade do Porto. Faculdade de Ciências
Typesetting and Layout: Paula Alexandra Gonçalves
Authors: Several
Format: Electronic
Document type: PDF
Publication Year: 2026
ISBN: 978-989-36122-8-6

Organizing Committee

Chair: Dr. Carolina Fonseca - University of Minho, Portugal

Dr. Paula Alexandra Gonçalves - University of Porto, Portugal

Dr. Cristina Freire - University of Porto, Portugal

Dr. João Graciano Mendonça Filho - Federal University of Rio de Janeiro, Brazil

Dr. Luís Vítor Duarte - University of Coimbra, Portugal

Dr. Bruno Valentim - University of Porto, Portugal

Dr. Joana Ribeiro - University of Coimbra, Portugal

Mariana Costa - University of Porto, Portugal

Scientific Committee

Dr. Angeles Borrego - INCAR-CSIC, Spain

Dr. Ashok Kumar Singh - CSIR-CIMFR, India

Dr. Bruno Valentim - University of Porto, Portugal

Dr. Carolina Fonseca - University of Minho, Portugal

Dr. Henrik Petersen - GEUS, Denmark

Dr. Joana Ribeiro - University of Coimbra, Portugal

Dr. João Graciano Mendonça Filho - Federal University of Rio de Janeiro, Brazil

Dr. Magdalena Misz-Kennan - University of Silesia, Poland

Dr. Nicola J. Wagner - University of Johannesburg, South Africa

Dr. Paul Hackley - USGS, USA

Dr. Paula Alexandra Gonçalves - University of Porto, Portugal

Dr. Polla Khanaqa - Center for Future Studies, Sulaimaniyya, Kurdistan Region-Iraq

Dr. Sandra Rodrigues - The University of Queensland, Australia

Dr. Shifeng Dai - China University of Mining & Technology, China

Dr. Stavros Kalaitzidis - University of Patras, Greece

Contents

Preface viii

Symposium on Organic Petrology for a Changing World
Oral Presentations

Rare earth and critical element enrichment in South African discard coal: Advancing sustainable waste valorisation
Sanki Biswas, Nicola J. Wagner 2

Viability of Mpumalanga discard coal as a source of critical elements
Mpeoana Lydia Majake, Nicola Wagner, Sanki Biswas 4

Integrated geological and geochemical assessment of critical and toxic element resources deposited in coal waste impoundments
Dmytro Khomenko, Zbigniew Jelonek, Iwona Jelonek 6

An initial assessment of low-rank coals for advanced industrial applications: case studies from Greece
Maria Georgaki, Malgorzata Wojtaszek-Kalaitzidi, Adam Cygan, Stavros Kalaitzidis 7

Effects of self-heating on the petrographic and Rock-Eval 7S parameters of coals from the Na Duong mine, Vietnam
Weronika Cyran, Dariusz Więcław, Marta Waliczek, Khuong The Hung, Pham Nhu Sang 9

Evolution in physicochemical properties and carbon permanence of biochar with increasing carbonization temperature
Henrik I. Petersen, Rasmus Jakobsen, Priyanka Kaushal, Abhijeet Anand, Arka Rudra, Kasper H. Blinkenberg, Hamed Sanei 11

Petrography of black mass - identification of carbon forms
Małgorzata Wojtaszek-Kalaitzidi, Bruno Valentim, Alexandra Guedes, Sónia Pereira 12

Microscopically distinguishable components of naturally graphitized coals
Li Kuo, Lu Hao, Duan Xiaoyu 14

On the origin of micrinite, the red herring of organic petrology
Paul C. Hackley, Brett J. Valentine, Ryan J. McAleer, Aaron M. Jubb, Javin J. Hatcherian, Jing Qu, Yuying Zhang 16

Experimental comparison of the maturity of organic matter based on vitrinite reflectance and autofluorescence measurements
Anna Maciejewska, Marcin Barski, Marta Waliczek 18

Digitalization and computer vision applied to palynofacies and thermal maturity studies
Gil Machado, Diogo Machado, André Sanches 20

Thermal conditions of the coal-bearing series in the Upper Silesian Coal Basin (Poland) in the light of research findings on rock temperature and vitrinite reflectance
Sławomir Kędzior, Arkadiusz Drozd, Tomasz Słoczyński 22

Structural parameter evolution characteristics of coals in different rank under various metamorphic pathways
Chao Liu, Beilei Sun..... 24

Synthesis of organic petrography, core and logs to identify depositional facies and source rocks using several case studies
Greg Smith, Muhammad Firdaus, India Sadd..... *25*

The occurrence, distribution and origin of Bolsovian age splint coal in the Central Appalachian Basin, USA
Cortland F. Eble..... 27

Peat swamps in the interior of Tropical Pangea: an example from the Lower Lubná Coal (Middle Pennsylvanian), Kladno-Rakovník Basin, Czech Republic
Otto Salva, Stanislav Opluštil, Ralf Littke, Thorsten Bauersachs, Cortland Eble, Ivana Sýkorová 28

Petrographic and geochemical analysis of burned organic matter from forest material
Magdalena Misz-Kennan, Monika Kościelny, Monika Fabiańska..... 30

Poster Presentations

Nanoscale chemo-mechanical heterogeneity of graptolites and its reservoir implications
Ke Wang, Qian Sun 32

Maceral-specific molecular structural evolution during the huminite-to-vitrinite transition
Yu Liu, Tengwei Gao, Jiayue Feng 33

A Silurian Oceanic Anoxic Event documented by hexavalent uranium isotopes
Zhengfu Zhao..... 34

Aridity and polymetallic stress suppressed the terrestrial carbon sink during the T-OAE
Kai Zhou..... 35

Revisiting Marlies Teichmüller's bituminite concept in coals: a CLSM-based re-evaluation
Jolanta Kus, Martin Blumenberg, Georg Scheeder 37

Semantic segmentation for identification of coal macerals and mineral matter
Na Xu..... 39

Assessment of fossil fuels-derived contaminants in soils from a protected area in the Portuguese coast (Cabo Mondego)
Fernando Michels, Maria Helena Henriques, Joana Ribeiro..... 40

Optical microscopy for biochar characterization: insights into reflectance, composition and methodological considerations
Konrad Ziemianin 42

Decoding primary and recycled organic-matter signals in Middle Jurassic fine-grained deposits of the Pieniny Klippen Belt, Western Carpathians
Magdalena Zielińska, Jolanta Kus, João Graciano Mendonça Filho, Ewa A. Szram, Martin Blumenberg, Monika Fabiańska..... 44

Organic petrology and biomarker constraints on peat formation in the Upper Eocene Nikolaevo deposit (Central Bulgaria)
Alexander Zdravkov, Reinhard F. Sachsenhofer, Johannes Weitz, David Misch, Dimitar Dimitrov, Valentin Kabadiyski, Stoyan Stoyanov, Bogomil Zlatkov 45

Climatically driven change of the peat-forming environments during the Eocene to Pliocene on the territory of Bulgaria: insights from organic petrology and biomarker analysis46
Alexander Zdravkov 46

Bioindicative and phytoremediation potential of *Spirodela polyrhiza* (L.) Schleid. in the presence of coal mine slurry
Zbigniew Jelonek, Zdzisława Romanowska-Duda, Iwona Jelonek, Casey Woźniak..... 47

Petrographic evidence of lipid impregnation in vitrinites as the control on the ultra-high fluidity of the Barro Branco coal seam (Paraná Basin, Brazil)
Bruno Deves Flores, Angeles Gomez Borrego, Anderson Azevedo Agra, Guilherme Liziero Ruggio da Silva, Antônio Cezar Faria Vilela, Eduardo Osório 48

Petrography of the ferrospheres from Talcher coal ash (Angul district, Odisha, India)
Bruno Valentim, Bibhuranjan Nayak, Sónia Pereira, Nilima Dash, Alexandra Guedes, Sasmita Prusty 50

Preliminary data on the anisotropy of reflectance of vitrinite in oriented samples from the Douro Carboniferous Basin (NW of Portugal)
Mariana Costa, Eduardo Ferreira da Silva, Ary Pinto de Jesus, Deolinda Flores 52

Insights into organic matter and depositional conditions in lacustrine carbonates of the Barra Velha Formation
Jaqueline Torres de Souza, Antonio Donizeti de Oliveira, Joalice de Oliveira Mendonça, Leonardo Borghi, João Graciano Mendonça Filho 54

Petrographic variability of biochar produced in a bench-scale Mass Loss Calorimeter to explore differences in combustibility
Angeles G. Borrego, M. Carmen Niembro, Cristina Carrillo García, Mercedes Guijarro Guzman, Javier Madrigal Olmo..... *55*

Decoding Late Oligocene fern life: assessing plant communities, depositional environments, and maceral genesis in the Petroșani Basin (Romania)
Roxana Pirnea, Izabela Mariș, Mihai Emilian Popa, Georgeta Predeanu, Doina Maria Ghiran 57

Evolution of effective CO_2 flow during successive adsorption steps in coal
Y. Bueno-Yamamoto, C.A. Rodrigues, J.J. Enciso-Cárdenas, I.D. García-Calvillo, P.F. Moreira, D.M. Garza-Cavazos, A. Bueno-Tokunaga, L.F. Camacho-Ortegón, G. De La Rosa-Rodríguez, M.J. Lemos de Sousa..... 58

Upgrading carbon residues from coking processes: A microscopic characterization study
Patricia Álvarez,Uriel Sierra, Marcos Granda, A. Concheso, A. Vigil 60

Vitrinite reflectance: A link between thermal history, kerogen evolution and basin modelling
D.M. Garza-Cavazos, C.A. Rodrigues, J.J. Enciso-Cárdenas, Y. Bueno-Yamamoto, F. Núñez-Useche, G. De La Rosa-Rodríguez, E. González-Partida, M.J. Lemos de Sousa..... 62

Characterization of biochar as reducing material for phosphorus recovery from anthropogenic waste ashes by petrographic, SEM/EDS and Raman spectroscopical methods
Ozben Kutlu, Georgeta Predeanu, Bruno Valentim, Alexandra Guedes, Mihaela Bălănescu, Bogdan Stefan Vasile, Valerica Slăvescu, Pinar Boluk, Mehmet Ihsan Kulas, Nezaket Duran, Marius Florin Drăgoescu 64

Design and efficiency assessment of a passive treatment system for acid mine drainage
Ruiwen Yan..... 66

Dispersed organic matter composition and thermal maturity of Upper Ordovician Boas River Formation from Hudson Platform in Northern Ontario, Canada
Julito Reyes, Denis Lavoie, Derek Armstrong..... 67

Occurrence and thermal transformation of lithium in Late Permian coal-bearing strata from the Xian'an Coalfield, Guangxi Province, South China
Xiaoyun Yan, Zhipeng Wang, Jie Sun, Yurong Zhu 69

Tracing coal-derived organic matter in Appalachian watersheds using organic petrography
Jennifer Nedzweckas, Matthew Varonka, Javin Hatcherian, Rebecca Smith, Paul Hackley..... 70

Advances on the impact of broad ion beam milling techniques on organic-rich samples
Brett J. Valentine, Paul C. Hackley, Jennifer Nedzweckas, Javin J. Hatcherian , Margaret M. Sanders 71

How feedstock and pyrolysis conditions influence biochar soil phytotoxicity
J.N.G.V. Canedo, C. Garcia Neto, L. Coelho, P. Souza Alonso, P. Mourão, R. Castillo Corrêa, A. Silva Trindade, D. Flores, F. Silva, L. Tarelho, S. Prats 72

Oil-source rock correlation in the Ediacaran of Pakistan tested through hydrous pyrolysis
Paul C. Hackley, Michael Lewan..... 76

Catalytic graphitisation of wood-derived biochar using manganese ore
Malgorzata Wojtaszek-Kalaitzidi, Aneta Michałek, Anna Rodź, Bartosz Mertas, Rui Rocha 77

Study on the coupling mechanism of sulfur migration and carbon structure evolution during coal heating
Tang Yuegang, Xue Liping, Bai Xiangfei, Gao Shuo..... 79

Organic petrographical and geochemical reappraisal of the Mesozoic sedimentary formations in Kurdistan Region, Northern Iraq
Maria Elli Damoulianou, Polla Khanaqa, Ibrahim M.J. Mohialdeen, Kamal Y. Kolo, Stavros Kalaitzidis 80

Organic matter characterization across the Upper Triassic–Lower Jurassic succession of the Lusitanian Basin (Portugal)
Paula Alexandra Gonçalves, Augusto Silva, Dariusz Więcław, João Graciano Mendonça Filho, Deolinda Flores..... 82

Petrographic and mineralogical study of the Pliocene Ptolemais Lignite sequence of the Southern Field, Ptolemais Basin, NW Greece
Y. Dimitriou, K. Christanis, G. Iliopoulos, A. Patra, S. Kalaitzidis..... 83

Organic record of the Coimbra Formation: from restricted to open-marine conditions during the Sinemurian of the Lusitanian Basin (Portugal)
C. Fonseca, D. Marques-Lima, S. Gomes, N. Franco, J.G. Mendonça Filho, L.V. Duarte, D. Flores 84

A library of North American metallurgical coal samples
Paul Hackley, Jennifer Nedzweckas, Joe Marquez 86

Organic petrography of lithium deposits in Thacker Pass, NV, USA
Javin J. Hatcherian, Randal Burns, Christopher D. Henry, Paul C. Hackley 87

Pilot study on the feasibility of geopolymers development using mining wastes from São Pedro da Cova Coal Mine (Northern Portugal) - Preliminary results
J. Paranhos, J. Espinha Marques, P. Santos, D. Arduin, A. Santos, S. Andrejkovičová, H. Sant'Ovaia, F. Rocha 88

Author Index 90

Preface

On behalf of the Organizing Committee, it is our great pleasure to welcome you to Porto and Lisboa and to the **77th Annual Meeting of the International Committee for Coal and Organic Petrology (ICCP)**. For the fourth time, Portugal has the honor of hosting the Annual ICCP Meeting. The Meeting will be held in Porto, at the Faculty of Sciences of the University of Porto, while the Symposium "Organic Petrology for a Changing World", as part of the meeting, will take place in Lisbon at the historic Lisbon Academy of Sciences.

The Symposium brings together a broad spectrum of scientific topics, highlighting recent advances in organic petrology and geochemistry and their integration with geology. The contributions address the formation, transformation, preservation, and reactivity of organic matter across diverse geological and environmental settings. Emphasis is placed on emerging challenges, including critical and rare-earth element recovery, carbon permanence and biochar, CO_2 storage, environmental remediation, and the valorization of carbon-rich wastes. Together, these contributions illustrate how **Organic Petrology** continues to expand beyond its traditional applications, connecting geological archives and processes with emerging questions in energy, resources, climate, and environmental science. The selected papers from this Symposium will be published in a special issue of the International Journal of Coal Geology.

We warmly welcome all contributing authors and co-authors who have submitted abstracts and take this opportunity to thank the Scientific Committee for their valuable support in reviewing the submissions.

We hope that the contributions presented at the Symposium will provide a stimulating overview of current research in organic petrology and reflect the breadth and vitality of the international community. We trust that they will encourage further scientific discussion and contribute to new ideas and perspectives.

We wish you a productive and enjoyable 77th Annual ICCP Meeting in Porto and a stimulating Symposium in Lisbon. We hope that, alongside the scientific program, you will have the opportunity to discover and appreciate the distinctive character, rich cultural heritage, and welcoming spirit of both cities, making your stay in Portugal a memorable experience of scientific exchange, collaboration, and shared discovery.

The Organizing Committee

77th Annual ICCP Meeting

Symposium on

Organic Petrology for a Changing World

Oral Presentations

Rare earth and critical element enrichment in South African discard coal: Advancing sustainable waste valorisation

Sanki Biswas[1*], Nicola J. Wagner[1]

[1] Carbon Ore Research Group, Department of Geology, University of Johannesburg, Johannesburg, South Africa

** Corresponding Author: sankib@uj.ac.za*

Discard coal and coal-ash are increasingly being recognized as potential secondary resources for critical elements as well as rare earth elements (REY) owing to the growing global demand, supply-chain uncertainties, and strategic importance of these critical raw materials. In this study, the discard coal collected from two processing plants (P-1 and P-2) in South Africa were investigated to evaluate the occurrence, distribution, mineralogical associations, and potential of REY and associated critical elements. A comprehensive analytical approach combining organic petrology, X-ray diffraction (XRD), inductively coupled plasma–mass spectrometry (ICP-MS), and mineral liberation analysis (MLA) was applied to characterize the samples. The discard coal samples are characterized as high-ash coal (66.6 wt.%), with inertinite dominated organic matter (avg. 21.0 vol.%), low vitrinite (3.4 vol.%) and liptinite (2.0 vol.%) (Fig. 1). The volatile matter content ranging from 12.8 to 18.6 wt.%, indicates that these discard coals contain some organic fraction, which makes discard coal valuable for further utilization. Mineralogically, the samples are dominated by kaolinite (46.6 wt.%), and quartz (avg. 21.3 wt.%), along with varying amounts of muscovite, pyrite, calcite, dolomite, microcline and gypsum. Total REY concentration ranges from 41.5 to 231.6 ppm (avg. 184.7 ppm; coal basis), exceeding global averages for both world hard coals (79.1 ppm) and Chinese coals (136 ppm) (Taylor and McLennan, 1985; Dai et al., 2025). Plant P-1 samples show enrichment in L-M-REY, whereas P-2 samples are characterized by M-H-REY enrichment (Fig. 2). Mineralogical hosts identified through MLA-BSE imaging include monazite, xenotime, Ce-REE phases, and REE-bearing silicates. The percentage of critical-REY (Nd, Eu, Tb, Dy, Y, and Er) account for 27.9% to 32.7% of the total REY and the outlook coefficients (Coutl) ranging from 0.66 to 0.86, indicating some are promising to recovery REY from these discard coal, although further technological optimization is required.

In addition to REY, the discard coal is enriched in several critical elements with concentration coefficients (CC) of 3.4-8.6, including Li (79.8), Ga (20.5) Nb (21.0), Zr (308.0), Hf (8.0), and Ta (1.9). Lithium is mainly associated with clay and carbonate, Ga-Nb-Ta with kaolinite, and Zr-Hf with zircon, consistent with Dai et al. (2021) and Li et al. (2020). The enrichment of Li-Nb(Ta)-Zr(Hf)-Ga-REY-Th-U highlights the strong multielement resource potential of these South African discard coal. Overall, integrating organic petrology with mineralogical and geochemical studies provides essential insights into organic and inorganic matter distribution, supporting the potential of coal waste as a sustainable secondary resource for REY and critical elements and its further utilization.

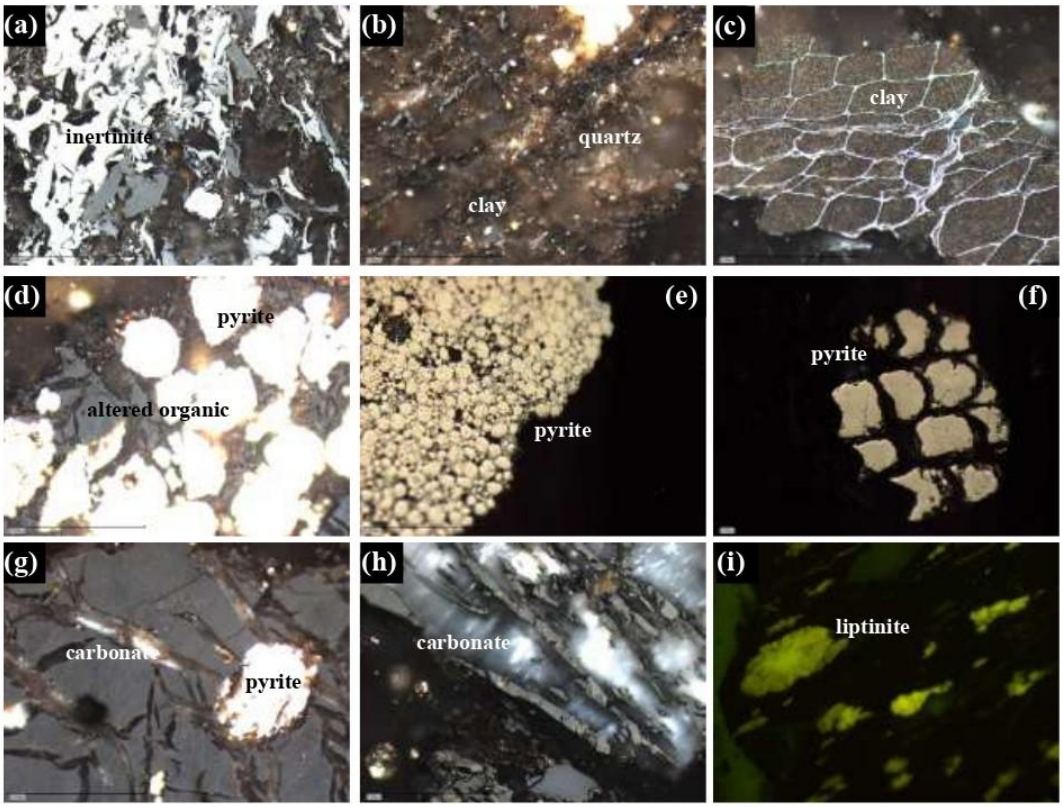

Figure 1. Photomicrographs of macerals and minerals observed in the discard coal samples under white light (a-h) and fluorescence light (i)

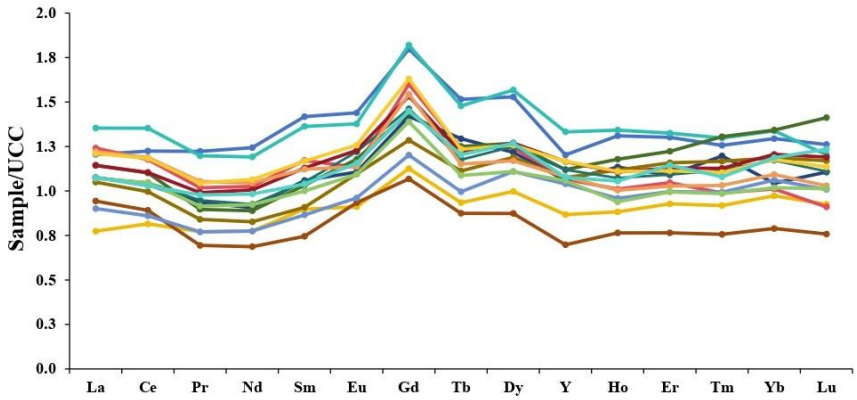

Figure 2. Upper Continental Crust (UCC) normalized rare earth elements (REY) distribution patterns of the discard coals, South Africa (following Taylor and McLennan, 1985).

References

Dai, S., Finkelman, R.B., French, D., Hower, J.C., Graham, I.T., Zhao, F., 2021. Modes of occurrence of elements in coal: A critical evaluation. Earth Sci. Rev. 222, 103815.

Dai, S., Hower, J.C., Finkelman, R.B., Ketris, M.P., Yudovich, Y.E., Zhang, Y., Liu, J., Zhao, C., Xu, N., Graham, I.T., French, D., 2025. Abundances of elements in global coals. Int. J. Coal Geol. 311, 104899.

Li, B., Zhuang, X., Querol, X., Moreno, N., Córdoba, P., Shangguan, Y., Yang, L., Li, J., Zhang, F., 2020. Geological controls on the distribution of REY-Zr (Hf)-Nb (Ta) enrichment horizons in late Permian coals from the Qiandongbei Coalfield, Guizhou Province, SW China. Int. J. Coal Geol. 231, 103604.

Taylor, S.R., McLennan, S.M., 1985. The continental crust: Its Composition and Evolution. Blackwell, Oxford, 312p.

Viability of Mpumalanga discard coal as a source of critical elements

Mpeoana Lydia Majake[1*], Nicola Wagner[1], Sanki Biswas[1]

[1]University of Johannesburg, Johannesburg, South Africa

** Corresponding Author: lydiamajake06@gmail.com*

The global shift towards low-carbon industrialization and advanced digital technologies has increased the demand for critical elements, including rare earth elements (REEs), germanium, gallium, vanadium, and uranium. This study investigates the mode of occurrence, mineral hosts, and distribution of these critical elements potentially occurring in discard coal from the Witbank Coalfield, South Africa (Fig. 1), using organic petrology, mineralogical [scanning electron microscopy with energy dispersive spectroscopy (SEM-EDS) and X-ray diffraction (XRD)], and geochemical [inductively coupled plasma-mass spectrometry (ICP-MS)] techniques. The discard coal has ash yields of 45-65 wt.%. Inertinite is the dominant maceral (16-54 vol.%), followed by vitrinite (≤15 vol.%) and minor liptinite (≤1 vol.%). Mineral matter (37-74 vol.%) exceeds the total maceral content.

Mineralogical analysis shows quartz and kaolinite are the dominant minerals, with lesser quantities of carbonates, pyrite, and minor microcline, muscovite, and gypsum. Total REE concentrations vary from 113.2 to 248.3 ppm, with an average of 175.9 ppm, exceeding the REE concentration (~168.4 ppm) of the upper continental crust (UCC) reported by Taylor and McLennan (1985). Germanium, gallium, and uranium reported high values of 1.5, 22.5, and 5.0 ppm, respectively, relative to the reported global coal median values (Dai et al., 2025). The REY def, rel% vs Coutl plot (Seredin, 2010), classified nine samples as 'promising' for REY recovery, while others fell into the 'unpromising' category. The backscattered electron (BSE) imaging in SEM-EDS identified monazite-hosted REEs with particle sizes around 6-12 μm, indicating the presence of REY-bearing mineral phases in discard coal. However, this technique was unable to identify host minerals for germanium, gallium, and uranium; therefore, further investigations are required.

Heavy-liquid density separation pre-concentration technique using a centrifuge was applied to evaluate the distribution of critical elements across various density fractions (i.e., RD 2.0, 2.5, and 3.0). Sodium polytungstate (SPT) separated minerals by density, producing fractions: float-1 (organic-rich), float-2 (clay-dominated), float-3 (quartz and carbonates), and sink (RD > 3.0; pyrite-rich). Proximate analysis showed increasing ash content with density, from ~28-37 wt.% in float-1 to 85.91 wt.% in float-3 and 73.54 wt.% in sink. Fixed carbon decreased with ash yield, confirming effective separation of organic and inorganic matter. The XRD and ICP-MS results will be presented to evaluate the distribution of critical elements in the density-separated products. The findings intend to demonstrate the suitability of density-based pre-concentration via centrifugation as a technique for increasing the concentration of critical elements in discard coal floats and sinks.

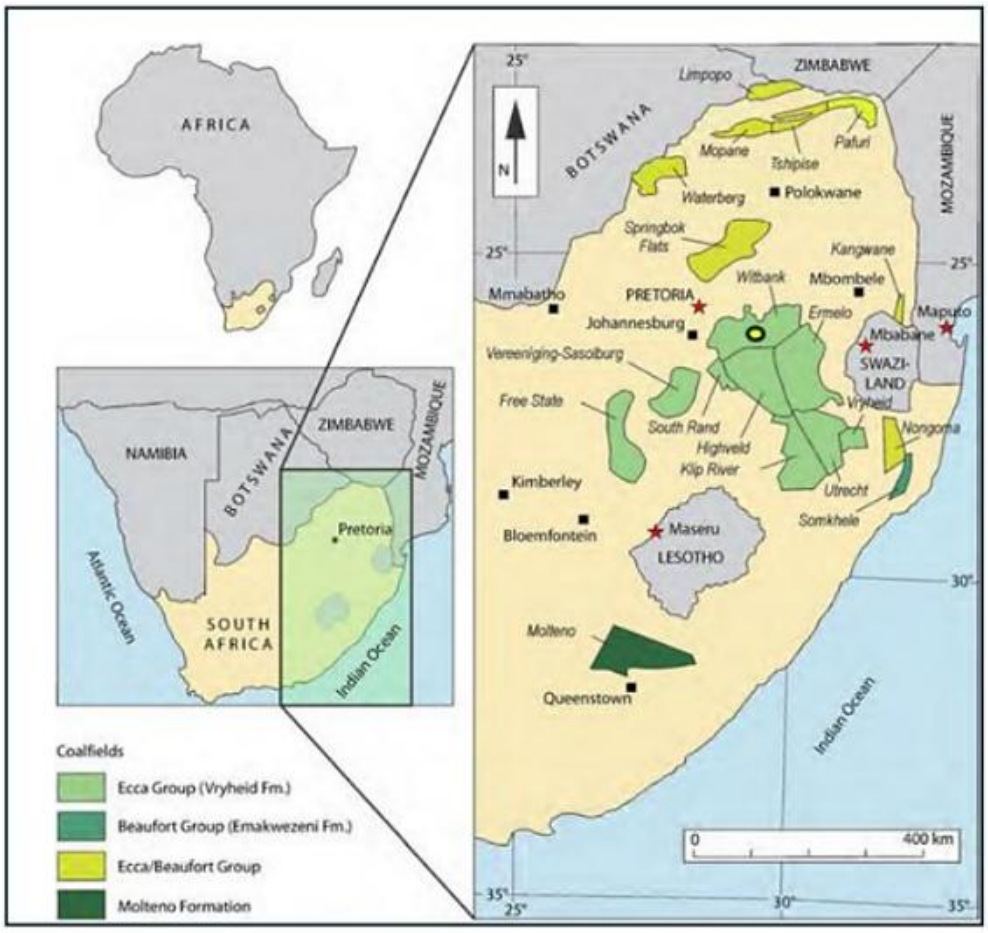

Figure 1. Map of South African coalfields showing major coal-bearing formations and the study area denoted by the yellow circle (Hancox, 2016), modified after Snyman (1998).

References

Dai, S., Hower, J.C., Yudovich, Y.E., Finkelman, R.B., Zhang, Y., French, D., Liu, Y., Liu, J., Yan, R., Zhao, Z., Ketris, M.P., Zhao, C., Xu, N., Graham, I.T., 2025. Abundances of elements in global coals. Int. J. Coal Geol. 311, 104899.

Hancox, P.J., 2016. The coalfields of south-central Africa: A current perspective. Episodes 39(2), pp. 404-428.

Taylor, S.R., McLennan, S.M., 1985. The Continental Crust: Its Composition and Evolution. Blackwell, Oxford. 312pp.

Seredin, V.V., 2010. A new method for primary evaluation of the outlook for rare earth elements. Geol. Ore Depos. 52, 428-433.

Snyman, C.P., 1998. Coal. In: Wilson, M.G.C. and Anhaeuesser C.R. (editors), The Mineral resources of South Africa, Hand Book 16. Council for Geoscience Publication 16, pp.136-205.

Integrated geological and geochemical assessment of critical and toxic element resources deposited in coal waste impoundments

Dmytro Khomenko[1,2*], Zbigniew Jelonek[1], Iwona Jelonek[1]

[1]University of Silesia, Faculty of Natural Sciences, Institute of Earth Science Katowice, Poland; [2]International Environmental Doctoral School associated with the Centre for Polar Studies at the University of Silesia(IEDS), Katowice, Poland

** Corresponding Author: dmytro.khomenko@us.edu.pl*

The progressive decarbonization and liquidation of mining and processing plants have brought the environmental management and potential economic utilization of coal waste storage areas to the forefront of modern geological research. While traditional reclamation remains economically unprofitable, comprehensive geological surveys offer a viable alternative by assessing the occurrence, distribution, and extraction prospects of critical elements, alongside the feasibility of holistic waste processing. This study focuses on flotation waste sediments deposited in settling tanks at the PGG SA KWK Piast-Ziemowit mine in Poland, aiming to determine the distribution patterns and content of both valuable and hazardous elements within these anthropogenic deposits.

Our integrated methodological approach combines ground-penetrating radar (GPR) surveys using GSSI SIR-20 and MALA ProEx systems with 270 MHz and 100 MHz antennas, a 25×25 m drilling grid with 80 mm diameter core sampling, and multi-stage laboratory analyses including flotation, sedimentation, XRF, ICP-OES, XRD, SEM/EDS, and petrographic microscopy. GPR surveys revealed that the coal sludge thickness reaches up to 4.7 meters, with the upper 1.0-1.5 m containing a higher proportion of coarse coal particles and elevated organic matter content. The mineral fraction (<0.02 mm), where critical elements primarily concentrate, was isolated and analyzed. Petrographic analysis identified vitrodetrinite and inertodetrinite as the dominant macerals. Grain-size dispersion analysis showed an average fine fraction content of 17.32% (standard deviation ±1.68%), with particles <1 μm and >45 μm indicating significant heterogeneity. XRF and XRD analyses confirmed the presence of quartz, kaolinite, illite/mica, pyrite, dolomite/ankerite, gypsum, and halite. ICP-OES results demonstrated that the enriched flotation waste contains economically promising concentrations of Ge, Ga, Li, and rare earth elements (REEs), alongside elevated levels of toxic elements such as As, Pb, Cd, Cr, and Se, which are preferentially associated with sulfide phases and organic matter.

Beneficiation tests, including froth flotation and sedimentation, achieved 65-90% recovery of critical elements from the -1+0.03 mm size fraction. The processed concentrate showed improved calorific value and technical parameters suitable for fuel briquette production. The residual mineral mass, after carbon extraction, retains significant concentrations of critical metals, with preliminary economic estimates indicating a potential value of approximately 70 million metric tons of recoverable material. Statistical and cluster analyses further defined distinct paragenetic associations and enrichment patterns, providing a robust basis for resource estimation.

The study establishes a scientific framework for trace element geochemistry in anthropogenic deposits and demonstrates that integrated GPR and drilling surveys, combined with detailed laboratory characterization and beneficiation testing, can effectively identify zones enriched in critical elements while simultaneously assessing environmental risks. These findings support a zero-waste strategy for coal waste impoundments, offering a pathway for full recovery of coal (as briquettes), critical elements (Ge, Ga, REEs), and mineral mass for construction, contributing to circular economy and strategic raw material security.

An initial assessment of low-rank coals for advanced industrial applications: case studies from Greece

Maria Georgaki[1], Malgorzata Wojtaszek-Kalaitzidi[2], Adam Cygan[2], Stavros Kalaitzidis[1*]

[1]Department of Geology, University of Patras, Patras, Greece; [2]Institute of Energy and Fuel Processing Technology, Zabrze, Poland

** Corresponding Author: skalait@upatras.gr*

Greece has historically been one of the most lignite-dependent countries in Europe, due to abundant coal resources in Western Macedonia and the Megalopolis Basin in the Peloponnese. However, a key part of the EU Green Deal is the gradual phase-out of lignite use. Alternative uses of lignite are the main objectives of several studies worldwide (e.g., Kalaitzidis et al., 2006; Giannouli et al., 2009; Cheng et al., 2018), as a solution for the future utilization of lignite. Lignite-based advanced materials, such as carbonized materials (e.g., activated carbon), constitute important alternative applications.

In the current study, six low-rank coals from Greece are examined to address a critical knowledge gap regarding the characteristics and potential utilization pathways of Greek lignites in the post-lignite energy transition era. The samples were obtained from four peat/coal bearing basins across Greece: Ptolemais (PT1, PT2), Prosilio (PR1, PR2), Xyniada (XY) and Almyros (AL). Pyrolysis and activation were performed on all samples. Raw, pyrolyzed, and activated fractions were subjected to proximate, ultimate, and petrographic analyses in order to obtain a comprehensive evaluation of the samples characteristics. In addition, electrical resistivity and conductivity measurements were carried out to evaluate their potential applications in electrode production.

For raw samples, the carbon content ranges from 28.8 to 55.7% (on a dry basis), while hydrogen and nitrogen fluctuate from 3.3 to 5.4% and from 0.3 to 1.9% (on a dry basis), respectively, whereas sulphur content ranges from 0.6 to 3.2% (on a dry basis). For the pyrolyzed samples, the carbon content ranges from 31.5 to 79.8% (on a dry basis), hydrogen and nitrogen range from 0.2 to 0.8% and from 0.3 to 0.4% (on a dry basis), respectively, while the sulphur content ranges from 1.2 to 4.2% (on a dry basis). For the activated samples, the carbon content varies from 14.6 to 76.4% (on a dry basis), hydrogen and nitrogen up to 0.5% and 0.2% (on a dry basis), respectively, and the sulphur content ranges from 0.3 to 4.3% (on a dry basis). Pyrolyzed and activated samples show higher carbon content values than raw samples, as reasonably expected. During the pyrolysis and activation, anisotropy developed in the samples (Fig. 1), with the bireflectance of the pyrolyzed and activated samples ranging from 1.46 to 1.85%.

The pyrolyzed and activated samples exhibit relatively good electrical conductivity, with values ranging from 2 to 17.6 S/cm. The pyrolyzed samples show the highest conductivity values, indicating their potential for application in electrode production. Overall, the results indicate that pyrolysis and activation significantly influence the physicochemical and electrical properties of Greek low-rank coals. Further work will include sorption experiments for dyes (e.g., Methylene blue and Safranin O) and phenanthrene to assess the adsorption capacity of the studied samples.

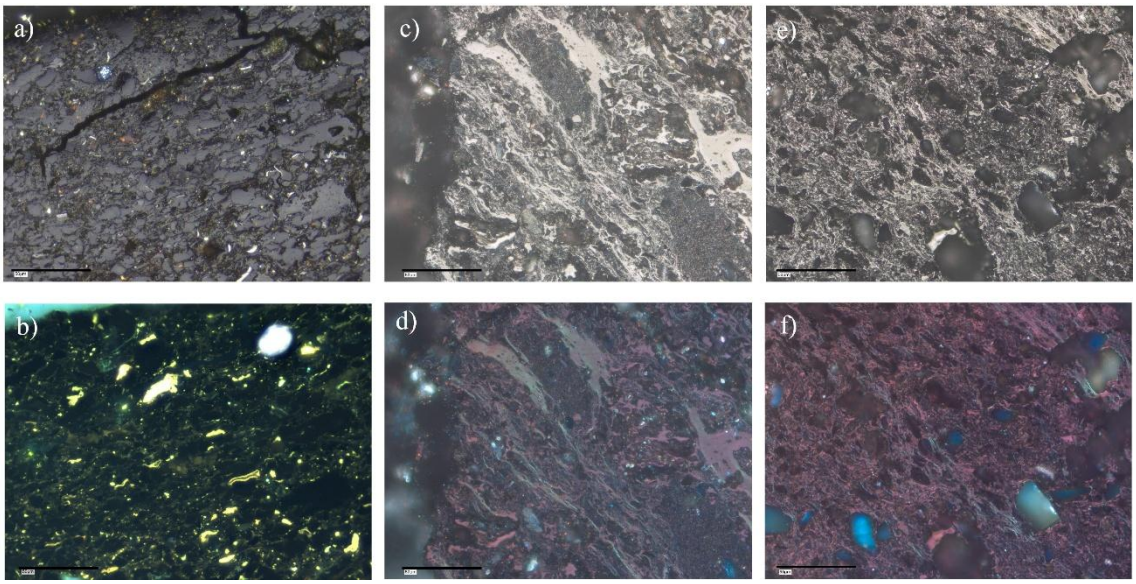

Figure 1. Photomicrographs of PT2 sample: a, b) raw lignite; c, d) pyrolyzed lignite; e, f) activated lignite; under incident white light (a, c, e); blue light excitation (b) and inserting λ plate under polarized light (d, f); oil immersion; X50 objective; total magnification X500.

References

Cheng, G., Zhang, C.X., Zhang, X.M., Zhang, Z.L., 2018. Preparation of lignite-based activated carbon and its flue gas desulfurization performance. Mater. Res. Express 6(2), 025603.

Giannouli, A., Kalaitzidis, S., Siavalas G., Chatziapostolou, A., Christanis, K., Papazisimou, S., Papanikolaou, C., Foskolos, A., 2009. Evaluation of Greek low-rank coals as potential raw material for the production soil amendments and organic fertilizers. Int. J. Coal Geol. 77, 383-393.

Kalaitzidis, S., Karapanagioti, H., Christanis, K., Bouzinos, A., Iliopoulou, E., 2006. Evaluation of peat and lignite phenanthrene sorption properties in relation to coal petrography: the impact of inertinite. Int. J. Coal Geol. 68, 30-38.

Effects of self-heating on the petrographic and Rock-Eval 7S parameters of coals from the Na Duong mine, Vietnam

Weronika Cyran[1*], Dariusz Więcław[1], Marta Waliczek[1], Khuong The Hung[2], Pham Nhu Sang[2]

[1]Faculty of Geology, Geophysics and Environmental Protection, AGH University of Krakow, Krakow, Poland; [2]Faculty of Geosciences and Geoengineering, Hanoi University of Mining and Geology, Hanoi, Vietnam

** Corresponding Author: weronika2002.cyran@gmail.com*

In the Na Duong open-pit coal mine in northern Vietnam, self-heating and spontaneous combustion processes occur. This study presents preliminary results on the petrological and geochemical effects of these processes in coals and coaly rocks from this mine. Sixteen rock samples (including 12 containing original (unchanged) material taken from exposed coal seams and 4 subjected to self-heating collected from temporary coal waste pile) were investigated using vitrinite reflectance measurements, petrographic observations, and Rock-Eval 7S pyrolysis to evaluate self-heating-related changes in the organic matter. All original samples exhibited VR_o values ranging from 0.39 to 0.54% and Tmax from 399 to 424°C, respectively, indicating a sub-bituminous range of analysed coals. The high pyritic sulphur, reaching 2.7 wt.% and organic sulphur contents up to 2.6 wt.%, respectively, suggest anoxic sedimentary conditions and that the exothermic oxidation of pyrite and organic sulphur compounds in humid conditions is the main cause of coal self-heating. Three samples displayed substantially higher reflectance values (2.62-3.04 $\%VR_o$), indicating advanced thermal alteration associated with self-heating. One of these samples showed a wide reflectance range (1.40-4.88 $\%VR_o$), suggesting heterogeneous heating conditions within the coal. The elevated reflectance values were restricted to samples collected from area subjected to spontaneous combustion. Furthermore, one sample collected from the self-heating zone, characterising a mean reflectance value of 0.39% and Tmax of 407°C, respectively, exhibited the tarry cover and localized increases in reflectance near the sample margins. The elevated value of the sulphur index of this sample (SI; Carvajal-Ortiz et al., 2021), reaching 85 mg S/g TOC, suggests a significant share of S compounds in the organic products of the self-heating. Petrographic observations of altered samples revealed features indicative of the high temperature influence, including devolatilisation pores, brighter rims, and fractures affecting the organic matter. Rock-Eval 7S data revealed significant differences between altered and unaltered samples. Self-heated samples exhibited substantially lower S2 and hydrogen index (HI) values, whereas samples with low reflectance values had relatively high HI values (201-401 mg HC/g TOC) suggesting a contribution of sapropelic organic matter. These samples were characterized by the presence of hydrogen-rich organic constituents, particularly liptinite-group macerals such as resinite, fluorinite, suberinite, sporinite, and cutinite, supporting the Rock-Eval data. The observed decrease in HI values in the altered samples was accompanied by a reduction in TOC. The obtained results indicate that self-heating in the Na Duong coals is associated with distinct petrographic and geochemical signatures reflecting different degrees of thermal alteration.

Acknowledgments
This research was partially funded by the subsidy granted to the AGH University of Krakow by the Ministry of Science and Higher Education.

References

Carvajal-Ortiz H., Gentzis T., Ostadhassan M., 2021. Sulfur differentiation in organic-rich shales and carbonates via open-system programmed pyrolysis and oxidation: insights into fluid souring and H_2S production in the Bakken Shale, United States. Energy Fuels 35, 12030-12044.

Evolution in physicochemical properties and carbon permanence of biochar with increasing carbonization temperature

Henrik I. Petersen[1*], Rasmus Jakobsen[1], Priyanka Kaushal[2], Abhijeet Anand[2], Arka Rudra[3], Kasper H. Blinkenberg[4], Hamed Sanei[3]

[1]Geological Survey of Denmark and Greenland (GEUS), Copenhagen, Denmark; [2]Centre for Rural Development and Technology (CRDT), Indian Institute of Technology Delhi, New Delhi, Indi; [3]Lithospheric Organic Carbon (LOC), Department of Geoscience, Aarhus University, Aarhus, Denmark; [4]Department of Geosciences and Natural Resource Management, University of Copenhagen, Copenhagen, Denmark

** Corresponding Author: hip@geus.dk*

Biochar is increasingly considered a viable method to mitigate climate change through long-term carbon storage. The storage potential depends on the physicochemical characteristics of the feedstock and the distribution of carbon fractions in the biochar, particularly the inertinite (inert carbon) fraction, which is a function of the carbonization temperature (CT) (Sanei et al., 2024). This study investigates the physicochemical properties and the fraction of inertinite of three series of biochar produced at 350-650°C from wheat straw, rice straw, and rice husk biomasses. The degree of thermal carbonization of the biomasses was measured by random reflectance (%R_o). The substantial silica content in rice husk retards the thermal carbonization, and the increase in mean R_o with increasing CT is markedly slower compared to the two other feedstocks (Petersen et al., 2027). The heating-induced carbonization of the biomasses into an increasingly condensed polyaromatic structure is accompanied by an increase in organic carbon (C_{org}) content that reaches >72% in rice straw and wheat straw biochar at CT's >550°C, a drastic decrease in the H/C molar ratio, a decrease in volatile matter, and an increase in ash content. Furthermore, a marked increase in specific surface area (BET) and pore volume, the latter controlled by the formation of micropores <2 nm, is observed. Also, the thermal stability recalcitrance index (R_{50}) was high (0.76-0.88) for rice straw and wheat straw biochar produced at >550°C and moderate (0.67-0.75) for rice husk biochar. The inertinite content in the biochar samples was quantified using the Inertinite Benchmark ($IBR_o2\%$) methodology (Sanei et al., 2025), which stipulates that inert carbon must yield R_o values >2%. Up to about 450°C, the content of inertinite is nil. However, the inertinite fraction (F_{inert}) increases substantially at CT's >550°C. Together with the increase in inertinite, the fraction of inert carbon ($C_{inert} = C_{org} \times F_{inert}$) increases. The percentage of C_{inert} can be converted to CO_2 equivalents to represent its carbon storage potential. Among the investigated biomasses, wheat straw biochar shows the greatest carbon storage potential, followed by rice straw biochar. The silica content in rice husk retards the carbonization and limits the carbon content and thus the storage potential. This study showcases the evolution in physicochemical properties of three biochar types with increasing CT, which can used to tailor-make biochar for specific purposes beside carbon storage.

References

Petersen, H.I., Kaushal, P., Anand, A., Blinkenberg, K.H., Sanei, H., 2027. A relationship between biochar reflectance and carbonization temperature. Fuel 428, 140432.

Sanei, H., Rudra, A., Przyswitt, Z.M.M., Kousted, S., Sindlev, M.B., Zheng, X., Nielsen, S.B., Petersen, H.I., 2024. Assessing biochar's permanence: an inertinite benchmark. Int. J. Coal Geol. 281, 104409.

Sanei, H., Wojtaszek-Kalaitzidi, M., Schovsbo, N.H., Stenshøj, R., Zhou, Z., Schmidt, H.-P., Hagemann, N., Chiaramonti, D., Kiaitsis, T., Rudra, A., Lehner, A.J., Brown, R.W., Gill S., Dorr, E., Kalaitzidis, S., Goodarzi, F., Petersen, H.I., 2025. Quantifying inertinite carbon in biochar. Int. J. Coal Geol. 310, 104886.

Petrography of black mass - identification of carbon forms

Małgorzata Wojtaszek-Kalaitzidi[1*], Bruno Valentim[2], Alexandra Guedes[2], Sónia Pereira[2]

[1]Institute of Energy and Fuel Processing Technology, Zabrze, Poland; [2]Faculty of Sciences, University of Porto, Porto, Portugal

* *Corresponding Author: mwojtaszek@itpe.pl*

Black mass generated during recycling of electronic and electrode materials is an important secondary resource for graphite, other carbon materials, and critical metals. However, its heterogeneous composition, fine particle size, and variable origin make reliable identification and quality assessment of carbon-rich fractions challenging (Valentim, 2024). This study presents petrographic characterisation of six black mass samples obtained from physical and chemical separation processes, with emphasis on carbon forms relevant to graphite concentrate recovery.

The analysed materials included isolated fractions enriched in graphite-related particles originating from lithium-ion batteries, graphite linings, and electronic device components. The main aim was to establish robust analytical criteria for determining the quality, structure, purity, and recyclability of carbon in black mass. A complementary approach combining incident-light microscopy, SEM-EDS, and Raman spectroscopy was applied. Petrographic observations enabled recognition of carbon forms, morphology, optical properties, particle associations, and degree of liberation. SEM-EDS provided information on textural relationships between carbon-rich particles, mineral matter, metallic fragments, and critical metals-bearing phases. Raman spectroscopy was used to assess structural ordering of graphite and other carbonaceous materials, including graphene layer organisation and defect intensity.

Based on these complementary structural and chemical investigations, preliminary classification criteria for carbon types in black mass were developed. The proposed approach distinguishes graphite from functional carbon structures, amorphous or disordered carbon, composite carbon-metal fragments, and particles that contain or are associated with critical metals (Fig. 1). The classification includes graphite flakes, spheroidal graphite, spheroidised graphite, pressed graphite, pyrolytic carbon, amorphous carbon, calcined cokes, carbon fibres, glass fibres, metal and metal oxide particles, synthetic polymers, and other components.

Qualitative and quantitative analyses were performed in accordance with the adopted classification criteria. This enabled the evaluation of sample variability, the proportion of recoverable graphite-rich fractions, and the occurrence of carbon forms that may influence subsequent processing routes in complex recycled carbon-rich materials.

The results demonstrate that petrography, supported by Raman spectroscopy and SEM-EDS, provides a reliable basis for identifying, classifying, and quantifying crushed black mass particles. The developed protocol may support industrial recycling assessment by improving control of graphite concentrate quality, evaluating carbon recyclability, and guiding high-value applications for recovered graphite and other carbon materials. Consequently, the study contributes to circular resource use and standardised petrographic procedures for black mass quality assessment and resource recovery.

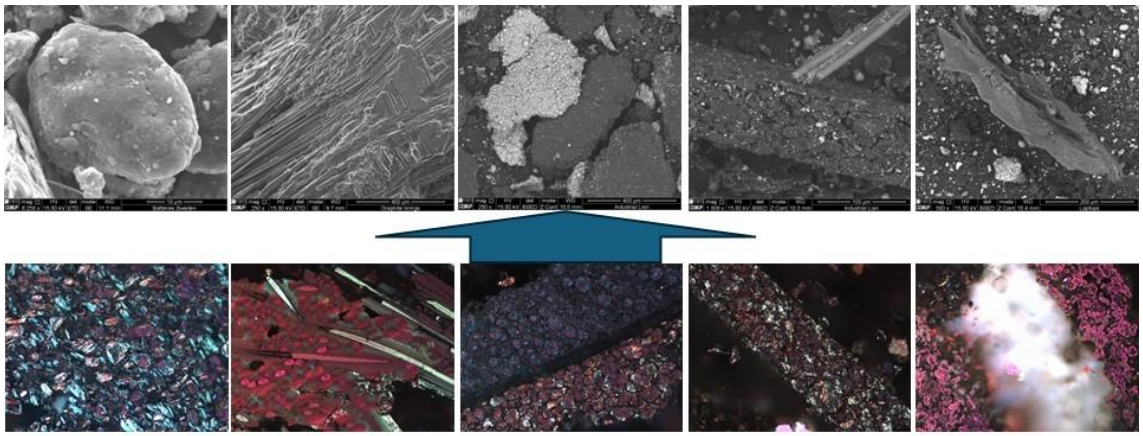

Figure 1. Black mass mixed materials observed with use of SEM (upper row) and polarized microscope (lower row); From left: spheroidised graphite, carbon fibers, cathode and anode chunks, anode chunk, synthetic polymer.

Acknowledgement

This project has received funding from the European Union's Horizon Europe research and innovation programme under grant agreement No 101131765 (EXCITE2) for Transnational Access conducted at Faculdade de Ciências da Universidade do Porto.

References

Valentim, B., 2024. Teaching Aid Regarding the Application of Advanced Organic Petrography in Recycling End-of-Life Lithium-Ion Batteries. Batteries 10, 391.

Microscopically distinguishable components of naturally graphitized coals

Li Kuo[1*], Lu Hao[1], Duan Xiaoyu[1]

[1]China University of Mining and Technology, Beijing, China

** Corresponding Author: kuo.li@cumtb.edu.cn*

Naturally, graphitized coals form in coal-bearing strata affected by large-igneous intrusions (Zheng et al., 1996). To reveal how the microscopically distinguishable components change during natural graphitization, a series of naturally graphitized coals from three mines in the Lutang graphite mining area were studied by coal petrographic approach. The Lutang graphite mining area is the biggest natural coal-derived graphite deposit in China, which located at the south of Chenzhou city, Hunan Province, where the Longtan coal measures were intruded by the Yanshanian granite batholith intrusion (Li, 2019).

In the less graphitized anthracite sample (LTG5-1), vitrinite with a homogeneous texture and minor residual inertinite were observed (Fig. 1a). The brightness of vitrinite has already surpasses inertinite. Vitrinite displayed high anisotropy (green interference colors under crossed polarized light) and high reflectance (R_r = 6.09%). With increasing metamorphism, the original macerals decreased markedly. In the highly graphitized sample series (LTG6), cryptocrystalline graphite became the dominant component (>80%), with sporadic high bright microcrystalline graphite particles also present (Fig. 1b-e). In addition, pyrolytic carbon (PC) and needle graphite (NG) were identified (Taylor et al., 1998). PC occurs as linings along fracture and pore walls, forming rim-like or filling textures, and commonly develops wormlike or spherulitic internal structures (Li et al., 2025). Under reflected cross-polarized light, PC displays strong anisotropy with cross or banded extinction, and the wormlike and spherulitic textures are key diagnostic features for identifying PC (Fig. 1e,f). NG is observed occasionally within pores and cracks, less commonly than PC. It shows needle-like or elongated shapes, some growing into fine flaky aggregates, and is typically oriented along the fracture direction (Fig. 1c,d). This distinctive needle-like morphology and preferred orientation distinguish NG from PC and microcrystalline graphite.

In the highly graphitized coals, no coal components (vitrinite and inertinite) remained, cryptocrystalline graphite takes the main constitution, suggesting the cryptocrystalline was transformed from coal components. The occurrence at pores and cracks of pyrolytic carbon and needle like graphite indicates these components formed from fluid precursors. It has been suggested the pyrolytic carbon in naturally graphitized coal formed by gaseous hydrocarbon, like CH_4 and CO_2; the needle-like graphite formed from liquid hydrocarbon, like coal tar (Li et al., 2018, 2026).

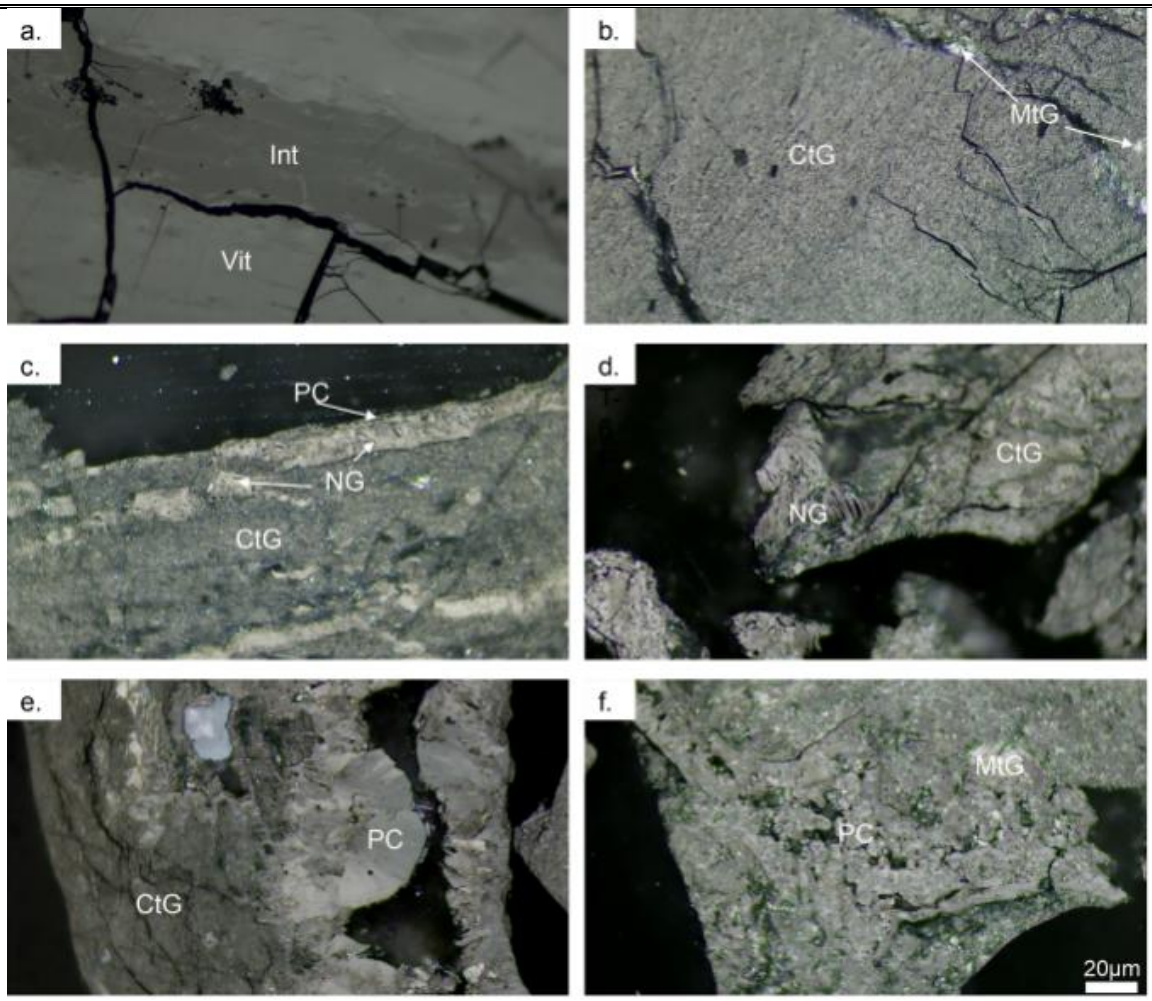

Figure 1. Representative photomicrographs of components in naturally graphitized coals. All images taken under white light with a 50× oil immersion objective, a) sample LTG5-1; b, c) sample LTG6-13; d) sample LTG6-4; e, f) sample LTG6-17. Vit–vitrinite, Int–inertinite, PC–pyrolytic carbon, CtG–cryptocrystalline graphite, MtG–microcrystalline graphite, NG–needle-like graphite. Scale bar = 20 μm indicated in panel f).

References

Li, K., Rimmer, S.M., Liu, Q., 2018. Geochemical and petrographic analysis of graphitized coals from Central Hunan, China. Int. J. Coal Geol. 195, 267-279.

Li, C., 2019. Petrology, Petro-Geochemistry and Tectonic Significance of the Qitianling Granite Body. Chengdu University of Technology, Hunan Province (In Chinese with English Abstract).

Li, J., Qin, Y., Shen, J., Chen, Y., Li, G., Zhu, P., 2025. Petrolographic characteristics of graphitic carbon in coal-based graphite: Implications for the applicability of reflectance. Int. J. Coal Geol. 310, 104884.

Li, K., Lu, H., He, X., Xu, Z., Liu, Q., 2026. Petrographic and carbon isotopic evidence for the sources and evolution of natural coal-derived graphite in Lutang area, South China. Int. J. Coal Geol. 105027.

Taylor, G., Teichmüller, M., Davis, A., Diessel, G.F.K., Littke, R., Robert, P., 1998. Organic Petrology. Gebruder Borntraeger, Berlin, pp. 169.

Zheng, Z., Zhang, J., Huang, J.Y., 1996. Observations of microstructure and reflectivity of coal graphites for two locations in China. Int. J. Coal Geol. 30, 277-284.

On the origin of micrinite, the red herring of organic petrology

Paul C. Hackley[1*], Brett J. Valentine[1], Ryan J. McAleer[1], Aaron M. Jubb[1], Javin J. Hatcherian[1], Jing Qu[2], Yuying Zhang[2]

[1]U.S. Geological Survey, Reston, USA; [2]University of Delaware, Newark, USA

* *Corresponding Author: phackley@usgs.gov*

Micrinite is a highly reflective, granular (<2 μm according to International Committee for Coal and Organic Petrology definition) microscopically identified component presenting mostly in bituminous coal and in immature to oil window-maturity source rocks. Previous workers have suggested micrinite is a refractory organic residue remaining from volatilization of lipid-rich organic matter during elevated temperatures of sedimentary burial. Others have demonstrated micrinite is comprised of fine-grained minerals which appear bright due to diffuse scattering of incident light. Micrinite identification and composition are important industrial considerations in metallurgy, where micrinite is considered an inert diluent in bituminous coking coals, or in source rocks where micrinite may signal incipient petroleum generation. Here we use a correlative petrographic approach (optical and electron microscopies, optical photothermal infrared spectroscopy) to show that micrinite can be composed of both organic and inorganic material. Micrinite in immature Bakken and Kimmeridge Formation source rock samples (Fig. 1A-G) is comprised of spherical (Fig. 1E inset) carbon forms, which we interpret as soot from the combustion of organic matter under an oxygenated atmosphere prior to burial. Soot forms of micrinite appear brighter than surrounding organic matter in secondary electron imaging of mechanically polished samples, possibly related to differences in edge density. Sulfur is present in low concentrations in soot micrinite relative to adjacent bituminite (Fig. 1D, F-G), consistent with combustion. On the other hand, micrinite in immature Boquillas and Pantokrator Formation source rock samples is comprised of sub-micron sized mineral phases including clays, quartz, feldspars (Fig. 1H-L), carbonates, and phosphates. In North American bituminous coals, micrinite consists of both organic and inorganic materials even in the same microscope field of view (Fig. 1M). The observation that micrinite is both organic and inorganic points to sub-micron size as the common feature and causal agent for its white color and apparent high reflectance. We assert that the white color of micrinite is caused by Mie scattering, where the typical sub-micron size of micrinite (Fig. 1N), whether formed as organically sourced soot or as inorganic minerals, causes all wavelengths of the interacting white light (approximately 380 to 740 nm) to be scattered equally, resulting in the appearance of micrinite as a white material. That is, micrinite can be both organic and inorganic, as suggested and demonstrated by prior workers, respectively, is white in color due to Mie scattering, and its apparent high reflectance is a red herring in regards to its origin.

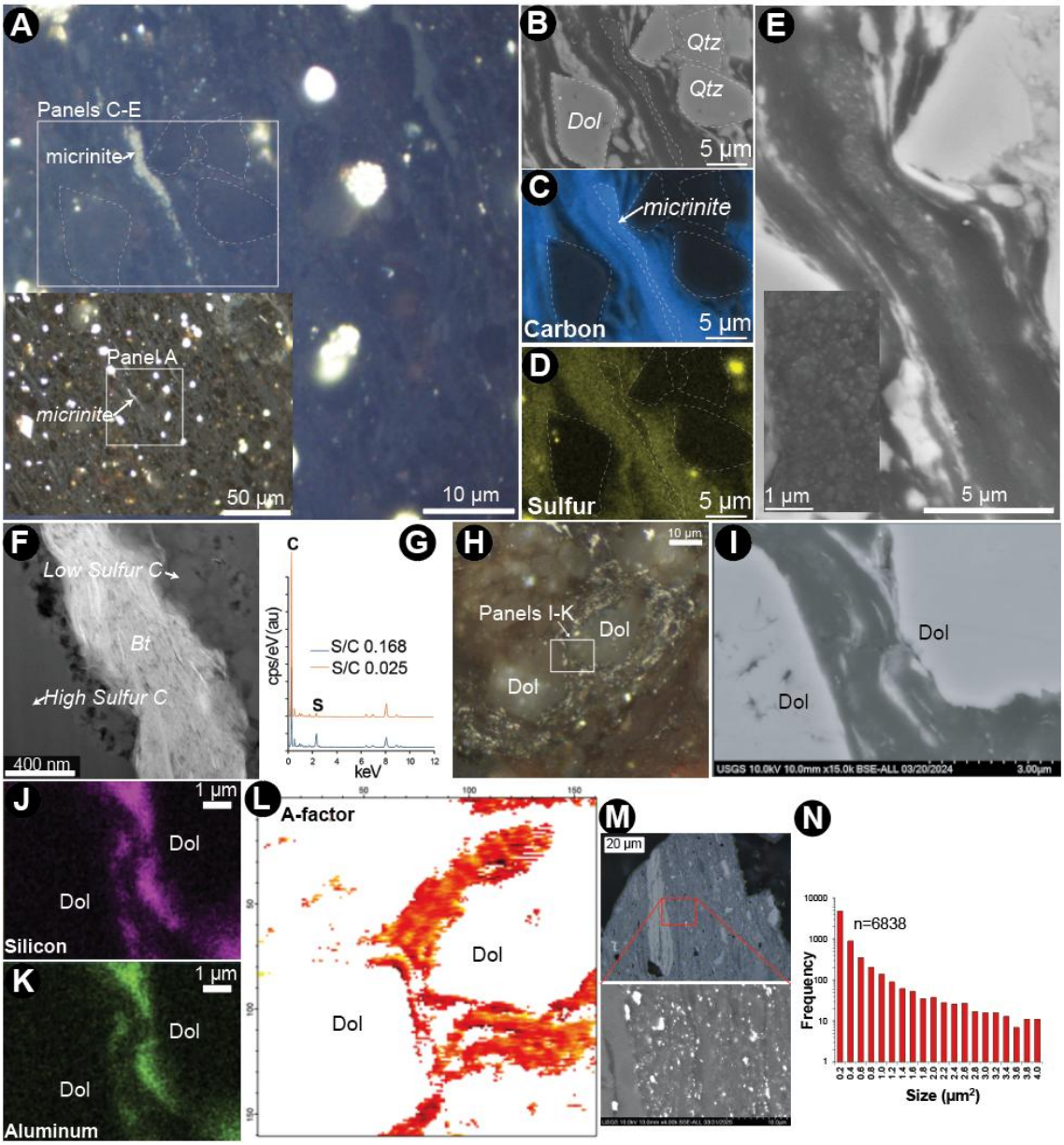

Figure 1. A. Micrinite in Bakken Formation, white light oil immersion (WLOI). B. Secondary electron (SE) image of micrinite in panel A. C. Carbon X-ray map for panel B. D. Sulfur X-ray energy dispersive spectroscopy (EDS) map for panels B-C. E. SE image zoom-in to micrinite in panels A-D, inset shows spherical micrinite forms at high magnification. F. Low sulfur (soot micrinite) and high sulfur (bituminite) carbon forms in Kimmeridge Clay Formation via transmission electron microscopy (TEM) darkfield imaging. G. TEM-EDS X-ray spectra from locations in panel F. H. Micrinite in Pantokrator Formation, WLOI. I. Backscatter electron (BSE) image of bituminite with clays from location in Panel H. J. EDS silicon X-ray map for panel I. K. EDS aluminum X-ray map for panel I. L. A-factor map from optical photothermal infrared spectroscopy showing absence of signal in locations of clay minerals. M. Micrinite in bituminous coal in WLOI and backscattered electron showing micrinite is organic and inorganic in same field. N. Histogram of micrinite sizes in WLOI image of panel M.

Experimental comparison of the maturity of organic matter based on vitrinite reflectance and autofluorescence measurements

Anna Maciejewska[1], Marcin Barski[1], Marta Waliczek[2]

[1]University of Warsaw, Faculty of Geology, Warsaw, Poland; [2]AGH University of Krakow, Faculty of Geology, Geophysics and Environmental Protection, Krakow, Poland

* *Corresponding Author: ak.maciejewska2@uw.edu.pl*

The thermal maturity of organic matter (OM) yields critical insights into hydrocarbon potential, sedimentary basin evolution, and burial history. It can be assessed using various indicators that quantify changes occurring during diagenesis. While results from different methods are generally correlated, the conversion, precision, and applicability of these approaches remain insufficiently understood. Fifteen core samples from the Jurassic basement of the Carpathians Foredeep and the Polish Outer Carpathians were measured for their thermal maturity values. Two approaches have been employed: spores' colouration and autofluorescence (R_o%), as well as vitrinite reflectance measurements (VR_o%).

Rock samples from Oleśnica 3, Łętowice 20, Zalasowa 2, and Zagorzyce 6 were macerated with hydrochloric and hydrofluoric acids, filtered, and prepared as microscopic slides. Dinoflagellate cysts present in the samples were assessed for colouration and autofluorescence under both white and ultraviolet light. The Staplin (1969) Thermal Alteration Index and the colour chart developed by Pearson (1984) were used to convert these observations to vitrinite reflectance equivalents. Subsequently, following the methodology of Tahoun et al. (2018), photographs of each cyst were analysed for RGB (red, green, and blue) values using GIMP 2.10.38 software. This evaluation of colour channels reduced the subjectivity inherent in colouration and autofluorescence analyses and enabled calculation of R_o% from R channel values (Tahoun et al., 2018).

The second approach involved measuring vitrinite reflectance, defined as the percentage of white light reflected from a polished vitrinite surface (Mukhopadhyay, 1994). Measurements were conducted on both polished block samples and kerogen concentrates embedded in epoxy resin to assess the applicability of the latter preparation method for samples with low OM content.

Results from colouration and autofluorescence analyses ranged from 0.4 to 1.2 R_o%, indicating predominantly mature OM. The vitrinite reflectance equivalent calculated from the R channel in white light corresponded closely with values obtained from colouration analysis. Therefore, the RGB method appears to be a promising tool for validating results and minimizing the influence of subjective colour perception. With one exception, VR_o% measurements corroborated the outcomes of the first method; the single outlier was attributed to liptinite contamination. In summary, the use of two complementary analytical methods provides extensive information on the region's thermal history. Establishing a conversion factor between these methods will enhance future research in organic petrology. The study is ongoing and will incorporate Rock- Eval pyrolysis to obtain more comprehensive data.

References

Mukhopadhyay, P.K., 1994. Vitrinite reflectance as a maturity parameter: Petrographic and molecular characterization and its applications to basin modeling. In: Mukhopadhyay, P.K., Dow, W.G. (Eds.), Vitrinite Reflectance as a Maturity Parameter: Applications and Limitations. ACS Symposium Series. American Chemical Society, Washington, DC, pp. 1-24.

Pearson D.L. 1984. Pollen/Spore colour 'standard'. Phillips Petroleum Company Exploration Projects Section (reproduced in Traverse A., 1988. Paleopalynology, Plate 1. Unwin Hyman, Boston).

Staplin, F.L., 1969. Sedimentary organic matter, organic metamorphism, and oil and gas occurrence. Bull. Can. Pet. Geol. 17(1), 47-66.

Tahoun, S.S., Deaf, A.S., Gentzis, T., Carvajal-Ortiz, H., 2018. Modified RGB-based kerogen maturation index (KMI): Correlation and calibration with classical thermal maturity indices. Int. J. Coal Geol. 190, 70-83.

Digitalization and computer vision applied to palynofacies and thermal maturity studies

Gil Machado[1,2*], Diogo Machado[3], André Sanches[4]

[1]Chronosurveys Lda, Almada Portugal; [2]GeoBioTec, Almada, Portugal; [3]Timeless Expression, Caldas da Rainha, Portugal; [4]RockRose Lda, Mértola, Portugal

** Corresponding Author: gil.machado@chronosurveys.com*

The digitalization of palynological slides has been gaining momentum as high-resolution scanners are increasingly used. There are multiple advantages of using digital versions of slides, such as independence from the physical version (the analyst can be located anywhere in the World, without the need of a microscope); permanent record of all the information contained in the slide (critical in vintage collections that may be degrading due to poor mounting medium); reproducibility and multiple analyses using the same dataset, especially when annotations are used.

A step forward is the use of computer vision approaches for this data, enabling automatic and semi-automatic analyses of the digital slides. Segmentation and classification models are widely used in computer vision. For palynological slides, the main challenge is the proper segmentation of juxtaposed and overlapping particles. Classification can be done using a supervised approach (pre-trained models), unsupervised, or a user-in-the-loop approach, where the model is built by the user, in real time, using multiple classification-validation iterations for each class (palynological particle type). The latter allows a more flexible definition of classes, adjustable to each project, and reduces interpretation time from days to hours.

Here, we present a software solution developed to analyze scanned palynological slides automatically, with a user-in-the-loop approach. The software – TaxaLens (Fig. 1) – uses adapted YOLO and SAM systems (Convolutional Neural Networks-based) to segment particles in a slide. To ease the classification of different particles by the user, the images are separated into clusters based on their visual similarity. These clusters can be matched directly to particle types (classes) or fine-tuned to train the model to identify classes more accurately. Several classification-validation cycles may be used to improve accuracy.

The outputs of the system are counts and proportions of different particles in each slide (spores, dinocysts, pollen, etc.), which can be displayed stratigraphically, in ternary plots, paleoenvironmental indexes, among other useful graphical and numerical displays. Taxonomic work can be done using the extracted images of a specific palynomorph group (even when they are rare), virtually eliminating time-consuming tasks of searching for them under the microscope or computer screen.

The software is presented in modules and future developments include thermal maturity measurements (Palynomorph Darkness Index) and charcoal analysis.

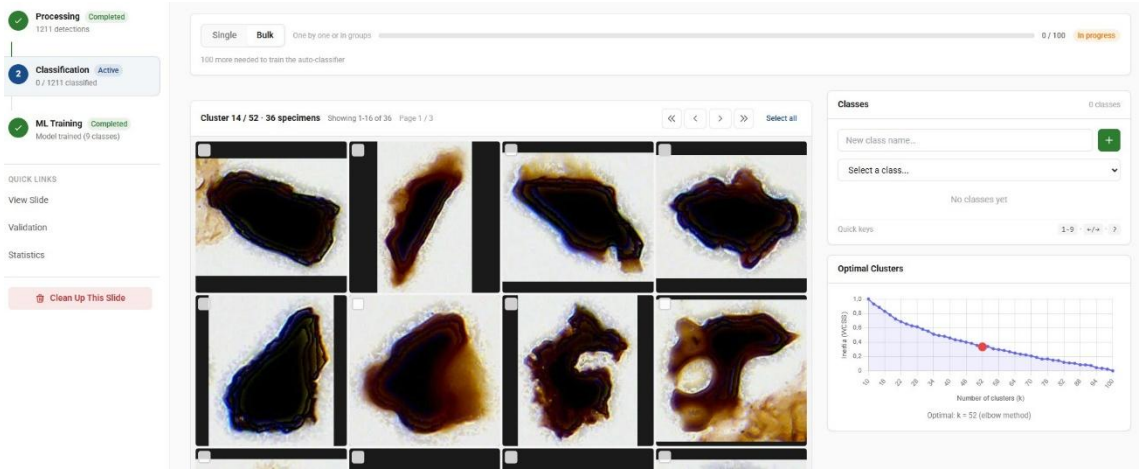

Figure 1. Example of clustering and classification in TaxaLens. From TaxaLens software.

Thermal conditions of the coal-bearing series in the Upper Silesian Coal Basin (Poland) in the light of research findings on rock temperature and vitrinite reflectance

Sławomir Kędzior[1*], Arkadiusz Drozd[2], Tomasz Słoczyński[2]

[1]University of Silesia, Katowice, Poland; [2]Oil and Gas Institute- National Research Institute, Kraków, Poland

* *Corresponding Author: slawomir.kedzior@us.edu.pl*

The Upper Silesian Coal Basin (USCB) is characterised by a higher heat flow (>75 mW/m²) compared with neighbouring areas (65-75 mW/m²) (Szewczyk and Gientka, 2009). This study reviews the available temperature data from boreholes. It also utilises vitrinite reflectance (Ro) data to reconstruct the thermal conditions of the USCB in the geological past. These data were processed using Schlumberger's PetroMod software, designed to reconstruct the geological history of oil basins (Słoczyński and Drozd, 2018). 1D modelling was carried out in selected deep (>1500 m) USCB wells to reconstruct the thermal evolution of Carboniferous formations based on temperature and Ro measurements. An attempt was also made to assess the factors influencing the current temperature distribution of the rock mass in the USCB by constructing maps of temperature variation at depth levels.

Thermal modelling showed that the Saddle Beds, with the thickest 510 seam, were within the range of maximum temperatures reaching 150-200°C at the Carboniferous–Permian boundary (approximately 300 Ma), when the series reached its maximum subsidence. Subsequently, the coal-bearing series cooled gradually in association with uplift to the current recorded temperature of several dozen degrees (Fig. 1). This finding is consistent with the results of apatite fission and helium dating conducted by Botor (2014).

Currently, significant variation in temperature is observed at individual depth levels. The differences reach over a dozen degrees (Karwasiecka, 1996). Positive temperature anomalies often accompany regional faults with displacements of up to 1,000 m to the south (e.g., Jawiszowice and Bzie-Czechowice faults; Fig. 2). Modelling of the temperature distribution in the fault zone of the southern part of the USCB (Leśniak and Leśniak, 1994, Kędzior, 2001) showed the best agreement of heat propagation with a conduction model characterised by anisotropy and radiogenic heat generation; however, the convection model should not be neglected. Thus, tectonic zones rooted in deep subsurface strata may act as migration pathways for the Earth's heat.

Furthermore, coal seams, which account for approximately 5% of the total thickness of the Upper Carboniferous strata, are characterised by very low thermal conductivity, averaging 0.5-0.7 W/m·K (Plewa, 1994), which should slow down heat transfer within the rock mass and thereby contribute to an increase in rock temperature in the USCB.

The above studies may prove helpful in identifying areas suitable for geothermal energy extraction, which is important from the perspective of utilising a zero-emission energy source.

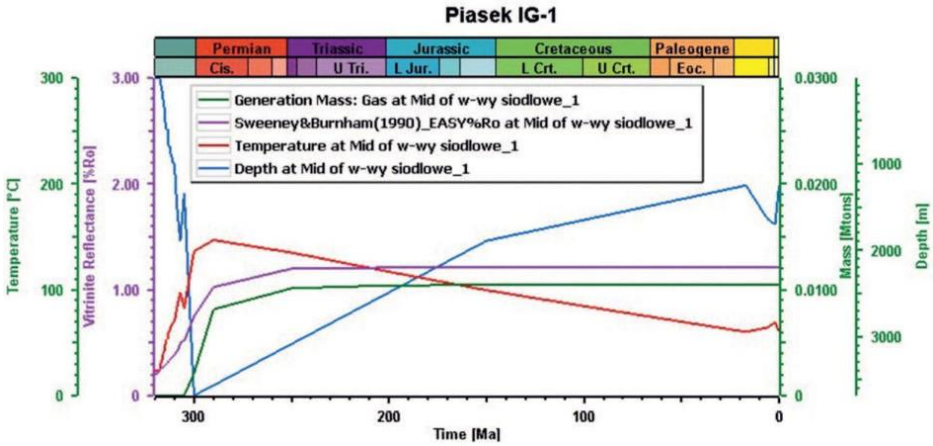

Figure 1. An example of thermal history modelling against the background of the geological development of the USCB coalfield (Słoczyński and Drozd, 2018).

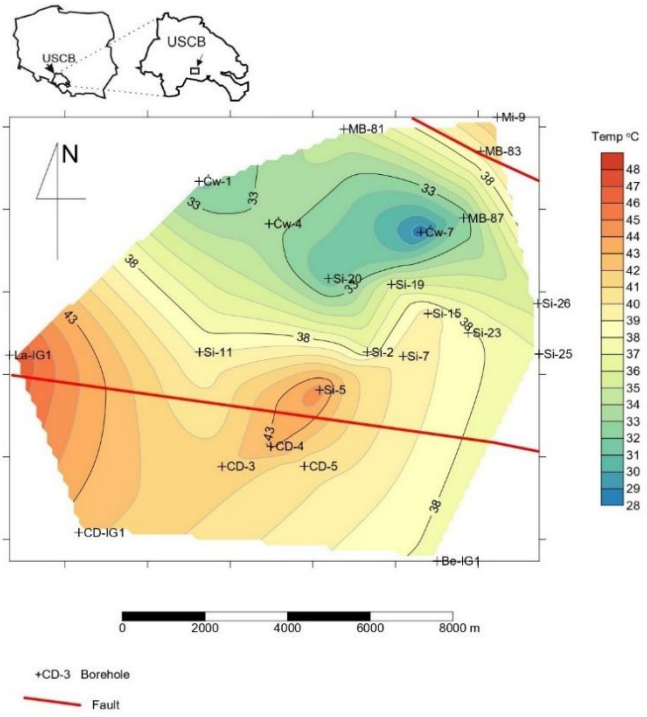

Figure 2. Temperature variation at a depth of 750 m below sea level (approximately 1000 m below ground level) in the southern part of the USCB.

References

Botor, D., 2014. Timing of coalification of the upper carboniferous sediments in the Upper Silesian Coal Basin on the basis of the apatite fission track and helium dating. Min. Res. Manag. 30, 85-104.

Karwasiecka, M., 1996. Geothermal atlas of the Upper Silesian Coal Basin, Polish Geological Institute, Warszawa.

Kędzior, S., 2001. Geothermal conditions of the Silesia mine coal deposit. Tech. Posz. Geol. Geosynoptyka i Geotermia, 5. ISSN 0304-520X.

Leśniak, L., Leśniak, A., 1994. Modelling the temperature distribution in the fault zone in the Czechowice region. AGH Quarterly, Geology 20, 221-235. ISSN 0138-0974.

Plewa S., 1994. Distribution of geothermal parameters on the territory of Poland. Wyd. CPPGSMiE PAN, Kraków. ISBN 83-86286-15-6.

Słoczyński, T., Drozd, A., 2018. Methane potential of the Upper Silesian Coal Basin carboniferous strata – 4D petroleum system results. Nafta-Gaz 10, 703-714.

Sweeney, J.J., Burnham, A.K., 1990. Evaluation of a simple model of vitrinite reflectance based on chemical kinetics. AAPG Bulletin 74, 1559-1570.

Szewczyk, J., Gientka, D., 2009. Terrestrial heat flow density in Poland – a new approach. Geol. Quart. 53 (1), 125-140.

Structural parameter evolution characteristics of coals in different rank under various metamorphic pathways

Chao Liu[1], Beilei Sun[1]

[1]Taiyuan University of Technology, Taiyuan, China

** Corresponding Author: tyutliuchao@163.com*

The molecular structure of coal governs its chemical reactivity and behavior during combustion, pyrolysis, liquefaction, and gasification. Deciphering the structural evolution of coal is fundamental to unlocking its efficient utilization. A comprehensive analysis of molecular structural parameter evolutionary patterns and underlying mechanisms across metamorphic pathways is necessary. In this study, a coal with vitrinite reflectance (VR_o) of 0.7% was selected and thermal simulation experiment was conducted to artificially advance the rank. The thermal simulation was conducted using a WYMN-3 semi-enclosed high-temperature and -pressure simulator. Approximately 105 g of coal was crushed to a particle size range of 3-8 cm and divided evenly into seven portions (~15 g each) to minimize the effects of sample heterogeneity. Each portion was loaded into the reaction chamber. The experiment was conducted across seven temperature points: 300°C (TA-2), 350°C (TA-3), 400°C (TA-4), 450°C (TA-5), 500°C (TA-6), 550°C (TA-7), and 600°C (TA-8). With increasing temperature in thermal simulation experiments, the vitrinite reflectance of coal samples progressively rises, reaching 4.38% at 600°C. The molecular structural characteristics of coal samples were analyzed via Fourier transform infrared (FTIR) spectroscopy, X-ray diffraction (XRD), and confocal laser Raman spectroscopy. FTIR results indicate that coalification leads to the conversion of aliphatic side chains into aromatic ring structure, with a gradual increase in methylene-type side chains and progressive elongation of aliphatic side chains. XRD results reveal that the lateral size (La), stacking height (Lc), and interlayer spacing (d_{002}) of coal molecules are 25.18-45.82, 14.40-35.61, and 3.43-3.59 Å, respectively. The d_{002} gradually decreases with increasing maturity. Although La and Lc values fluctuate owing to coalification jumps, they exhibit an overall increasing trend. Raman spectroscopy results indicate that the structural disorder degree of coal fluctuates during coalification, ultimately transforming into a highly ordered structure. Based on the molecular structural parameters of coal under different metamorphic pathways, the factors influencing coal molecular structures during metamorphism are discussed. The results reveal that temperature promotes hydrogen detachment from aliphatic side chains in coal, inducing carbon cyclization, and serves as the dominant control factor driving aromatic condensation growth and the cleavage of side chains/functional groups. Additionally, temperature progressively reduces methylene-type side chains and shortens aliphatic chain lengths. Time provides a kinetic buffer for dehydrogenation-cyclization reactions of aliphatic chains and C-H structural modifications in aromatic systems, facilitating their evolution toward thermodynamic equilibrium. As a secondary factor, pressure significantly influences physical structural parameters (La, Lc, d002).

Synthesis of organic petrography, core and logs to identify depositional facies and source rocks using several case studies

Greg Smith[1*], Muhammad Firdaus[1], India Sadd[1]

[1]Curtin University, Perth Australia

** Corresponding Author: gregory.c.smith@curtin.edu.au*

Studies of organic rich samples from several Mesozoic-Cenozoic basins which have core, log and seismic control indicate that organic petrography is a good indicator of depositional facies (Sadd et al., 2023; Smith, et al., 2023). This also makes organic petrography an excellent tool for source potential but is rarely used for source rock studies whereas vitrinite reflectance is the only common measurement. The results here also question the use of Rock-Eval results that indicate 2-5 wt.% TOC indicates very good source rocks.

A good model of depositional setting can be deduced by synthesis of organic petrography with core logs, downhole logs and high resolution seismic data which together allow modelling of likely extent and source rock volumes (Fig. 1). The main organic depositional facies can be identified with characteristic petrographic compositions (Diessel, 1992). Commonly six or more organic facies occur: they may include thick, humic coals developed in ombrogenous coastal plain bogs/swamps, with overall Vitrinite (V) >> Liptinite (L); and thinner coals in lower coastal plain mainly topogenous, swamps, marshes and deltas, with V > L and more mineral matter. Thinner coals also occur in upper coastal plain environments where Inertinitic (I) durain bands are more prevalent (V > I > L).

Humic coals transition laterally and vertically to sapropelic coals (Hutton, 1987; Cook and Sherwood, 1991) with OM >70% and L ≥ V, mainly deposited in floodplain lakes during drowning of peat swamps, or laterally adjacent to peat marshes around fringes of interdistributary bays. Vertically thin coals transition to coaly mudstones (OM 30-70%, V>L) developed above thin coals or splays, with extensive beds from late stage fill of localized swamps or marshes. Carbonaceous mudstones (OM 20-30%, L ≥ V) are mainly deposited in floodplain lakes, restricted interdistributary bays and back-barrier lakes, or on vegetated supra-tidal bars in distributary channels. Laminated mudstones with OM 5-10% and low Vitrinite, Liptinite and/or Inertinite (I) occur in more distal lower coastal plains or delta fronts, restricted shallow lakes and seas in rift settings.

Sapropelic coals, coaly mudstones and carbonaceous mudstones are commonly logged as mudstones by sedimentologists focused on sandstones for reservoir studies. Samples of organic rich beds are mainly taken for destructive palynological analyses, while Rock-Eval samples focus on claystones that mostly have < 5-10% OM.

Hence, the best source rocks are missed by the petroleum industry while the coal industry focuses on the humic coals. Consequently, the database for organic rich source rocks is significantly biased and potential input from organic petrologists is untapped.

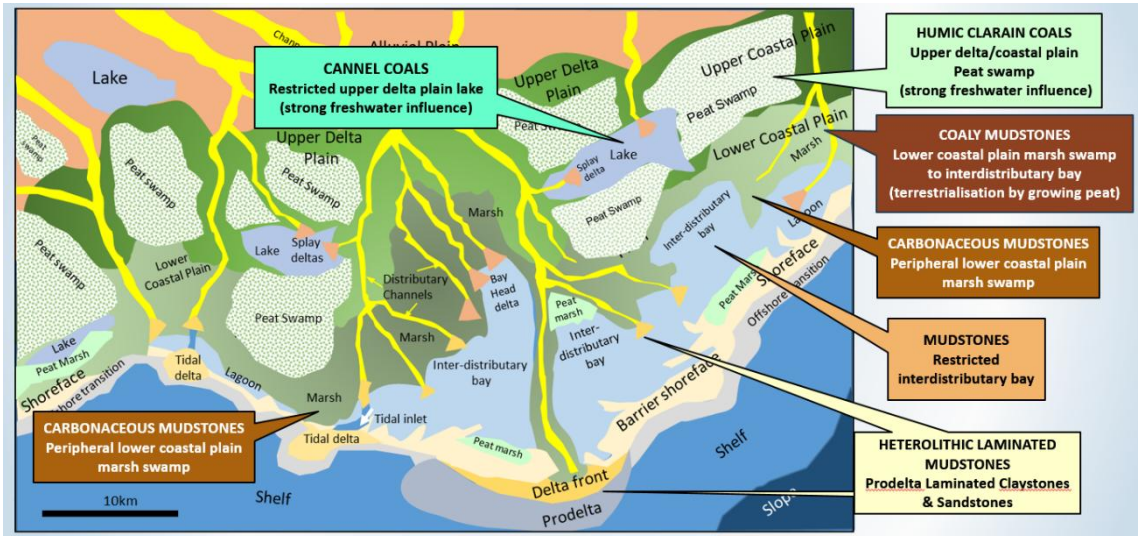

Figure 1. Schematic relationship of some organic facies to depositional facies in a lower coastal plain setting

References

Cook, A., Sherwood, N., 1991. Classification of oil shales, coals and other organic-rich rocks. Org. Geochem. 17(2), 211-222.
Diessel, C.F., 1992. Coal-bearing Depositional Systems. Springer-Verlag, Berlin, 356pp.
Hutton, A., 1987. Petrographic Classification of Oil Shales. Int. J. Coal Geol. 8(3), 203-231.
Sadd, I., Smith, G., Hanich, T., Sun, X., Minken, J., 2023. Organic Depositional Facies Control on Hydrocarbon Occurrence in the early Middle Triassic, Roebuck Basin, WA. Brisbane: Australian Society of Exploration Geophysicists.
Smith, G., Lang, S., Charles, A., Watts, C., Horan, S., Hoffman, N., 2023. Marked Depositional and Organic Facies Change across the Paleocene-Eocene in the Gippsland Basin, Australia. AEGC. ASEG. Retrieved from https://doi.org/10.5281/zenodo.7980222

The occurrence, distribution and origin of Bolsovian age splint coal in the Central Appalachian Basin, USA

Cortland F. Eble[1*]

[1] University of Kentucky, Lexington, KY, USA

** Corresponding Author: eble@uky.edu*

The Central Appalachian Basin occurs along the eastern portion of the USA, covering an area that includes southern West Virginia, SW Virginia, NE Tennessee and eastern Kentucky. Bituminous coal from this region has been mined for more than 100 years, most of which occurs as humic coal with minor occurrences of sapric coal. Splint coal has a dull luster, is extremely hard, and is equivalent to durain and mattkohle. Although bands of splint coal occur in many beds throughout the Pennsylvanian section, the lithotype is especially common in mid-Middle Pennsylvanian (Bolsovian) age coal beds that occur between the Magoffin and Stoney Fork Shale Members of eastern Kentucky. Coals in this interval are commonly >1 m thick and are important economic mining targets.

Petrographically, splint coal layers contain elevated amounts of liptinite and inertinite, commonly comprising >40 % of the mineral matter free maceral assemblage. This contrasts with brighter-appearing coal layers (e.g., clarain) that are dominated by vitrinite (commonly >70 %). Palynologically, splint coal layers contain elevated amounts of crassicingulate spore taxa (e.g., *Densosporites*, *Cristatisporites*, *Radiizonates*; sometimes referred to as "densospores"), which were produced by the subarborescent lycopsid *Omphalophloios*. Tree fern spores are also abundant and taxonomically diverse in splint coal layers. Spores and pollen representing other Pennsylvanian floral groups (e.g., calamites, cordaites, pteridosperms) are present and locally abundant. Lycospora, the dispersed spore of several large, lycopsid trees (e.g., *Lepidophloios*, *Lepidodendron*, *Paralycopodites*) occurs in reduced amounts in splint coal layers and is common to abundant in bright coal lithotypes. Geochemically, splint coal layers are typically low in ash (<10 %) and sulfur (<1 %) and have low Hardgrove Grindability Indexes (HGI <40). Inorganic partings occur frequently but are ephemeral and usually cannot be traced laterally for any great distance.

The origin of splint coal layers remains enigmatic. Early work by Rheinhardt Thiessen (1936) suggested that splint coal owed its origin to the presence and abundance of an unidentified plant that produced a "salve-shaped" microspore and a "winged" megaspore found in association with splint coal. He later considered that splint coal originated from highly degraded peat. Charles Davis (1913) suggested that biological decay could be accelerated by dry conditions, allowing for aeration of the peat acrotelm layers, or wet conditions, provided the water was oxygenated. More recent work has suggested that splint coal forms from the apex areas of domed, ombrogenous peats.

References

Thiessen, R., 1936. Splint Coal. Transactions of the Institute of Mining and Metallurgical Engineering,

Whie, D., Thiessen, R., 1913. The Origin of Coal with a chapter on the formation of peat by C.A. Davis. United States Bureau of Mines Bulletin 38.

Peat swamps in the interior of Tropical Pangea: an example from the Lower Lubná Coal (Middle Pennsylvanian), Kladno-Rakovník Basin, Czech Republic

Otto Salva[1*], Stanislav Opluštil[1], Ralf Littke[2], Thorsten Bauersachs[2], Cortland Eble[3], Ivana Sýkorová[4]

[1]Institute of Geology and Palaeontology, Faculty of Science, Charles University, Prague, Czech Republic; [2]Institute of Geology and Geochemistry of Petroleum and Coal, Energy and Mineral Resources Group, Lochnester. Aachen, Germany; [3]Kentucky Geological Survey, University of Kentucky, Lexington, KY, USA; [4]Institute of Rock Structure and Mechanics, Academy of Sciences of the Czech Republic, Prague, Czech Republic.

** Corresponding Author: salvao@natur.cuni.cz*

Four sections of the high-volatile bituminous Lower Lubná Coal (reflectance values of vitrinite between 0.62% and 0.78%; Upper Radnice Member; Middle Pennsylvanian, Bolsovian) from the Kladno-Rakovník Basin were investigated using petrological, palynological, and geochemical methods to determine peat-forming conditions in the interior of tropical Pangea. All coal profiles are dominated by the dull coal lithotype, with dull coal being abundant, banded dull coal subordinate, and banded coal represented by only a single sample. Bands of carbonaceous mudstone and mudstone are locally present. Vitrinite macerals dominate in most samples, whereas liptinite content ranges from 0 to 44.2 vol.% and inertinite from 0.8 to 84.2 vol.%. Collotelinite is the prevailing maceral within the vitrinite group (up to 92.8 vol.%), sporinite within liptinite (up to 42.3 vol.%), and fusinite and semifusinite within inertinite (up to 30.2 vol.% and 49.8 vol.%, respectively). Most samples across all profiles display high ash yields (ranging from 5.7 to 73.2 wt.%, dry basis) and high mineral contents, dominated by detrital clay minerals with minor admixtures of quartz and pyrite. Palynological analyses indicate an alternation between two dominant plant assemblages: one dominated by lepidodendrid lycopsids producing *Lycospora* and the other by subarborescent lycopsids of the genus *Omphalophloios* producing densospores. The maceral and palynological compositions align well with organic geochemical data. Molecular analyses reveal a marked predominance of methylnaphthalenes and phenanthrene over other compounds, alongside a prevalence of pristane over phytane. Together with the dominance of C29 steranes, these biomarker distributions confirm a terrestrial plant origin for organic matter. Biomass-burning-derived PAHs (e.g., pyrene, fluoranthene, methylfluoranthene) were identified, consistent with high inertinite contents, providing further evidence of wildfire activity. These characteristics indicate a peat mire subjected to alternating conditions: periods of frequent fires (marked by elevated abundances of macroscopic inertinite macerals and low inorganic input) and intervals of higher water levels (Jerrett et al., 2011) driven by flooding from nearby fluvial systems (Opluštil, 2005a, b). Petrographic indices (GWI and A/I) were utilized to conclude that most of the profiles formed in rheotrophic to mesotrophic settings. The hydrological regimes of these peat mire precursors were broadly similar to time-equivalent Bolsovian coal seams from the Ruhr Basin, Germany (Zieger and Littke, 2019), which also include ombrotrophic mires. However, while the Ruhr Basin coals formed in coastal settings within the foreland of the rising Variscan Orogen, the Lower Lubná Coal in the Kladno–Rakovník Basin (Czechia) developed in landlocked mires within the interior of tropical Pangea. The conclusion is that although the climate was humid in both regions, higher moisture availability near the sea (Ruhr Basin) favored the development of ombrogenic raised peat swamps, indicating a minor-to-moderate precipitation gradient across this part of equatorial Pangea.

Acknowledgments

This study was funded by the Grant Agency of the Charles University (grant No. 456325) and Grant Agency of the Czech Republic (Project No 25-16958S).

References

Jerrett, R.M., Flint, S.S., Davies, R.C., Hodgson, D.M., 2011. Sequence stratigraphic interpretation of a Pennsylvanian (Upper Carboniferous) coal from the central Appalachian Basin, USA. Sedimentology 58, 1180-1207.

Opluštil, S., 2005a. Evolution of the Middle Westphalian river valley drainage system in central Bohemia (Czech Republic) and it palaeogeographic implication. Palaeogeogr. Palaeoclimatol. Palaeoecol. 222, 223-58.

Opluštil, S., 2005b. The effect of paleotopography, tectonics and sediment supply on quality of coal seams in continental basins of central and western Bohemia (Westphalian), Czech Republic. Int. J. Coal Geol. 64, 173-203.

Zieger, L., Littke, R., 2019. Bolsovian (Pennsylvanian) tropical peat depositional environments: The example of the Ruhr Basin, Germany. Int. J. Coal Geol. 211, 103209.

Petrographic and geochemical analysis of burned organic matter from forest material

Magdalena Misz-Kennan[1*], Monika Kościelny[1], Monika Fabiańska[1]

[1]University of Silesia, Sosnowiec, Poland

** Corresponding Author: magdalena.misz@us.edu.pl*

Vegetation fires are widely discussed in terms of their environmental impacts, i.e., on the atmosphere and soil. Apart from large-scale fires affecting wide areas, small fires covering areas of a few tens of square meters that occur in forests, shrubs, and grass also change the macroscopic, microscopic, and chemical properties of plants. This research focuses on alterations in the geochemical and petrographic features of plants from the Włodowice forest (Poland). The collected samples comprised tree branches, pine cones, pine bark, pine branches, and moss that were subjected to wildfire. They were embedded in epoxy resin and polished blocks were prepared for microscopic investigations. Microscopic investigations revealed that plants were commonly altered to a limited degree, as reflected in reflectance measurements that, for individual samples, vary widely, sometimes from <0.1% in unaltered plants to >3.0% in pyrofusinite. The range of changes depends on the type of plants, fire temperature and its duration. Based on reflectance measurements, the fire temperature, 265-375°C, can be estimated, allowing the type of fire to be determined as ground and surface fire. The petrographic analysis also showed the dependence of fusinite transformation on the intensity of the fire. Geochemical analysis (GCMS) showed the presence of various phenol groups in the samples, mainly methoxy- and methyl groups and PAHs, mostly naphthalene, phenanthrene, anthracene, fluoranthene, pyrene, chrysene, benzo(ghi)fluoranthene and large amounts of retene. The last compound dominated in alkyl PAHs making it a useful marker of past fires, preserved in soil. Soil sample had the highest contents of fluoranthene and pyrene. PAH diagnostic ratios point out to their pyrolytic source, i.e., recent fire. Distribution of phenolic compounds, derived from thermally destructed lignin, reflect the species of a parent plant. Pine cones, wood and branches produced primarily vanillin as well as other compounds with coniferyl-type of a molecular structure. Further fractionated lignin thermal products such as p-propyl phenols and xylenols were present as minority. Syringyl structures were absent. Both phenols and PAH are considered toxic and carcinogenic, and high amounts of these compounds could negatively affect the plant development, the life of living organisms and soil properties. The geochemical analysis is needed to gain information about possible endangerment of the forest environment by noxious post-fire compounds.

77th Annual ICCP Meeting

Symposium on

Organic Petrology for a Changing World

Poster Presentations

Nanoscale chemo-mechanical heterogeneity of graptolites and its reservoir implications

Ke Wang[1*], Qian Sun[1]

[1] School of Energy Resources, China University of Geosciences, Beijing, China

** Corresponding Author: wangk2019@163.com*

Graptolites are a major organic component in many pre-Devonian marine shales and are widely regarded as important contributors to hydrocarbon generation, pore development, and fluid migration. However, the nanoscale heterogeneity of different graptolite types and its significance for organic petrology and subsurface energy applications remain poorly constrained. The granular and non-granular graptolites in the Longmaxi shale of the Sichuan Basin, China, was investigated using an integrated workflow combining optical microscopy, scanning electron microscopy, atomic force microscopy (AFM), and AFM-based infrared spectroscopy (nano-IR).

The results reveal clear chemo-mechanical differences between the two graptolite types. Granular graptolites exhibit rougher surfaces, with roughness values nearly twice those of nongranular graptolites, and commonly display a more "depressed" morphology relative to the surrounding minerals. In contrast, non-granular graptolites are smoother and mechanically stiffer. AFM modulus mapping shows that granular graptolites have lower moduli of about 9-12 GPa, whereas non-granular graptolites yield higher values of 20-24 GPa. Granular graptolites also commonly contain abundant pores and locally loose textures, suggesting stronger hydrocarbon generation and expulsion-related modification.

The nano-IR analyses further demonstrate that both graptolite types are dominated by oxygenated functional groups together with O- and N-bearing heteroatomic moieties. Granular graptolites show relatively stronger signals related to aliphatic ethers and alcohol compounds and lower CH_3/CH_2 ratios, indicating longer and more mobile aliphatic chains than in nongranular graptolites. These geochemical differences are consistent with the lower stiffness of granular graptolites and may help explain their enhanced pore development.

The results indicate that nanoscale heterogeneity among graptolite types is important for evaluating organic matter evolution, shale reservoir quality, and rock mechanical behavior. Granular graptolites may contribute more significantly to hydrocarbon generation, gas storage space, and flow pathways, whereas non-granular graptolites may play a greater role in maintaining whole-rock stiffness. This study highlights how advanced nanoscale organic petrographic characterization can improve understanding of shale gas systems and may also provide useful insights into CO_2 storage and enhanced gas recovery in organic-rich shales.

Maceral-specific molecular structural evolution during the huminite-to-vitrinite transition

Yu Liu[1*], Tengwei Gao[1], Jiayue Feng[1]

[1]College of Geoscience and Survey Engineering, China University of Mining and Technology , Beijing, China

** Corresponding Author: liuyu@cumtb.edu.cn*

The huminite-to-vitrinite transformation is a key threshold in coalification, marking the transition from biochemically dominated processes to geochemically controlled evolution. Although substantial knowledge has been gained regarding the overall huminite-to-vitrinite transition, maceral-specific transformation pathways remain poorly understood. This knowledge gap limits our understanding of the precursor materials and formation mechanisms of different vitrinite macerals. In this study, matrix lignite and xylite samples were collected, while peat, wood, cellulose, and lignin were used as comparative precursor materials. Thermal simulation experiments were conducted to simulate the transformation of huminite macerals into vitrinite macerals. Nano-FTIR spectroscopy and solid-state nuclear magnetic resonance, combined with organic petrography and reflectance measurements, were employed to characterize the molecular structural evolution and optical changes of different huminite macerals during coalification. The results indicated that xylite and highly degraded lignite converged toward similar molecular characteristics, accompanied by a marked increase in aromaticity. However, it should be noted that the molecule structural evolution pathways of different huminite macerals differ markedly. Interestingly, textinite has a lower aromatic structural content than corpohuminite, but this relationship is reversed after vitrinite formation, with telinite showing a higher proportion of aromatic structures than corpogelinite. This reversal is mainly attributed to the temperature-induced aromatization of cellulose residues in telinite. Cellulose residues mainly form molecular structures with a high proportion of aromatic components through the aromatization of carbohydrate-derived cyclic structure, whereas corpohuminite, which is primarily derived from aromatic-rich precursors, exhibits further increased aromaticity mainly through bond cleavage and loss of aliphatic structures and oxygen-containing groups. This mechanism provides explanations for the differences in reflectance and molecular structure among different vitrinite macerals and offer a potential basis for identifying cellulose-derived materials in relatively high-rank coals. These findings also help to refine the theoretical framework of vitrinite formation and evolution, while providing a more nuanced understanding of the distinct hydrocarbon-generation and pyrolysis behaviors of different vitrinite macerals.

A Silurian Oceanic Anoxic Event documented by hexavalent uranium isotopes

Zhengfu Zhao[1,2*]

[1] College of Geoscience and Survey Engineering, China University of Mining and Technology, Beijing, China; [2]Department of Geosciences and Natural Resource Management, University of Copenhagen, Copenhagen, Denmark

** Corresponding Author: zhaozf2023@gmail.com*

Marine anoxia has profoundly shaped the evolution of Earth's ecosystems, biogeochemical cycles, and climate state, yet most Phanerozoic oceanic anoxic events are commonly interpreted as consequences of greenhouse warming. Here we identify the Silurian Ireviken Biogeochemical Event (IBE; ~432–430.5 Ma) as a global marine deoxygenation event whose development and termination were closely regulated by global cooling. Using a novel anaerobic extraction technique that selectively isolates carbonate-hosted hexavalent uranium (U^{6+}_{carb}), we reconstructed the evolution of seawater uranium isotopes ($\delta^{238}U_{SW}$) from the Altajme core, Gotland, Sweden. The U^{6+}_{carb} record displays a pronounced negative $\delta^{238}U$ excursion of -0.44‰, larger than the coeval shift recorded by conventional bulk carbonate δ^{238}Ucarb (-0.30‰). The average offset between $\delta^{238}U^{6+}_{carb}$ and $\delta^{238}U_{carb}$ (-0.25 ± 0.11‰) is consistent with modern seawater–carbonate fractionation, but this offset increases during peak anoxia, indicating locally intensified reducing conditions that compromised the fidelity of conventional bulk carbonate $\delta^{238}U$ records. To quantify the timing, magnitude, and rate of marine redox change, we apply a probabilistic, physics-informed inverse U-cycle model to the $\delta^{238}U^{6+}_{carb}$ record. The results reveal a progressive expansion of anoxic seafloor area, culminating in a 10 ± 2-fold increase relative to the pre-event baseline. This expansion coincides with a positive carbonate carbon isotope excursion of ~+4‰, consistent with enhanced organic carbon burial within expanding oxygen-deficient marine environments. However, unlike many warming-driven anoxic events, the IBE was followed by global cooling, which likely increased seawater oxygen solubility and strengthened ocean ventilation. These cooling-related processes appear to have dampened further anoxic expansion and promoted the eventual recovery of marine redox conditions. Nevertheless, excess organic carbon burial persisted for an additional ~0.6 Myr after peak anoxia, indicating that the marine carbon cycle and ocean redox system remained perturbed well after the onset of climatic cooling. Our findings reveal a negative climate-redox feedback in which cooling did not initiate anoxia but regulated its later evolution by limiting the persistence and intensity of global marine deoxygenation. This provides a new perspective on how Earth's climate system can modulate, and potentially terminate, largescale oceanic anoxic events.

Aridity and polymetallic stress suppressed the terrestrial carbon sink during the T-OAE

Kai Zhou[1*]

[1] China University of Mining and Technology, Beijing, China

** Corresponding Author: zkai_cumt@163.com*

The Toarcian Oceanic Anoxic Event (T-OAE, ~183 Ma) represents a pronounced Mesozoic carbon-cycle perturbation, characterized by marine anoxia, a negative carbon-isotope excursion, and global warming. However, terrestrial ecosystem responses remain poorly constrained, and whether vegetation–climate feedbacks could amplify the crisis has not been quantitatively assessed. Here, a high-resolution multiproxy record is presented from the lacustrine succession of the Qaidam Basin (China), a mid-latitude continental basin preserving a nearly continuous T-OAE interval. The data reveal pronounced aridity, evidenced by sedimentary facies shifts and pollen assemblages, coinciding with polymetallic enrichment. Concentrations of Hg, As, Cu, Cr, Cd and Pb increase sharply at the event onset and correlate strongly with a rise in aberrant (teratological) palynomorphs (from <1% to 7.74%; Fig. 1). Additional evidence includes: a decline in silicate weathering (CIA), Hg–As enrichments with volcanogenic isotopic signatures (δ^{202}Hg), a collapse of ferns, expansion of opportunistic *Classopollis*, and increased inertinite (charcoal) indicating heightened wildfire frequency. Collectively, these observations indicate severe vegetation disruption, characterized by plant reproductive failure, loss of canopy cover, and a shift to fire-prone, species-poor landscapes. It is proposed that this ecological disruption acted as a positive feedback on the carbon cycle. Aridity directly weakened the silicate-weathering carbon sink, while metal toxicity (especially As and Cu) impaired plant reproduction and reduced biological weathering. Simultaneously, accumulated dead biomass and increased fire activity promoted oxidative release of terrestrial organic carbon. Mass-balance modelling suggests that, if this mechanism operated regionally, the Qaidam Basin alone could have released an additional 80–83 Gt C to the atmosphere. This extra carbon flux would have shortened the T-OAE carbon-cycle anomaly by 0.3–2.0 kyr, assuming constant volcanic CO_2 input. The results demonstrate that a single mid-latitude continental basin can measurably modulate global carbon-cycle dynamics during a major environmental crisis. Whether such terrestrial feedbacks were globally significant requires similarly high-resolution records from other continental basins.

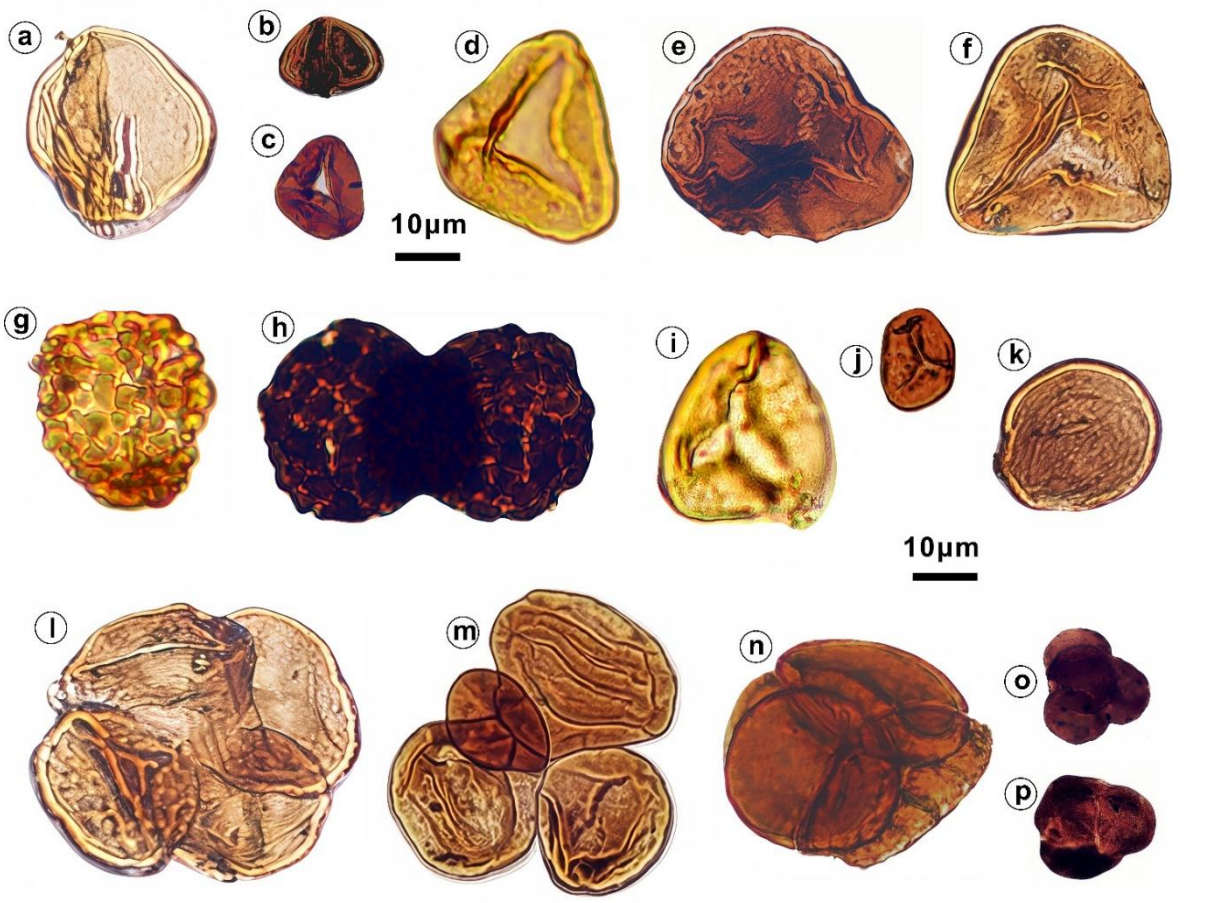

Figure 1. Selection of normal and teratological spores and pollen grains from the Dameigou section. Scale bar for all images is 10 µm. a, *Cyathidites*, normal. b, c, Dwarfed *Cyathidites*. d, *Cyathidites, normal*; e, f, Aberrant Cyathidites spores, with deformed trilete leasurae. g, *Leptolepidites*, normal. h, Conjoined *Leptolepidites* spores. i, *Deltoidospora*, normal. j, Dwarfed Deltoidospora. k, *Classopollis annulatus*, normal. l, *Classopollis* tetrad, normal. m, Asymmetrical deformed *Classopollis annulatus* tetrad with one underdeveloped grain and three normal-sized, larger, spores. n, Asymmetrical *Classopollis annulatus* tetrad with three underdeveloped spores. o, p, Fused small-sized *Classopollis* tetrads.

Revisiting Marlies Teichmüller's bituminite concept in coals: a CLSM-based re-evaluation

Jolanta Kus[1], Martin Blumenberg[1], Georg Scheeder[1]

[1]Federal Institute for Geosciences and Natural Resources (BGR), Hannover, Germany

* *Corresponding Author: J.Kus@bgr.de*

In the 1970s, Marlies Teichmüller, a pioneering German coal and organic petrologist, introduced the concept of bituminite as a coal maceral to describe its unfigured and "amorph" outline. For decades, Teichmüller's definition served as the standard framework for the identification of bituminite in coals.

However, with the advent of advanced analytical techniques – such as confocal laser scanning microscopy (CLSM) – the traditional boundaries of the bituminite concept have been extended. This study reveals that what Marlies Teichmüller classified as bituminite in coals exhibits high optical and spectral variability. Consequently, research by the ICCP as well as the Identification of Dispersed Organic Matter Working Group (IDOM WG) has highlighted the need to revisit the nomenclature of bituminite and refine the generic model related to its origin and optical properties.

This study provides a CLSM-based re-evaluation of Marlies Teichmüller's "bituminite in coal" concept within the framework of CLSM application. Coal petrographic observations challenge the view of bituminite as bearing no clear indication of its organic precursors. Instead, microscopic identification and spectral profiles strongly indicate its existence as a genetic and optical continuum. This continuum ranges from well-defined sporinite – and to a lesser extent, cutinite and resinite – through degraded and altered sporinite, to entirely unfigured bituminite. This transition from mainly structured sporinite to unfigured bituminite represents a progressive loss of structural integrity driven by degradation within the peat-forming environment and by transformation during the in-situ hydrocarbon generation stage.

The advancement of both processes towards altered sporinite and ultimately unfigured bituminite with formation of exsudatinite induces a systematic shift in spectral properties (Fig. 1). In parallel, the emission intensity varies greatly. The degradation-driven changes reflect the breakdown of highly fluorescent structural units and the accumulated oxygenated functional groups. Transformation-related generation of liquid hydrocarbons acting as chemical quenchers dissipate the CLSM-related excitation energy non-radiatively. As this quenching occurs inside altered sporinite and unfigured bituminite, the generated hydrocarbons can be expelled and begin to be absorbed by micro-porosity of adjacent vitrinite macerals and start also to bleed out into micro-fractures and form exsudatinite. Unlike marine shales, the coals studied herein did not generate secondary solid bitumen other than exudatinite during transformation.

Ultimately, this work presents organic petrological and organic geochemical data and bridges the gap between classic and modern coal petrology, honoring Teichmüller's legacy while updating her concept for the current state of geoscientific research.

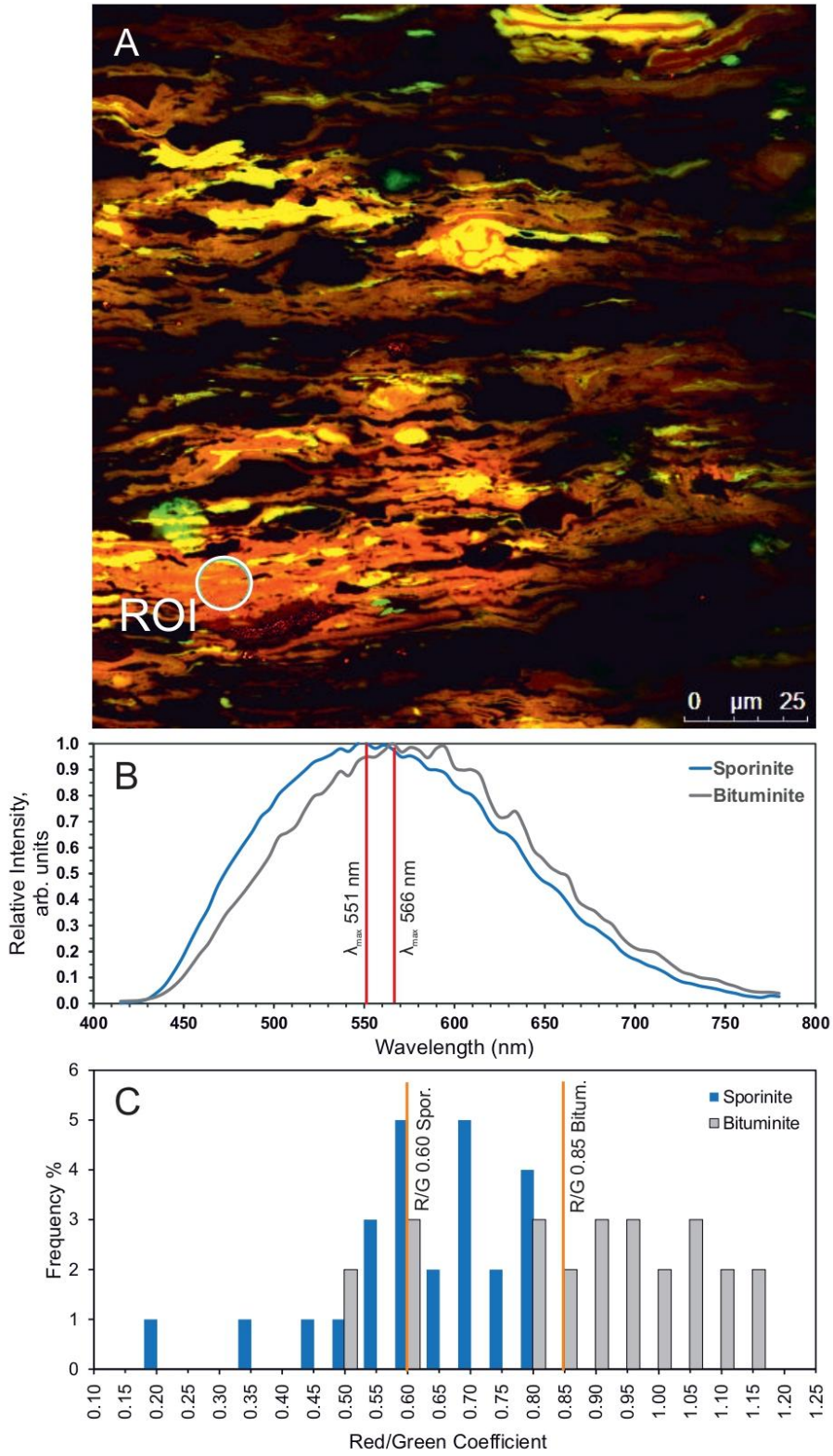

Figure 1 . CLSM-based data for Fröhn well, Saarland region, Germany. A – Confocal laser scanning microscopy (CLSM) images of bituminite and sporinite. B – Averaged emission spectra of bituminite and sporinite. C – Frequency distribution histograms of Red/Green coefficient for bituminite and sporinite.

Semantic segmentation for identification of coal macerals and mineral matter

Na Xu[1*]

[1]China University of Mining and Technology, Beijing, China

** Corresponding Author: xuna1011@gmail.com*

Coal macerals and mineral matter are important for coal petrographic analysis and quantitative evaluation. In recent years, deep learning methods have made great progress in identifying coal macerals, while research on mineral matter recognition remains insufficient (Xu et al., 2025). Besides, mineral matter is prone to being misclassified as certain coal macerals in microscopic images (Xu et al., 2026). Its occurrence and distribution also differ greatly across various coalfields, which raises additional challenges for automatic identification (Dai et al., 2016). Therefore, it is necessary to develop an effective model for the joint identification of coal macerals and mineral matter. In this study, a pixel-level annotated dataset of coal microscopic images was established, and an enhanced SegFormer-based semantic segmentation model, termed ECSegFormer, was proposed. An edge enhancement module and a color attention module were further introduced to improve boundary representation and the discrimination of visually similar categories. Experimental results show that ECSegFormer achieved good performance in the identification of coal macerals and mineral matter, especially in boundary-complex regions and sparse small-target areas. Compared with some state-of-the-art models, ECSegFormer showed superior overall performance. In addition, comparison with the traditional point-counting method further confirms its reliability for quantitative analysis. These results indicate that ECSegFormer provides an effective technical approach for the automatic identification and quantitative analysis of coal macerals and mineral matter in coal microscopic images.

References

Dai, S., Liu, J., Ward, C.R., Hower, J.C., French, D., Shaohui Jia, S., Hood, M.M., Trent M. Garrison, T.M., 2016. Mineralogical and geochemical compositions of Late Permian coals and host rocks from the Guxu Coalfield, Sichuan Province, China, with emphasis on enrichment of rare metals. Int. J. Coal Geol. 166, 71-95.

Xu, N., Wang, Q., Li, P., Kong, J., Li, Q., Engle, M.A., Hower , J.C., Wei Zhu, W., 2025. Intelligent identification of coal macerals using improved semi-supervised semantic segmentation methods. Int. J. Coal Geol. 300, 104712.

Xu, N., Jiao, F., Hower, J.C., Wang, Q., Li, P., Wang, Y., Zhu, W., 2026. An improved U-net model for the identification of coal macerals. Int. J. Coal Prep. Util., 1-20.

Assessment of fossil fuels-derived contaminants in soils from a protected area in the Portuguese coast (Cabo Mondego)

Fernando Michels[1*], Maria Helena Henriques[1], Joana Ribeiro[2]

[1]University of Coimbra, Geosciences Centre, Coimbra, Portugal; [2]University of Coimbra, Dom Luiz Institute, Coimbra, Portugal

* *Corresponding Author: fernandohmichels@gmail.com*

Cabo Mondego (central Portugal) is nationally and internationally recognized for its geodiversity and geoheritage, and it is designated as a Natural Monument of Portugal. The area of Cabo Mondego also encompasses a history of potentially contaminating activities associated with long-term coal mining and industrial operations that used fossil fuels. The industrial activities in Cabo Mondego were principally focused on cement and lime production and, over time, also included the manufacture of glass, bricks, tiles, ceramics, and coal coke briquettes, all of which operated using high-temperature ovens fueled by fossil fuels. This study aims to evaluate the quality of soil in the Cabo Mondego area through petrographic analysis for identification of type and source of fossil fuels-derived particles. The petrographic analysis was conducted on polished pellets prepared from soil samples. A LEICA DM750P microscope equipped with reflected white light and with a 50× immersion oil objective was used. The nomenclature established by the International Committee of Coal and Organic Petrology (ICCP, 1998; 2001; Sýkorová et al., 2005; Pickel et al., 2017) and the classification systems proposed by Ligouis et al. (2005), Crelling et al. (2006), and Suárez-Ruiz et al. (2017) regarding anthropogenic organic particles and coal combustion-derived particles were applied. The quantitative analysis of organic particles was conducted by point-counting. The petrographic analysis was conducted at the University of Coimbra. The contaminant particles identified in soil included, principally, coal, coke, and char, followed by smaller amounts of agglomerates of fine particles, iron-rich spheres, and charcoal. Different types of coals were identified, including the local coal exploited in Cabo Mondego. The observed coke particles are characterized by predominantly banded and/or granular internal textures. The char particles exhibit vesiculate structure and dense particles, some of which show optical anisotropy. Samples collected in proximity to the industrial complex contain a significantly higher quantity of combustion-derived particles (coke and char) that decrease towards more distant areas. This distribution suggests that these anthropogenic particles were likely emitted as airborne contaminants through stack emissions from the industrial complex. The distribution of coal particles exhibits a distinct pattern compared to that of combustion-derived particles and is attributed to the coal handling and transport associated with both mining and industrial operations. The distribution of charcoal particles is likely associated with forest fires since they were identified in samples collected at greater distances from the industrial complex.

Acknowledgements
The author F. Michels acknowledges the financial support from FCT: scholarship 2021.06231.BD.

References

Crelling, J., Glikson, M., Huggett, W., Borrego, M.A.G., Hower, J., Ligouis, B., Mastalerz, M., Misz, M., Suárez-Ruiz, I., Valentim, B., 2006. Atlas of anthropogenic particles. In M. Mastalerz & J.C. Hower (Eds.), International Committee for Coal and Organic Petrology and Indiana Geological Survey (CD-ROM).

ICCP, International Committee for Coal and Organic Petrology, 1998. The new vitrinite classification (ICCP System 1994). Fuel 77, 349-358.

ICCP, International Committee for Coal and Organic Petrology, 2001. The new inertinite classification (ICCP system 1994). Fuel 80, 459-471.

Ligouis, B., Kleineidam, S., Karapanagioti, H.K., Kiem, R., Grathwohl, P., Niemz, C., 2005. Organic petrology: a new tool to study contaminants in soils and sediments. In: E. Lichtfouse, S. Dudd, D. Robert (Eds.), Environmental chemistry. Green Chemistry and Pollutants in Ecosystems. Springer, Berlin, pp. 89-98.

Pickel, W., Kus, J., Flores, D., Kalaitzidis, S., Christanis, K., Cardott, B.J., Misz-Kennan, M., Rodrigues, S., Hentschel, A., Hamor-Vido, M., Crosdale, P., Wagner, N., ICCP, 2017. Classification of liptinite – ICCP system 1994. Int. J. Coal Geol. 169, 40-61.

Suárez-Ruiz, I., Valentim, B., Borrego, A.G., Bouzinos, A., Flores, D., Kalaitzidis, S., Malinconico, M.L.; Marques, M., Misz-Kennan, M., Predeanu, G., Montes, J.R., Rodrigues, S., Siavalas, G., Wagner, N,. 2017. Development of a petrographic classification of fly-ash components from coal combustion and co-combustion. (An ICCP Classification System, Fly-Ash Working Group – Commission III). Int. J. Coal Geol. 183, 188-203.

Sýkorová, I., Pickel, W., Christanis, K., Wolf, M., Taylor, G.H., Flores, D, 2005. Classification of huminite – ICCP system 1994. Int. J. Coal Geol. 62, 85-106.

Optical microscopy for biochar characterization: insights into reflectance, composition and methodological considerations

Konrad Ziemianin[1*]

[1]Oil and Gas Institute - National Research Institute, Kraków, Poland

* *Corresponding Author: ziemianin@inig.pl*

Biochar, a carbon-rich product of biomass pyrolysis, has gained increasing attention due to its applications in carbon sequestration, soil improvement, environmental remediation and industrial processes. Optical microscopy provides valuable information on biochar morphology, porosity and the degree of thermal transformation of individual particles. Nevertheless, studies utilizing microscopic data for biochar characterization remain relatively scarce. In recent years, increasing attention has been paid to the use of reflected-light microscopy and reflectance measurements as proxies for biochar stability and carbon permanence (Petersen et al., 2023; Chiaramonti et al., 2024; Rudra et al., 2024; Sanei et al., 2024; Mastalerz et al., 2025). Existing studies commonly employ approximately 500 reflectance measurements per sample, whereas 200 measurements have been proposed as a minimum recommendation (Mastalerz et al., 2023, 2025). A reflectance value of 2.0% is currently considered a threshold separating reactive and non-reactive biochar fractions (Sanei et al., 2024; Mastalerz et al., 2025).

The aim of this study was to evaluate the applicability of reflected-light optical microscopy for biochar characterization, with particular emphasis on reflectance analysis, compositional assessment and methodological optimization. Biochar samples produced from straw and sawdust were obtained through pyrolysis at temperatures of 500, 550, 600, and 650°C. Polished blocks were examined using reflected-light microscopy under oil immersion. The variability of reflectance (Fig. 1), the representativeness of subsamples, the influence of grain-size fractions and the effect of the number of measurements on analytical reliability were investigated.

The results demonstrate a systematic increase in mean reflectance with increasing pyrolysis temperature, reflecting the progressive carbonization of biomass. All samples exhibited pronounced heterogeneity, with reflectance values ranging from approximately 0.1% to over 4%. A key methodological outcome is the determination that at least 350 reflectance measurements are required to obtain stable and reproducible results. Grain-size effects were found to significantly influence analytical outcomes, particularly in sawdust-derived biochars, where the coarsest fractions contained disproportionately high amounts of less transformed material and could not be considered representative.

The integration of morphological observations with reflectance-based classification of reactive and non-reactive fractions enables a more comprehensive assessment of biochar properties and stability. The results demonstrate the considerable potential of optical microscopy as a practical tool for biochar characterization.

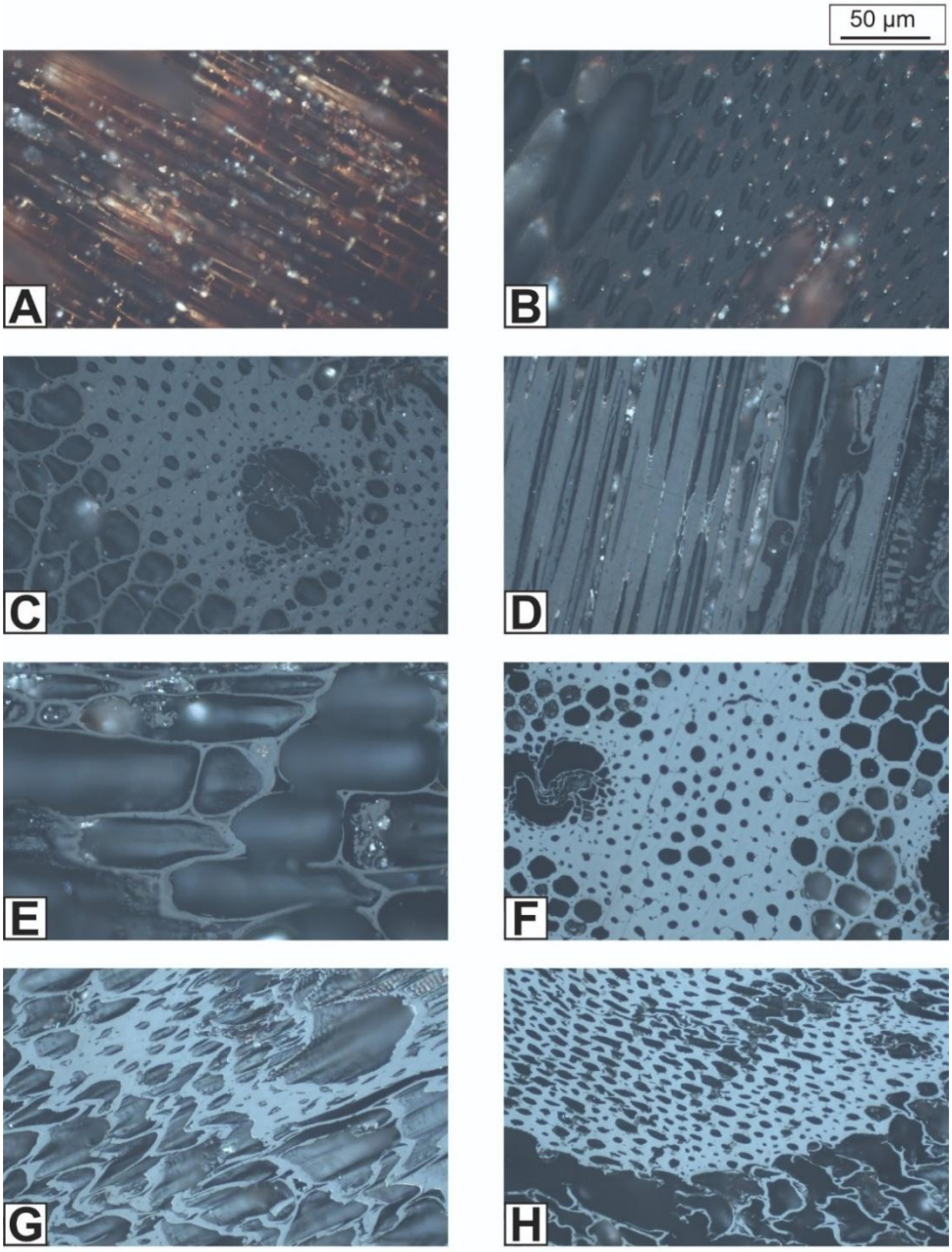

Figure 1. Examples of variability in the degree of carbonization among biochar fragments derived from straw (pyrolysis temperature: 500°C). A: fragment at an early stage of transformation; B: R_o = 0.28%; C: R_o = 0.69%; D: R_o = 0.93%; E: R_o = 1.19%; F: R_o = 1.81%; G: R_o = 2,14%; H: R_o = 2.26%.

References

Chiaramonti, D., Lotti, G., Vaccari, F.P., Sanei, H., 2024. Assessment of long-lived carbon permanence in agricultural soil: Unearthing 15-year-old biochar from a long-term field experiment in a vineyard. Biomass and Bioenergy 191, 107484.

Mastalerz, M., Drobniak, A., Briggs, D., Bradburn, J., 2023. Variations in microscopic properties of biomass char: Implications for biochar characterization. Int. J. Coal Geol. 271, 104235.

Mastalerz, M., Drobniak, A., Liu, B., Sauer, P.E., 2025. Reflectance as an indicator of biochar permanence. Int. J. Coal Geol. 306, 104809.

Petersen, H.I., Lassen, L., Rudra, A., Nguyen, L.X., Do, P.T.M., Sanei, H., 2023. Carbon stability and morphotype composition of biochars from feedstocks in the Mekong Delta, Vietnam. Int. J. Coal Geol. 271, 104233.

Rudra, A., Petersen, H.I., Sanei, H., 2024. Molecular characterization of biochar and the relation to carbon permanence. Int. J. Coal Geol., 291,104565.

Sanei, H., Rudra, A., Przyswitt, Z.M.M., Kousted, S., Sindlev, M.B., Zheng, X., Nielsen, S.B., Petersen, H.I., 2024. Assessing biochar's permanence: An inertinite benchmark. Int. J. Coal Geol. 281, 104409.

Decoding primary and recycled organic-matter signals in Middle Jurassic fine-grained deposits of the Pieniny Klippen Belt, Western Carpathians

Magdalena Zielińska[1*], Jolanta Kus[2], João Graciano Mendonça Filho[3], Ewa A. Szram[1], Martin Blumenberg[2], Monika Fabiańska[1]

[1]University of Silesia in Katowice, Faculty of Natural Sciences, Institute of Earth Sciences, Sosnowiec, Poland; [2]Federal Institute for Geosciences and Natural Resources (BGR), Hannover, Germany; [3]Laboratório de Palinofácies & Fácies Orgânica, Rio de Janeiro, Brazil

* *Corresponding Author: magdalena.zielinska@us.edu.pl*

The Middle Jurassic fine-grained deposits of the Szlachtowa Formation in the Pieniny Klippen Belt, Western Carpathians, have long been regarded as a key archive for reconstructing Jurassic sedimentation along the northern Tethyan margin. However, their organic-matter record is complicated by mixed provenance, reworking, variable preservation, and subsequent compressional deformation and tectonic imbrication of the Pieniny Klippen Belt. This study demonstrates how integrated organic petrology, fluorescence microspectrometry, palynofacies, Rock-Eval pyrolysis, and biomarker geochemistry can separate primary depositional signals from recycled organic components in a structurally complex orogenic Carpathian belt.

The most critical petrographic result is the recognition of several optically and genetically distinct vitrinite populations, including first-cycle vitrinite, phyllovitrinite, and recycled vitrinite. This distinction is essential for robust thermal maturity assessments, as undifferentiated vitrinite measurements would obscure the true thermal signal. First-cycle vitrinite indicates thermally mature organic matter, with random vitrinite reflectance ranging from 0.65% to 0.81%. The organic assemblage is dominated by terrigenous Type III kerogen, whereas marine Type II components, represented mainly by lamalginite and dinoflagellate cysts, occur subordinately. Fluorescence spectra show that lamalginite and dinoflagellate cysts have similar λmax values and red/green quotients, suggesting comparable fluorescence behaviour of these marine liptinite components. However, differences between measured spectral parameters and maturity estimates derived from them indicate that fluorescence-based maturity proxies should be interpreted with regard to organic facies and maceral composition.

Palynofacies are dominated by phytoclast groups rather than amorphous organic matter or marine palynomorphs, indicating strong terrigenous supply to a marine depositional system. Reworked, oxidized, and fragmented organic particles point to erosion of older sedimentary successions and recycling of organic matter into Middle Jurassic deposits. This recycled component, together with indigenous terrestrial and subordinate marine organic matter, records sediment redistribution from shelf and slope areas into deeper-water depositional settings. The data support deposition under predominantly heterolithic oxic shelf and dysoxic–suboxic shelf-to-basin transitional conditions, controlled by synsedimentary extensional tectonics, unstable slopes and fault-bounded blocks, with the Czorsztyn Ridge acting as a palaeogeographic high that modulated sediment supply and basinward redistribution.. Although these fine-grained deposits contain thermally mature organic matter, their low to fair generative potential is consistent with mineral dilution and strong terrigenous input, as indicated by low Hydrogen Index values, phytoclast-dominated palynofacies, subordinate amorphous organic matter and the common occurrence of fragmented or oxidized particles. The study shows that, in tectonically disrupted fine-grained successions, organic petrology is not only a thermal maturity tool but a critical approach for distinguishing depositional, recycled and post-depositional organic-matter signals.

Organic petrology and biomarker constraints on peat formation in the Upper Eocene Nikolaevo deposit (Central Bulgaria)

Alexander Zdravkov[1*], Reinhard F. Sachsenhofer[2], Johannes Weitz[2], David Misch[2], Dimitar Dimitrov[1], Valentin Kabadiyski[1], Stoyan Stoyanov[1], Bogomil Zlatkov[1]

[1] University of Mining and Geology, Sofia, Bulgaria; [2]Montanuniversität Leoben, Leoben, Austria

** Corresponding Author: alex_zdravkov@mgu.bg*

Carbonaceous mudstone and coal samples from the Upper Eocene Nikolaevo deposit in Central Bulgaria were studied for their organic petrological and geochemical characteristics. The samples are characterized by vitrinite reflectance in the range 0.51 – 0.71 % (avg. 0.61 %) and comparable maceral composition with dominant vitrinite (avg. 94.7 vol. %), low to moderate liptinite (avg. 4.2 vol. %), and very low inertinite (avg. 1.1 vol. %). Detrovitrinite (mostly vitrodetrinite) constitutes, on average, 68.3 vol. % of the organic matter. Lenticular highly gelified collotelinite (avg. 14.4 vol. %), similar to leaf-derived vitrinite associated with cutinite and locally fluorinite (i.e., phyllo-vitrinite; avg. 2.6 vol. %), is commonly detected. Gelovitrinite, mostly occurring as corpogelinite infillings in collotelinite and/or suberinite, is widely present, constituting on average 9.3 vol. %. Sporinite, liptodetrinite, and cutinite are the most abundant liptinite macerals, whereas resinite and alginite are rare. Primary and secondary roots (suberinite) are common, but the amounts are low (up to 2.9 vol. %). In many samples, the primary roots display semi-fusinized cell walls. Apart from that, inertinite is almost exclusively represented by funginite (up to 1.7 vol. %).

The extractable organic matter is dominated by asphaltenes (avg. 66 %) and polar compounds (avg. 26 %). The aliphatic fractions consist of *n*-alkanes, varying amounts of phyllocladane/abietane-type diterpenoids, and non-hopanoid triterpenoids (Di-/(Di-+Tri-)-terpenoid ratio = 0.07 – 0.98), and minor concentrations of steranes and hopanes. In all samples, the *n*-alkane distributions are dominated by mid- (C_{21}-C_{25}) and/or long chain (C_{26}-C_{31}) homologues. Notably, several samples are characterized by a maximum at either *n*-C_{22} or *n*-C_{26}, indicating periods of high-standing water table and a reducing depositional environment. The aromatized counterparts of the diterpenoids and the non-hopanoid triterpenoids dominate the aromatic fractions.

High ash yields (avg. 56 %, db) and moderate- to high sulfur contents (avg. 2.7 %, db) argue for peat accumulation within a low-lying mire with abundant siliciclastic input. Considering the petrographic and geochemical characteristics of the organic matter, peat formation most likely occurred in a waterlogged fen-type environment, vegetated predominantly with aquatic macrophytes and herbaceous/bushy angiospermous plants. Conifer plants likely existed around the mire margins or in tree islands within the mire and contributed leaf litter and/or heavily humified tissues.

Measured vitrinite reflectance and biomarker ratios argue for a transition from low- to medium rank of the studied coals.

Acknowledgements
Financial support from the Bulgarian National Science Fund through the bilateral project KP-06-Austria/2 and from ÖeAD through the project WTZ Bulgaria ("2025_BG") is greatly acknowledged.

Climatically driven change of the peat-forming environments during the Eocene to Pliocene on the territory of Bulgaria: insights from organic petrology and biomarker analysis

Alexander Zdravkov[1*]

[1]University of Mining and Geology, Sofia, Bulgaria

** Corresponding Author: alex_zdravkov@mgu.bg*

Petrographic and biomarker data from thirteen Bulgarian coals (Middle Eocene –Pliocene) document a long-term shift from angiosperm-dominated minerotrophic mires during the Eocene – Early Oligocene to gymnosperm-dominated forested mires during the Late Oligocene and Neogene. The Middle Eocene to Early Oligocene coals from Suhostrel, Burgas, Nikolaevo, and Pirin deposits are characterized by vitrinite-rich assemblages dominated by detrovitrinite. The poor tissue preservation reflects major input from herbaceous and shrubby angiosperm vegetation. Biomarkers display abundant long-chain *n*-alkanes and diverse angiosperm-derived triterpenoids. Diterpenoids occur in subordinate amounts and indicate limited conifer input. Peat accumulation took place in hydrologically active, meso- to rheotrophic fens with fluctuating redox conditions and often significant siliciclastic input. The warm and humid Eocene-Early Oligocene climate likely favored groundwater inflow, nutrient availability, and high angiosperm productivity. In the Late Oligocene Pernik and Bobov Dol deposits, the coals exhibit high proportions of telohuminite, extensive gelification, and abundant resinite, consistent with the predominance of woody, resin-rich gymnosperm vegetation. Biomarker assemblages are dominated by phyllocladane-, abietane-, and pimarane-type diterpenoids, whereas the concentrations of angiosperm-derived triterpenoids are greatly reduced. Peat accumulated in topogenous, waterlogged mires under mostly reduced and acidic conditions, and low nutrient availability. The global cooling and decline in atmospheric CO_2 during the Oligocene likely altered hydrological and nutrient cycling regimes, thereby promoting the development of densely forested, conifer-dominated mires.

The petrographic and biomarker characteristics of the Miocene–Pliocene Maritsa-East, Maritsa-West, Elhovo, Sofia, Beli Breg, Stanyantsi, Chukurovo, and Karlovo lignites indicate the establishment of mixed plant communities. Diterpenoid-rich biomarker profiles and persistent resinite indicate continued predominance of gymnosperms, although increasing abundances of angiosperm-derived triterpenoids suggest a progressively greater contribution from angiosperm vegetation. Locally (e.g., the Maritsa-West and Stanyantsi deposits), more minerotrophic conditions and/or higher pH favored angiosperm-dominated plant communities. Peat formation occurred in mesotrophic, low-lying mires with variable acidity, episodic flooding, and more pronounced seasonal water table fluctuations. These settings likely reflect the combined influence of a cooler, more seasonal Neogene climate and the tectonic evolution of the graben basins, which facilitated the development of poorly drained, locally nutrient-limited peatlands. The results indicate a major ecological change of the peat-forming environments during the Cenozoic transition from a global greenhouse to an icehouse setting. The observed changes in plant communities were likely driven by shifts in hydrology and nutrient availability associated with long-term atmospheric CO_2 decline and increasing climatic seasonality, particularly water-table stability.

Acknowledgements
Financial support from the Bulgarian National Science Fund through projects KP-06-H64/5 and KP-06-Austria/2 is greatly acknowledged.

Bioindicative and phytoremediation potential of *Spirodela polyrhiza* (L.) Schleid. in the presence of coal mine slurry

Zbigniew Jelonek[1*], Zdzisława Romanowska-Duda[2], Iwona Jelonek[1], Casey Woźniak[2]

[1]University of Silesia, Faculty of Natural Sciences, Institute of Earth Science, Katowice, Poland; [2]University of Lodz, Faculty of Biology and Environmental Protection, Department of Plant Ecophysiology, Lodz , Poland

** Corresponding Author: zbigniew.jelonek@us.edu.pl*

The management of post-mining coal waste, including sludge and slurry, presents a significant environmental challenge; however, these materials offer substantial potential as secondary raw materials and agricultural fertilizers due to their rich mineral content. This study aims to evaluate the fertilizer potential and associated environmental risks of post-mining coal sludge by utilizing the aquatic macrophyte *Spirodela polyrhiza* (L.) Schleid. as a bioindicator and phytoremediation agent.

An experiment was conducted over 10 days, cultivating *Spirodela polyrhiza* in aqueous media supplemented with coal sludge at concentrations ranging from 100 to 500 mg/100 ml. The study employed a multidisciplinary approach, including X-ray fluorescence (XRF) spectrometry for the physicochemical characterization of the waste and plant dry matter, macroscopic growth tracking via frond proliferation, and physiological assessments measuring the chlorophyll content index (SPAD) and photosystem II efficiency through chlorophyll fluorescence. Furthermore, petrographic microscopic analysis was performed to identify cytological and histological adaptations.

XRF analysis revealed that the addition of sludge significantly altered the elemental profile of the plant biomass, increasing the total elemental content by an average of 140%. Notably, the plants exhibited active transport and high bioaccumulation of essential macronutrients, demonstrating a threefold increase in calcium oxide, a more than twofold increase in phosphorus, and a fivefold increase in sulfur. Additionally, there was a fifty-fold increase in the accumulation of trace elements like zinc and cadmium, confirming the plant's excellent phytoremediation capabilities.

Growth dynamics indicated a distinct, non-linear stimulatory effect, with the optimal concentration identified at 400 mg/100 ml, yielding the highest frond count and demonstrating a significant positive correlation with the applied sludge dose. Similarly, the SPAD index reached its maximum at this concentration, reflecting enhanced pigment synthesis without functional disturbances to the photosynthetic apparatus. This was corroborated by stable chlorophyll fluorescence values across all experimental variants, indicating an absence of physiological stress. Microscopic observations further confirmed the positive biological response: plants cultivated with sludge developed larger, more uniform cell with thicker walls and a much more compact tissue structure compared to the control group.

Petrographic evidence of lipid impregnation in vitrinites as the control on the ultra-high fluidity of the Barro Branco coal seam (Paraná Basin, Brazil)

Bruno Deves Flores[1], Angeles Gomez Borrego[2], Anderson Azevedo Agra[3], Guilherme Liziero Ruggio da Silva[4], Antônio Cezar Faria Vilela[1], Eduardo Osório[1*]

[1]Universidade Federal do Rio Grande do Sul, Porto Alegre, Brazil; [2]Instituto de Ciencia y Tecnología del Carbono (INCAR-CSIC), Oviedo, Spain; [3]Tecnored, Pindamonhangaba, Brazil; [4]Gerdau Ouro Branco, Ouro Branco, Brazil

** Corresponding Author: eosorio@ufrgs.br*

The Barro Branco coal seam (Rio Bonito Formation, Lower Permian, Paraná Basin, southern Brazil) exhibits one of the most extreme thermoplastic behaviors reported for bituminous coals (Flores et al., 2020). This study combines petrographic, geochemical, and rheological analyses to demonstrate that this anomalous behavior is controlled by perhydrous vitrinites formed through lipid impregnation of vitrinite precursors during early diagenesis. A beneficiated Barro Branco coal (HV-BC; high-volatile A bituminous, R_r = 0.84%) was compared with three coking coals, including an iso-rank Appalachian coal (HV-US; R_r = 0.85%).

Despite identical rank, the two high-volatile coals differ profoundly. HV-BC plots above the humic coal band in the van Krevelen diagram (atomic H/C = 0.83; O/C = 0.027), the diagnostic signature of perhydrous vitrinites (Kalkreuth et al., 2004, 2010). Fluorescence spectral analysis of collotelinite reveals well-defined emission maxima between 500 and 650 nm in HV-BC, whereas the iso-rank reference is nearly non-fluorescing; this contrast cannot be explained by rank and is interpreted as secondary fluorescence resulting from lipid impregnation (Teichmüller and Durand, 1983; Lin and Davis, 1988). Exsudatinite filling fusinite cell lumens further documents the migration of lipid-derived compounds during coalification. These features are attributed to anaerobic, marine-influenced lagoon-barrier palaeomires with restricted drainage, where bacterial reworking of algal, spore, and cuticular material enriched the huminite precursors in hydrogen.

N-methyl-2-pyrrolidone (NMP) extraction quantified the lipid-derived molecular phase (Given, 1984) at 34.9% daf in HV-BC, the highest among the coals studied. This molecular phase governs the anomalous rheology: HV-BC reaches a Gieseler maximum fluidity of 168,308 ddpm over an exceptionally wide plastic range (146 °C vs. 82 °C for HV-US), while removal of the NMP-soluble fraction collapses fluidity by nearly two orders of magnitude (to 3,586 ddpm) and shifts the devolatilization onset from 335 to 411°C. The excess fluidity degrades coke quality, producing a high proportion of oversized and irregular pores (74% of porous area) that correlates inversely with drum strength (R^2 = 0.89).

The petrographic identification of perhydrous vitrinites, reflectance suppression, secondary fluorescence, and exsudatinite, thus provides a predictive tool for anticipating extreme thermoplastic behavior. Beyond conventional blending, the large molecular phase of such coals makes them natural sources of high-fluidity binder phases for briquettes combining coal and biomass-based carbon, broadening the contribution of organic petrology to low-carbon ironmaking in a changing world.

References

Flores, B.D., Agra, A.A., Gums, A., da Silva, G.L.R., Osório, E., Vilela, A.C.F., 2020. Thermoplastic interaction of ultra-high fluidity Brazilian coal with components of blends. J. Mater. Res. Technol. 9, 2737–2743.

Given, P.H., 1984. An essay on the organic geochemistry of coal. In: Gorbaty, M.L., Larsen, J.W., Wender, I. (Eds.), Coal Science, vol. 3. Academic Press, New York, pp. 65–339.

Kalkreuth, W., Sherwood, N., Cioccari, G., Corrêa da Silva, Z., Silva, M., Zhong, N., Zufa, L., 2004. The application of FAMM (Fluorescence Alteration of Multiple Macerals) analyses for evaluating rank of Paraná Basin coals, Brazil. Int. J. Coal Geol. 57, 167–185.

Kalkreuth, W., Holz, M., Mexias, A., Balbinot, M., Levandowski, J., Willett, J., Finkelman, R., Burger, H., 2010. Depositional setting, petrology and chemistry of Permian coals from the Paraná Basin: 2. South Santa Catarina Coalfield, Brazil. Int. J. Coal Geol. 84, 213–236.

Lin, R., Davis, A., 1988. The chemistry of coal maceral fluorescence: with special reference to the huminite/vitrinite group. The Pennsylvania State University, Special Research Report, University Park, PA.

Teichmüller, M., Durand, B., 1983. Fluorescence microscopical rank studies on liptinites and vitrinites in peats and coals, and comparison with results of the Rock-Eval pyrolysis. Int. J. Coal Geol. 2, 197–230.

Petrography of the ferrospheres from Talcher coal ash (Angul district, Odisha, India)

Bruno Valentim[1,2*], Bibhuranjan Nayak[3], Sónia Pereira[1,2], Nilima Dash[3], Alexandra Guedes[1,2], Sasmita Prusty[3]

[1]Faculdade de Ciências da Universidade do Porto, Porto, Portugal; [2]Instituto de Ciências Terra - Pólo Porto, Porto, Portugal; [3]CSIR-Institute of Minerals and Materials Technology, Bhubaneswar, India

** Corresponding Author: bvvalent@fc.up.pt*

In the state of Odisha, the coal ash generation was 25.393 Mt in 2024-25, and its utilization reached 86.9%. The majority of ash is being used in roads, low lying area and bricks industries (CEA, 2026). Metals recovering from fly ash (CFA) is an option (e.g., Dai et al., 2022). However, iron, a major element in CFA, is not being recovered despite being easily magnetically separated.

Coal and ash samples were collected from the Talcher Super Thermal Power Station (Odisha, India). The feed coal is mainly a blend of sub-bituminous to bituminous Talcher coal from Angul district, with very high ash content (40 wt.%, on average), and some Australian coals. The feed coal is pulverised before combustion at 1350-1500 °C.

The ferrospheres were manually collected from the ashes using a ferrite magnet and analysed via Scanning electron microscopy with Energy-dispersive spectroscopy (SEM-EDS), incident light optical microscopy, and Raman microspectroscopy.

The SEM-EDS analysis of the feed-coal allowed the identification of siderite as the main Fe-carrier, quartz, kaolinite, illite, and Ti-oxides. Pyrite is rare.

The ferrospheres' size ranges from 10-200 μm, and their internal structure comprises iron spheres encapsulated by glassy aluminosilicate, massive glassy aluminosilicate spheres embedding Fe-crystallites, and spheres with coarse Fe-crystals and residual aluminosilicate matrix (Fig. 1).

Under incident reflected light microscopy, most ferrospheres observed are made of gray magnetite dendrites, which are purple and isotropic under polarized light (Fig. 1B). The Raman microspectroscopy analyses of ten ferrospheres reveal a high-intensity Raman band at 675-692 cm^{-1} (A1g) together with a low-intensity band at 309-352 cm^{-1} (Eg), enabling the identification of magnetite in the spectra collection. The shift of the main band (A1g) to lower wavenumbers (692 to 675 cm^{-1}) is generally accompanied by a narrowing of this band, with a FWHM decreasing from 71 to 43 cm^{-1}, indicating a higher crystallinity for some of the particles.

Compared with Santos et al. (2023) study, there is a higher amount of glassy aluminosilicate covering the ferrospheres' surface while in Colombian coal ferrospheres, the surface is "clean". This seems related to the main Fe-bearing minerals contributing to the formation of the ferrospheres (pyrite in the case of the Colombian coal, and siderite in this study), and their association with the clay matrix.

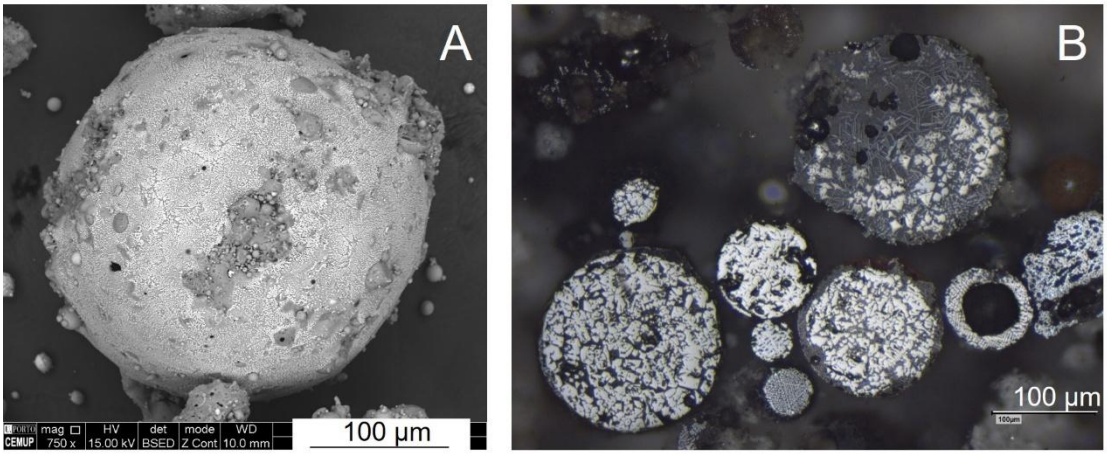

Figure 1. Ferrospheres: A) ferrosphere surface with magnetite (white) and aluminosilicate glass (gray) (SEM-EDS, backscattered electron mode); B) cross-section of different ferrospheres types (incident light microscopy).

Funding
Project CATCH by FCT (grant ref. 2023.16411.ICDTDOI, COMPETE2030-FEDER-00714500, https://doi.org/10.54499/2023.16411.ICDT), project INSUB by DST, India (grant ref. DST/INT/Portugal/P-05/2021 dated 12/07/2023), and FCT (grant ref. DRI/India/0315/2020, https://doi.org/10.54499/DRI/India/0315/2020).

References

CEA, 2026. Report on Ash Generation and Utilization For Grid-Connected Thermal Power Stations for the Year 2024–25. Government of India, Ministry of Power, Central Electricity Authority (CEA). New Delhi, January-2026, pages 43-44.

Dai, S., Arbuzov, S.I., Chekryzhov, I.Y., French, D., Feole, I., Folkedahl, B.C., Graham, I.T., Hower, J.C., Nechaev, V.P., Wagner, N.J., Finkelman, R.B., 2022. Metalliferous Coals of Cretaceous Age: A Review. Minerals 12, 1154.

Santos, A.C., Cruz, C., Font, E., French, D., Guedes, A., Moreira, K., Sant'Ovaia, H., Vieira, B.J.C., Waerenborgh, J.C., Valentim, B., 2023. Physicochemical Properties of Fe-Bearing Phases from Commercial Colombian Coal Ash. Minerals 13, 1055.

Preliminary data on the anisotropy of reflectance of vitrinite in oriented samples from the Douro Carboniferous Basin (NW of Portugal)

Mariana Costa[1*], Eduardo Ferreira da Silva[2], Ary Pinto de Jesus[1], Deolinda Flores[1†]

[1] Instituto de Ciências da Terra, Polo da Universidade do Porto e Departamento de Geociências, Ambiente e Ordenamento do Território, Faculdade de Ciências da Universidade do Porto, Porto, Portugal; [2]Departamento de Geociências, Universidade de Aveiro e GeoBioTec - GeoBioCiências, GeoTecnologias e GeoEngenharias, Aveiro, Portugal. † Decease

** Corresponding Author: up201201358@fc.up.pt*

The Douro Carboniferous Basin (DCB) constitutes the largest terrestrial Carboniferous outcrop in Portugal and is located within the Central-Iberian Zone. Dated from the Gzhelian, is an intramontane synorogenic basin, formed by a sinistral pull-apart tectonic setting, along the Douro-Beira Shear Zone. Meta-anthracite was extensively exploited throughout the basin, particularly in São Pedro da Cova and Pejão Coalfields.

Coal rank is primarily determined by vitrinite reflectance in accordance with ISO 11760:2018. Vitrinite reflectance is inherently isotropic but may develop anisotropy in relation to the stress regime associated with coalification process (Hower and Davis, 1981; Levine and Davis, 1989). This anisotropy is assessed under polarized light, yielding maximum, and minimum reflectance, with the mean reflectance calculated from these values. The three-dimensional patterns defined by those reflectance parameters can be represented by ellipsoidal forms, known as the Vitrinite Reflectance Indicating Surface (VRIS).

This study is based on maximum and minimum vitrinite reflectance measurements obtained from nine oriented polished blocks. Five meta-anthracite samples were collected from the Pejão Coalfield, and another four from the São Pedro da Cova Coalfield. As the samples were provided from existing collections, their precise geographic locations are unknown, with only their coalfield of origin being documented. However, it is known that the bedding orientation is N130°-140°E, with dips ranging between 50°-80°NE (e.g., Freire, 1981; Pinto de Jesus, 2003).

Preliminary results indicate that the bedding-parallel plane exhibits significantly higher reflectance values than the perpendicular planes. Maximum reflectance values range from 5.45% to 8.35% in the bedding-parallel plane and from 4.83% to 7.36% in the perpendicular planes. The ellipse flattening ratio, calculated from the difference between the major semi-axis (maximum reflectance) and the minor semi-axis (minimum reflectance) divided by the major semi-axis, ranges from 2.95% to 18.68% in the bedding-parallel plane, compared with 23.19% to 58.29% in the perpendicular planes, indicating marked differences in VRIS geometry.

The higher reflectance values observed in bedding-parallel sections, together with the marked differences in VRIS geometry between bedding-parallel and bedding-perpendicular planes, indicate a pronounced optical anisotropy in the Douro Basin meta-anthracites. These results are consistent with previous studies suggesting that vitrinite in high-rank coals commonly exhibits biaxial reflectance behavior associated with tectonic deformation and non-hydrostatic stress regimes during syntectonic coalification under a NE-SW compressive torque related to the latest Hercynian (Variscan) deformation phases. The VRIS geometry therefore provides valuable information on the structural evolution of the basin in addition to conventional coal-rank assessment (Cook et al., 1972; Kilby et al., 1988, 1991).

Acknowledgments
The authors would like to dedicate this work to Professor Deolinda Flores. The author M. Costa benefits from a PhD scholarship granted by FCT Ref: 2022.11145.BD. This work is supported by national funding awarded by FCT - Foundation for Science and Technology, I.P., through ICT – Earth Sciences Institute (UID/4683/2025), and through the GEOBIOTEC - Geobiosciences, Geotechnologies and Geoengineering research unit (UIDB/GEO/04035/2020). A special thanks to Armando Faria and his son, Rui Faria, for giving us the Fojo samples, and to the Museu Mineiro de São Pedro da Cova, particularly to Micaela Santos, for giving us the São Pedro da Cova samples.

References

Cook, A.C., Murchison, D.G., Scott, E., 1972. Optically biaxial anthracitic vitrinites. Fuel 51(3), 180-184.

Freire, J., 1981. Bacia Carbonífera do Norte de Portugal. Os jazigos de São Pedro da Cova e do Pejão. Estudos Notas e Trabalhos do Serviço de Fomento Mineiro 24(1-4), 1-380.

Hower, J.C., Davis, A., 1981. Application of vitrinite reflectance anisotropy in the evaluation of coal metamorphism. Geol. Soc. Am. Bull. 92(6), 350-366.

ISO 11760, 2018. Classification of coals. International Organization for Standardization. Geneva, Switzerland, 9 pp.

Kilby, W.E., 1988. Recognition of vitrinite with non-uniaxial negative reflectance characteristics. Int. J. Coal Geol. 9(3), 267-285.

Kilby, W.E., 1991. Vitrinite reflectance measurement – some technique enhancements and relationships. Int. J. Coal Geol. 19(1-4), 201-218.

Levine, J.R., Davis, A., 1989. Reflectance anisotropy of Upper Carboniferous coals in the Appalachian foreland basin, Pennsylvania, USA. Int. J. Coal Geol. 13(1-4), 341-373.

Pinto de Jesus, A., 2003. Evolução sedimentar e tectónica da Bacia Carbonífera do Douro (Estefaniano C inferior, NW de Portugal). Cad. Geol. Laxe 28, 107–125.

Insights into organic matter and depositional conditions in lacustrine carbonates of the Barra Velha Formation

Jaqueline Torres de Souza[1,2*], Antonio Donizeti de Oliveira[1], Joalice de Oliveira Mendonça[1], Leonardo Borghi[2], João Graciano Mendonça Filho[1]

[1]Laboratório de Palinofácies e Fácies Orgânica (LAFO), Universidade Federal do Rio de Janeiro, Brazil; [2]Laboratório de Geologia Sedimentar (LAGESED), Universidade Federal do Rio de Janeiro, Brazil

* *Corresponding Author: jaqueline@lafo.geologia.ufrj.br*

The Santos Basin, one of the largest oil and gas provinces in Brazil, covers approximately 350,000 km² and originated during the Neocomian as a result of the breakup of Gondwana and the opening of the Atlantic Ocean. The basin is recognized as one of the main regions for hydrocarbon exploration and production, holding considerable scientific and economic relevance. Nevertheless, studies focusing on organic matter within lacustrine carbonate reservoirs of the pre-salt succession remain limited. This study integrates both organic petrography analysis (palynofacies and thermal maturity) and organic geochemistry analysis (total organic carbon - TOC, and Rock-Eval pyrolysis) to characterize the sedimentary succession of the Barra Velha Formation in a pre-salt field in the Santos Basin. The study aimed to investigate depositional systems, identify the main controls on sedimentation, and evaluate the quality, preservation, and hydrocarbon generation potential of the organic matter. The results indicate the presence of amorphous organic matter derived from autotrophic photosynthetic bacteria and organisms of animal origin belonging to the Phylum Cnidaria, Class Hydrozoa. Geochemical analyses revealed intervals with significant hydrocarbon generation potential, presenting hydrogen index (HI) values up to 898 mg HC/gTOC, TOC content reaching 3.73 wt.%, and S2 values of 39.57 mg HC/grock. Despite this potential, thermal maturity analyses indicate that the organic matter remains thermally immature, with spore coloration index (SCI) values ranging from 4.0 to 4.5 (0.40 - 0.45% VR_{eq}). These findings expand the current understanding of organic matter in Brazilian pre-salt intervals and contribute to paleoenvironmental and petroleum system interpretations.

Petrographic variability of biochar produced in a bench-scale Mass Loss Calorimeter to explore differences in combustibility

Angeles G. Borrego[1*], M. Carmen Niembro[1], Cristina Carrillo García[2], Mercedes Guijarro Guzman[2], Javier Madrigal Olmo[2]

[1] INCAR/CSIC, Oviedo, Spain; [2]ICIFOR-INIA (CSIC), Madrid, Spain

* *Corresponding Author: angeles@incar.csic.es*

Organic petrology offers significant potential for characterizing biomass altered by forest fires, as demonstrated by the inertinite analogues observed in coal (Sanei et al., 2024). In this study, a bench-scale Mass Loss Calorimeter (MLC), which enables thermal exposure studies to be carried out under precise exposure conditions whilst observing the sample reaction and measuring the total heat release (Madrigal et al., 2013) has been used to simulate plant burning (Fig.1a). A single radiation intensity of 50 kW/m2 has been applied to 27 samples belonging to three species common in Mediterranean forest (*Pinus pinea*, *Arbutus unedo*, and *Quercus pyrenaica*) with three fuel moisture contents (FMC). The resulting biochar was analyzed by reflected-light microscopy to explore differences between species and combustion conditions.

A wide range of occurrences is observed in all the samples from virtually unaffected particles retaining the original fluorescence (reddish in the case of *A. unedo* and yellowish in *P. pinea* and *Q. pyrenaica*) to highly charred material, which indicates varying degrees of thermal alteration by the heat source (Fig.1c). The char reflectance in the pool of samples is in the range R_o=0.08-6.02%, which correspond to estimated temperature of 198-1043°C according to Jones et al. (1991). The *A. unedo* samples fell within the group exhibiting the lowest reflectance values and the highest scatter, whereas *P. pinea* contained the highest amount of high reflecting particles (R_o>5.0%), which could be related to its higher flammability (Dimitrakopoulos and Papioannou, 2001). No trend of variation in reflectance has been observed as a function of FMC. A k-means cluster generated three differentiated groups (Fig. 1b) highlighting that only *P. pinea* particles reached a char temperature higher than 800 °C (R_o≈5.0%; Jones et al., 1991).

Future works using different species and heating levels is suggested to explore the ability of this protocol to estimate burn intensity and severity with application in the field of prescribed burns, controlled burns, paleoecology, pyroecology, soil science, fire dynamics in the organic matter, and fire severity assessment.

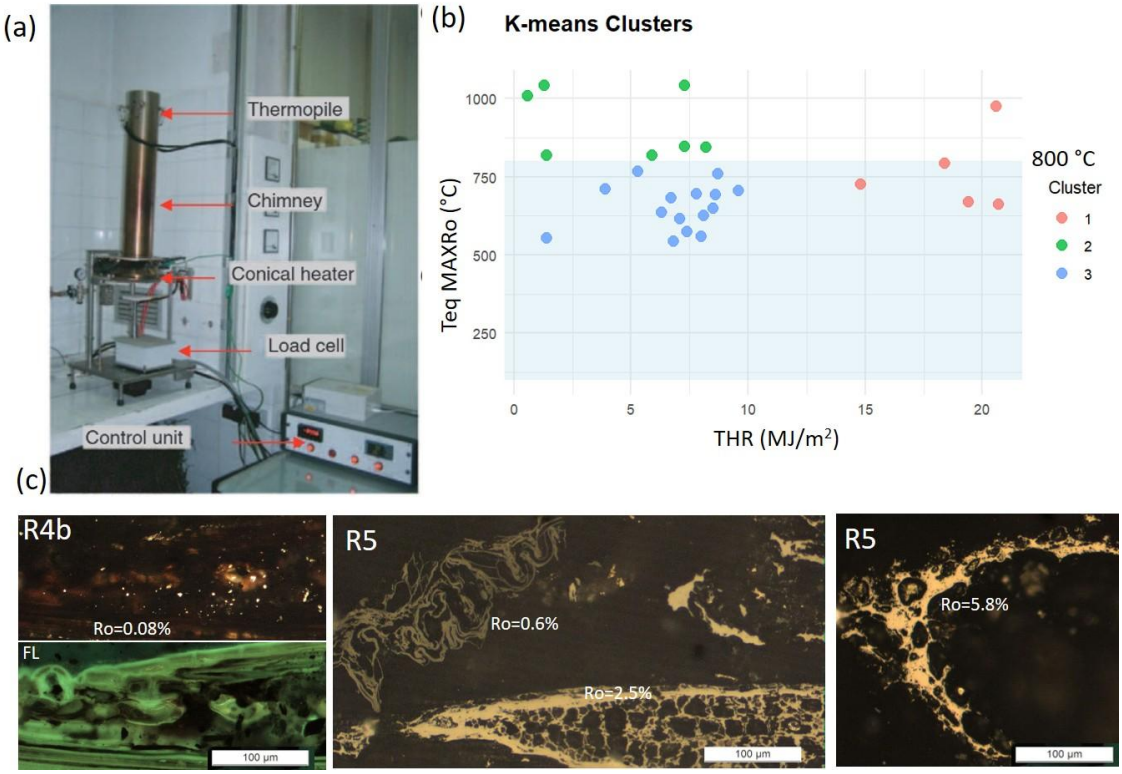

Figure 1. (a) Mass Loss Calorimeter device, further details in Madrigal et al. 2013; (b) Cluster analysis showing the relationship between Total Heat Release (Calorimetry) and Maximum Temperature of char calculated from the maximum reflectance value [3] and threshold at 800 °C: Cluster 1= *P. pinea* dry samples, Cluster 2= *P. pinea* fresh fuels, Cluster 3= comprises *A. unedo* and *Q. pyrenaica* samples; (c) Variability of *P. pinea* biochar; Images taken in reflected light oil immersion (Ro=reflectance in oil; FL=Fluorescence Light).

Acknowledgements

MLC tests was carried out thanks to SenforFire Project (SUDOE_SenForFire-S1/1-1/E0040) and ZEGIADAPT national project PID2023-146599OR-C51. Char petrography was supported by Composite Group Project IDE/2024/000737.

References

Dimitrakopoulos A.P., Papioannou K.K., 2001 Flammability assessment of Mediterranean forest fuels. Fire Technol. 37, 146-152

Jones T.P., Scott A.C., Cope M., 1991. Reflectance measurements and the temperature of formation of modern charcoals and implications for studies of fusain. Bull. Geol. Soc. France 162, 193-200.

Madrigal J., Hernando C., Guijarro M., Díez C., 2013. A new bench-scale methodology for evaluating the flammability of live forest fuels. J. Fire Sci. 31, 131-142.

Sanei H., Rudra A., Przyswitt Z.M.M., Kousted S., Sindlev M.B., Zheng X., Nielsen S.B., Petersen H.I., 2024. Assessing biochar's permanence: an inertinite benchmark. Int. J. Coal Geol. 281, 104409.

Decoding Late Oligocene fern life: assessing plant communities, depositional environments, and maceral genesis in the Petroșani Basin (Romania)

Roxana Pirnea[1*], Izabela Mariș[2,3], Mihai Emilian Popa[4], Georgeta Predeanu[5], Doina Maria Ghiran[2]

[1]Independent researcher, Timișoara, Romania; [2]OMV Petrom SA, Core and Cuttings Technologies Laboratory, Câmpina, Romania; [3]University of Bucharest, Faculty of Geology and Geophysics, Laboratory of Mineralogy, Bucharest, Romania; [4]University of Bucharest, Faculty of Geology and Geophysics, Doctoral School of Geology, Bucharest, Romania; [5]University Politehnica of Bucharest, Faculty of Applied Chemistry and Materials Science, Research Center for Environmental Protection and Ecofriendly Technologies, Bucharest, Romania

** Corresponding Author: roxana.pirnea@gmail.com*

The Late Oligocene terrestrial macroflora of the Petroșani Basin (Romania) records a distinct, low-diversity ecosystem dominated by swamp and mixed mesophytic forest habitats flourishing under a warm, humid, laurel-woodland-type climate. This study integrates paleobotanical records with organic petrography to reconstruct the depositional system and evaluate the roles of primary and secondary coal generators in shaping the basin bituminous coal deposits.

Five distinct fossil fern genera have been identified within a broader angiosperm-conifer-fern wetland association: *Pronephrium stiriacum* (Unger) Knobloch et Kvaček 1976 (Thelypteridaceae), *Osmunda lignitum* (Giebel 1857) Stur 1870 (Osmundaceae), *Blechnum dentatum* (Göppert 1836) Heer 1872 (Blechnaceae), *Odontosoria marekgaltieri* Pšenička, Sakala et Dašková 2022 (Lindsaeaceae) and *Aspidium cf. elongatum* Heer sensu Procházka 1951 (familiae et genera indeterminate). While primary coal generation was driven by taxodiaceous peat-forming swamp communities, ferns acted as secondary coal generators within specific micro-environments. *Osmunda lignitum* thrived within fern-dominated mats inside a lowland forest-broad swamp matrix, comparable to the modern Everglades. *Blechnum dentatum* occupied open habitats within taxodiaceous back-swamps, while *Pronephrium stiriacum* – frequently recovered from coal seam roof shales – is abundant, reflecting its ability to aggressively colonise mires during their closing, successional phases.

This distribution directly correlates with the maceral composition identified via Thermal Alteration Index (TAI), vitrinite reflectance, and epifluorescence microscopy. The dominance of Oligocene coniferous trees and early flowering plants is geochemically reflected by a high liptinite content, characterised by abundant resinite, sporinite, cutinite, and fossilized sporangia. While the coal samples remain rich in vitrinite, its distribution is structurally less uniform than that of older, Palaeozoic fern-rootlet matrices. This heterogeneity emphasises the transition from ancient Palaeozoic cellulose-dominated peat to resin- and wax-rich Cenozoic gymnosperm and angiosperm inputs.

Ultimately, the identified plant assemblages reveal an environment under persistent ecological constraints that could not support a high biodiversity. However, the localised accumulation of Betulaceae representatives and fern mats, paired with dominant taxodiaceous stands, provided the necessary biomass for extensive carbon sequestration. This multi-proxy approach establishes a definitive link between Oligocene plant ecology, successional dynamics, and the specific petrophysical and chemical properties of the Petroșani Basin coal seams.

Evolution of effective CO_2 flow during successive adsorption steps in coal

Y. Bueno-Yamamoto[1,2,3,4*], C.A. Rodrigues[2,4,5], J.J. Enciso-Cárdenas[1,3], I.D. García-Calvillo[3,6], P.F. Moreira[2,4], D.M. Garza-Cavazos[2,3,4], A. Bueno-Tokunaga[1], L.F. Camacho-Ortegón[1,3], G. De La Rosa-Rodríguez[1,2,4], M.J. Lemos de Sousa[2,4,5]

[1]Centro de Investigación en Geociencias Aplicadas - Universidad Autónoma de Coahuila (UAdeC), Nueva Rosita, Coahuila, Mexico; [2]Fundação/Universidade Fernando Pessoa, Porto, Portugal; [3]Centro de Estudios e Investigaciones Interdisciplinarios (UAdeC), Saltillo, Coahuila, Mexico; [4]ARNET/MARE, URI, Coimbra, Portugal; [5]Academia das Ciências de Lisboa, Lisboa, Portugal; [6] Centro de Investigación en Matemáticas Aplicadas (UAdeC), Saltillo, Coahuila, México

** Corresponding Author: buenoyuriko@gmail.com*

The continuous increase in atmospheric carbon dioxide (CO_2) concentrations has intensified interest in Carbon Capture, Utilisation and Storage (CCUS) technologies as a strategy for mitigating Greenhouse Gas (GHG) emissions (IPCC, 2005, 2007; Rodrigues et al., 2025). Among the potential geological formations under consideration for long-term CO_2 storage, coal seams represent a promising candidate due to their high adsorption capacity and strong affinity for CO_2 (IPCC, 2005; Liu et al., 2025). While storage capacity is commonly used to assess reservoir suitability, understanding gas flow behaviour within the coal matrix is equally important, as it directly influences injection performance and, ultimately, storage efficiency (Rodrigues et al., 2016; Liu et al., 2025). Consequently, characterising the evolution of flow properties during adsorption is essential for improving the understanding and assessment of geological CO_2 storage processes.

This study investigates the evolution of effective CO_2 flow across successive adsorption steps within the coal matrix, based on isothermal adsorption tests conducted using a volumetric sorption technique. Coal samples from the Sabinas Basin (Coahuila, Mexico) were prepared and conditioned before undergoing a sequence of controlled pressure increments at a constant temperature. Pressure and volume data were continuously recorded throughout the adsorption process and subsequently processed using noise-reduction techniques to improve data quality and ensure reliable parameter estimation.

The analysis focused on calculating diffusion coefficients for successive adsorption steps, which were used as indicators of effective CO_2 flow within the coal matrix (Rodrigues et al., 2016; Liu et al., 2020). The evolution of these coefficients was examined through successive adsorption steps as the coal matrix became increasingly saturated with CO_2.

Results revealed a substantial reduction in the effective CO_2 flow during the adsorption process. The estimated diffusion coefficients decreased from 3.35×10^{-7} m²/s in the initial adsorption step to approximately 10^{-10} m²/s in the final steps, representing a reduction of about three orders of magnitude. This behaviour suggests that CO_2 flow diminishes as the coal matrix becomes saturated (Zhao et al., 2019; Liu et al., 2020). Furthermore, the observed behaviour suggests distinct flow regimes, comprising an initial rapid flow stage, a transitional stage, and a final dynamic stable stage as the matrix approaches saturation.

The results suggest that effective CO_2 flow is not constant and may not be adequately represented by a single diffusion parameter. The observed trend provides experimental evidence that diffusion behaviour changes significantly throughout the adsorption process, with potential implications for the evaluation and modelling of underground geological CO_2 storage (IPCC, 2005; Liu et al., 2025).

References

Intergovernmental Panel on Climate Change (IPCC), 2007. Climate Change 2007: Synthesis Report. IPCC, Geneva, Switzerland.

Intergovernmental Panel on Climate Change (IPCC), 2005. Carbon dioxide capture and storage: Special report of the Intergovernmental Panel on Climate Change. Cambridge University Press, Cambridge, UK.

Liu, A., Liu, P., & Liu, S., 2020. Gas diffusion coefficient estimation of coal: A dimensionless numerical method and its experimental validation. International Journal of Heat and Mass Transfer 162, 120336.

Liu, X., Zhang, B., Fu, X., Lu, J., Huang, M., Zeng, F., 2025. Potential, Efficiency, and Leakage Risk of CO_2 Sequestration in Coal: A Review. Processes 13(6), 1680.

Rodrigues, C.F.A., Dinis, M.A.P., Lemos de Sousa, M., 2016. Gas content derivative data versus diffusion coefficient. Energy Exploration & Exploitation 34, 606-620.

Rodrigues, C.F.A., Rocha, H., Tasinari, C., Lemos de Sousa, M.J., 2025. Developments and Evolution of CCUS Technologies: A Review. Carbon Capture Utilization and Storage, Law, Policy and Standardization Perspectives. Springer Nature Sustainable Developments Goals Series.

Zhao, W., Cheng, Y., Pan, Z., Wang, K., Liu, S., 2019. Gas diffusion in coal particles: A review of mathematical models and their applications. Fuel 252, 77-100.

Upgrading carbon residues from coking processes: A microscopic characterization study

Patricia Álvarez[1*],Uriel Sierra[2], Marcos Granda[2], A. Concheso[2], A. Vigil[2]

[1]Instituto de Ciencia y Tecnología del Carbono (INCAR), CSIC Oviedo, Spain; [2]Laboratorio Nacional de Materiales Grafénicos, Centro de Investigación de Química Aplicada (CIQA), Coahuila, México.

* *Corresponding Author: par@incar.csic.es*

Carbon-rich deposits generated during industrial coking processes progressively accumulate on the inner walls of coke ovens and must be periodically removed. Due to the lack of established reuse routes, this material is generally classified as industrial waste, creating environmental and economic concerns for the steel industry. Nevertheless, its high carbon content and complex microstructure suggest that it could be considered as a precursor for advanced carbon materials. In recent years, increasing attention has been devoted to the upgrading of industrial carbon wastes through thermochemical treatments aimed at producing more carbon ordered structures such as graphene materials with potential technological applications (González-Ingelmo et al., 2024a,b). In this context, understanding of the structural evolution of these heterogeneous residues is essential for developing sustainable and energy-efficient valorisation strategies.

The study aims to evaluate the potential of this industrial residue as a low-cost feedstock for the production of graphite-like materials. The original sample (coke-like waste) was collected at the Industrial Minera Mexico, Nueva Rosita Plant, Coahuila, and was subjected to further graphitization (up to 2800ºC, graphite-like waste). Both were characterized using optical microscopy and scanning electron microscopy (SEM). Optical microscopy revealed textural heterogeneities and the development of anisotropic domains during thermal treatment. This behaviour suggests the presence of catalytic effects associated with metallic particles naturally occurring in the residue (Fig. 1). SEM analysis confirmed that the highly anisotropic domains formed during carbonization appear as a distinct coating surrounding and partially detached from the carbonaceous core (Fig. 2). The combined results obtained from both techniques provide a deeper understanding of the structural evolution of the material during the carbonization process.

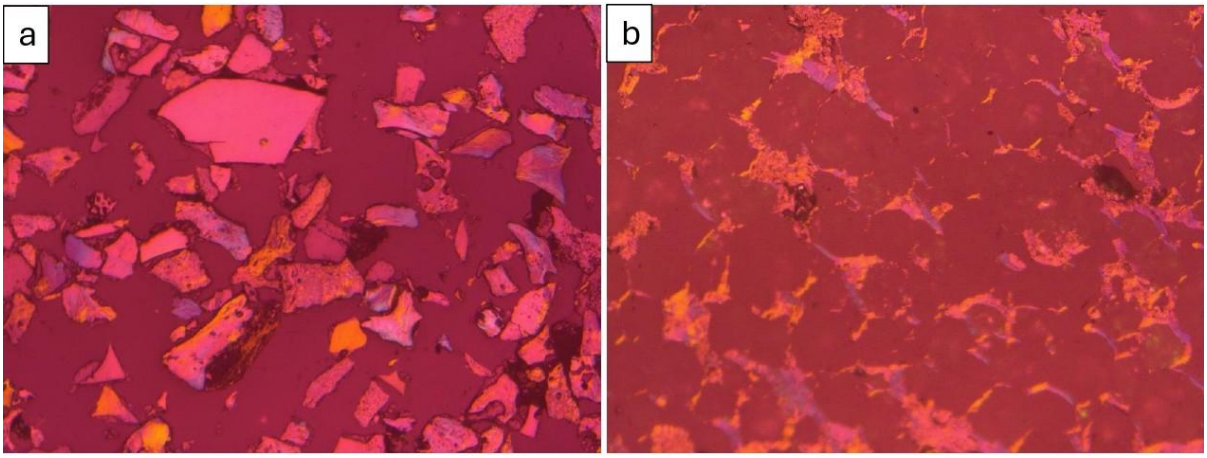

Figure 1. Optical micrographs of the coke-like waste (a) and graphite-like waste (b) obtained using a 20× oil-immersion objective under crossed polarized light with a 1λ retardation plate.

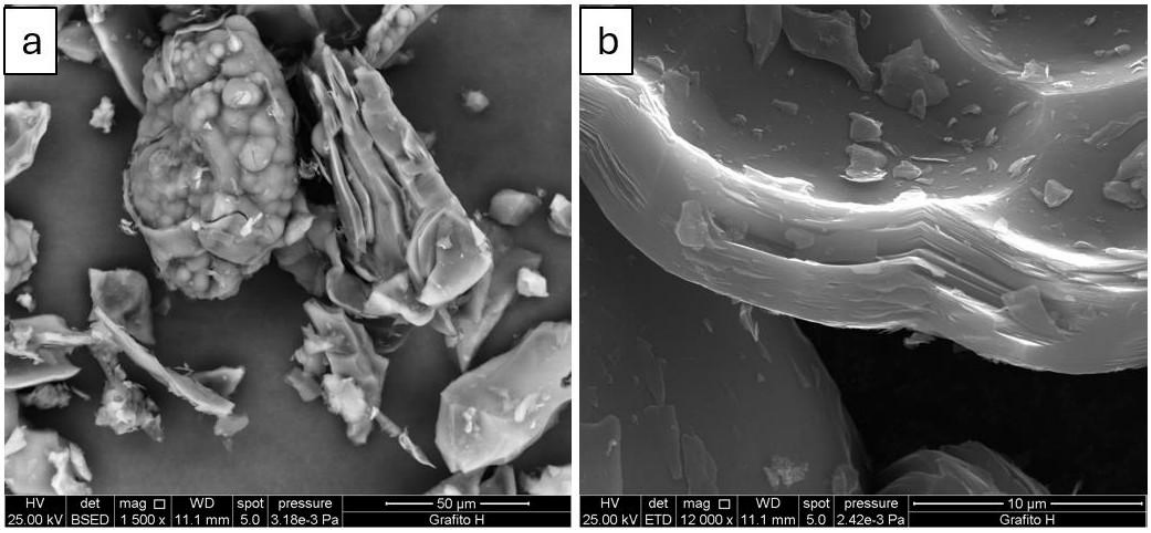

Figure 2. SEM images of Graphite-like waste a) 50 µm, b) 10µm

Acknowledgement
The authors thank the Spanish Council for Research (ICOOP program COOPPB24065) for their financial support.

References

González-Ingelmo M., Álvarez P., Granda M., Rocha V.G., González Z., Sierra U., Sánchez-Page B., Jiménez M.V., Pérez Torrente J.J., Blasco J., Subias G. 2024a. On the study of the preparation of graphene-anchored NHC-iridium catalysts from a coke-like waste with application in water splitting. Appl. Surf. Sci. 655, 159556.

González-Ingelmo M., Rocha V.G., González Z., Sierra U., Diaz Barriga E., Álvarez P. 2024b. Graphene Materials from Coke-like Wastes as Proactive Support of Nickel–Iron Electro-Catalysts.

Vitrinite reflectance: A link between thermal history, kerogen evolution and basin modelling

D.M. Garza-Cavazos[1,2], C.A. Rodrigues[2,3,4], J.J. Enciso-Cárdenas[1,5], Y. Bueno-Yamamoto[1,2,3,5], F. Núñez-Useche[6], G. De La Rosa-Rodríguez[2,3,5], E. González-Partida[7], M.J. Lemos de Sousa[2,3,4]

[1]Centro de Estudios e Investigaciones Interdisciplinarias, Universidad Autónoma de Coahuila (UAdeC), Mexico; [2]Fundação/Universidade Fernando Pessoa, Porto, Portugal; [3]ARNET/MARE, URI,Coimbra, Portugal; [4]Academia das Ciências de Lisboa, Lisboa, Portugal; [5]Centro de Investigación en Geociencias Aplicadas, Universidad Autónoma de Coahuila (UAdeC), Mexico; [6]Instituto de Geología, Universidad Nacional Autónoma de México (UNAM), Mexico; [7]Centro de Geociencias Campus Juriquilla, Universidad Nacional Autónoma de México (UNAM), Mexico

* *Corresponding Author: dianagarzacavazos@uadec.edu.mx*

Vitrinite reflectance (R_o) is one of the most widely used parameters for thermal maturity assessment and basin-model calibration. Although it is traditionally interpreted as a proxy for burial-related temperature, which is a time-dependent parameter, R_o evolution reflects broader chemical and structural transformations of organic matter throughout thermal maturation (Burnham, 2019; Tissot and Welte, 1984). This raises an important question for basin modelling: to what extent does vitrinite reflectance record thermal history alone, and to what extent does it reflect the compositional and kinetic evolution of organic matter?

Experimental and conceptual studies have linked increases in R_o to progressive dehydrogenation, aromatisation, and structural reorganisation during maturation (Burnham, 2019; Carr and Williamson, 1990; Tissot and Welte, 1984). From this perspective, vitrinite reflectance may be regarded as the optical expression of cumulative chemical and structural changes within organic matter rather than a simple empirical function of temperature and time.

The initial composition of organic matter, which is largely controlled by the depositional environment and biological precursors, governs the molecular structure of kerogen and its kinetic pathways of thermal transformation (Tissot and Welte, 1984). Consequently, kerogens with different compositions and kinetic properties may follow distinct maturation pathways and hydrocarbon-generation trajectories, even when subjected to comparable thermal histories (Lewan and Ruble, 2002; Tissot and Welte, 1984). Therefore, as vitrinite reflectance changes in response to variations in the chemical evolution of kerogen, it can be considered an indicator of both thermal history and organic matter evolution.

Recent studies showed that reflectance suppression often occurs when vitrinite coexists with liptinite, solid bitumen or immature bitumen (Peters et al., 2018; Sanders et al., 2022). These lower-reflecting substances can optically dilute or mask the true reflectance of vitrinite. In addition, experimental work suggests that free radicals and other byproducts generated during maturation of hydrogen-rich organic matter can modify the surrounding chemical environment, thereby influencing the aromatisation and condensation processes responsible for increasing R_o, although the underlying mechanisms remain under investigation (Sanders et al., 2022). These interactions do not chemically change vitrinite itself. Still, they can hinder the formation of more organised aromatic structures in the adjacent organic matter, resulting in suppressed or delayed Ro evolution in hydrogen-rich organic matter.

This review assesses the physical and chemical significance of vitrinite reflectance during thermal maturation by combining concepts from organic petrology, organic geochemistry, and basin modelling. Current evidence suggests that the interpretation of Ro should consider not only thermal evolution, but also the petrographic and geochemical characteristics of organic matter. In this context, vitrinite

reflectance can be considered as an integrated record of the chemical response of organic matter to thermal stress, connecting kerogen evolution, organic matter composition, and basin-model calibration.

References

Burnham, A.K., 2019. Kinetic models of vitrinite, kerogen, and bitumen reflectance. Organic Geochemistry 131, 50-59.

Carr, A.D., Williamson, J.E., 1990. The relationship between aromaticity, vitrinite reflectance and maceral composition of coals: Implications for the use of vitrinite reflectance as a maturation parameter. Organic Geochemistry 16(1-3), 313-323.

Lewan, M.D., Ruble, T.E., 2002. Comparison of petroleum generation kinetics by isothermal hydrous and nonisothermal open-system pyrolysis. Organic Geochemistry 33(33), 1457-1475.

Peters, K.E., Hackley, P.C., Thomas, J.J., Pomerantz, A.E., 2018. Suppression of vitrinite reflectance by bitumen generated from liptinite during hydrous pyrolysis of artificial source rock. Organic Geochemistry 125, 220-228.

Sanders, M.M., Jubb, A.M., Hackley, P.C., Peters, K.E., 2022. Molecular mechanisms of solid bitumen and vitrinite reflectance suppression explored using hydrous pyrolysis of artificial source rock. Org. Geochemistry 165, 104371.

Tissot, B. P., Welte, D. H., 1984. Petroleum formation and occurrence (2nd ed.). Springer-Verlag.

Characterization of biochar as reducing material for phosphorus recovery from anthropogenic waste ashes by petrographic, SEM/EDS and Raman spectroscopical methods

Ozben Kutlu[1*], Georgeta Predeanu[2,3], Bruno Valentim[4,5], Alexandra Guedes[4,5], Mihaela Bălănescu[2,3], Bogdan Stefan Vasile[2,6], Valerica Slăvescu[2,3], Pinar Boluk[1], Mehmet Ihsan Kulas[1]; Nezaket Duran[1], Marius Florin Drăgoescu[2,3]

[1] Ege University Solar Energy Institute, Turkey; [2]National University of Science and Technology POLITEHNICA Bucharest, Romania; [3]Research Centre of Environmental Protection and Eco-friendly Technologies; [4]Faculdade de Ciências da Universidade do Porto, Porto, Portugal; [5]Instituto de Ciências da Terra, Porto, Portugal; [6]Advanced Research Center for Innovative Materials, Products and Processes and National Research Center for Micro and Nanomaterials, Romania

** Corresponding Author: ozben.kutlu@ege.edu.tr*

One of the sustainable options of the PREWA project for future assurance of P supply in Romania, as well as in Türkiye consist in phosphorus (P) recovery from the food production and consumption chain which represents the strategy of P-recycling to reduce EU phosphate insecurity.

A sustainable thermal P extraction stream is based on recovery and reuse of anthropogenic secondary resources focusing on incineration and producing a P-rich ash from food production waste, and sewage sludge. The recovered P-rich ash has the potential to partially substitute phosphate rocks and reduce the consumption of phosphate rocks-based fertilizers (Kasina et al., 2023).

Research on P extraction from various ashes has been carried out within several projects (Fahimi et al., 2024, Predeanu et al., 2024a, 2025a, 2025b; Valentim et al, 2024). Extensive research has been developed to broaden the raw material base for obtaining carbon materials from lignocellulosic materials for the use in various purposes such as fuel (Drobniak et al., 2025) and carbon materials (biochar) produced by conventional and microwave heating (Predeanu et al., 2024b), which can be used also as reducing agents in the P extraction reaction from ashes.

The development of thermal P extraction process is based on a redox chemical reaction in which calcium phosphate mixed with carbon-rich biochar and silica, forms above 1300°C calcium silicate $CaSiO_3$ and phosphoric anhydride P_2O_5, which is then reduced by carbon. At high temperature, the calcium silicate melts to form a slag, while P vaporizes (Beral and Zapan, 1962).

This study describes the results of petrographic, SEM/EDS and Raman microspectroscopical analyses of biochar formed during carbonization of biomass by conventional and microwave heating at low temperatures up to 500°C. The properties of the resulting biochars were compared with those of BIOCHARNOVA, a commercial biochar produced from woody lignocellulosic biomass through high-temperature batch pyrolysis in a fixed-bed reactor. Petrographic analysis showed that microwave carbonization of fruit kernel biomass produced a porous biochar matrix with fine pores and an interconnected pore network (Fig. 1A-C). SEM/EDS revealed Mg- and P-containing oxide phases in sewage-sludge biochar, Si-dominated phases in spent mushroom compost biochar, and associated Ca-, K-, and P-containing phases in chicken-litter biochar (Fig. 1D-F). Raman spectra of the biochars exhibited similar characteristics, indicating predominantly amorphous carbon structures. These findings demonstrate differences in mineral-phase associations among the biochars and support their evaluation as reducing agents for thermal P recovery from anthropogenic ashes.

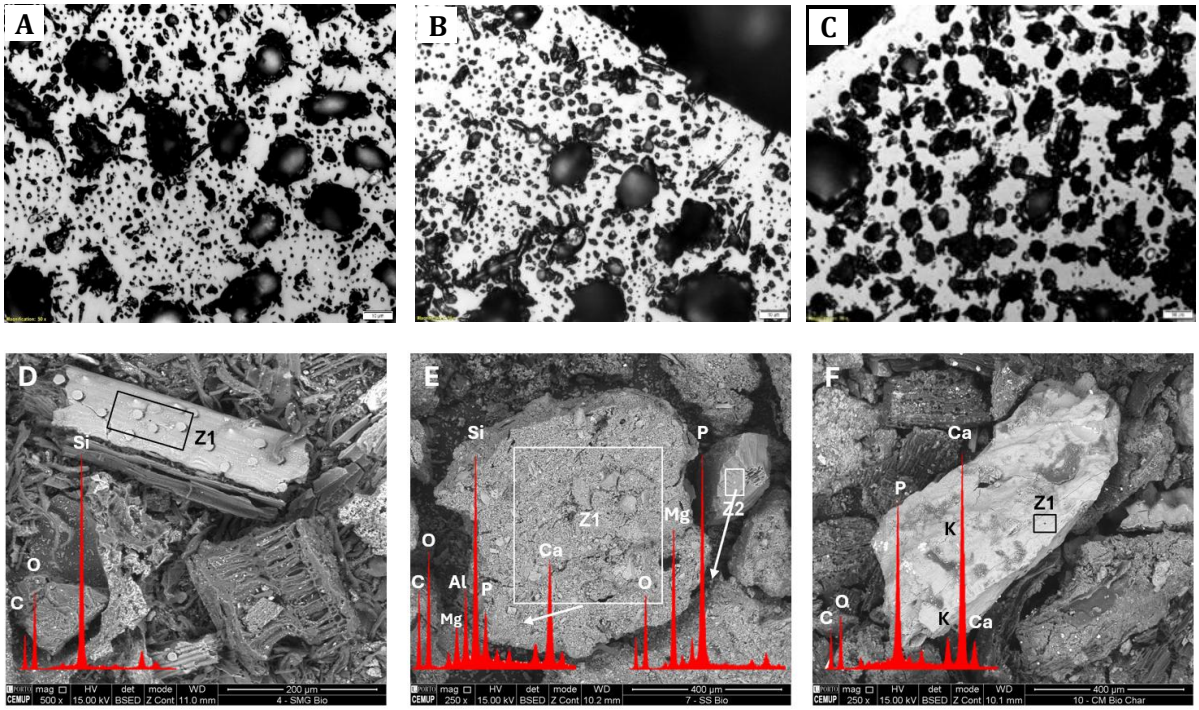

Figure 1. Petrographic Photomicrographs (A-C) and SEM/EDS images (D-F) of the biochar samples

Acknowledgements

Mobility Joint Call (2024) for funding the PREWA project "Sustainable Phosphorus Recovery from Waste through Integrated Environmental and Energy Management in the Clean Production Chain" through UEFISCDI-Romania (no. 10BMTR) and TUBITAK- Türkiye (no. 124N783). European Union's Horizon Europe program through the EXCITE2 project for TNA conducted at Porto University.

References

Beral, E., Zapan, M., 1962. Phosforus. In: Inorganic Chemistry. Editura Tehnic˘a, București, pp. 672.360–369 (in Romanian).

Drobniak, A., Mastalertz, M., Jelonek, Z., et al., 2025. Component Identification of Solid Biomass Fuels Using Reflected Light Microscopy: Interlaboratory Study 2. Inter. J. Coal Geol., 307, 104814.

Fahimi, A., Massa, M., Mousa, E., Ye, G., Predeanu G., Olgun, H., Mousavinezhad, S., Vahidi, E., Valentim, B., Białecka, B., Bontempi, E., 2024. Enhancing Phosphorus Recovery from Poultry Litter Ash through Microwave-Assisted Thermochemical Treatment for Improving Its Solubility. J. Environ. Manag. 379, 124802.

Kasina, M., Jarosz, K., Stolarczyk, M., Göttlicher, J., Steininger, R., Michalik, M., 2023. Characteristics of phosphorus rich compounds in the incinerated sewage sludge ashes: a case for sustainable waste management. Sci. Rep. 13, 1–11.

Predeanu, G., Slăvescu, V., Vasile, B.S., Valentim, B., Guedes, A., Santos, A.C., Ye, G., Mousa, E., 2024a. Characterization of the ash samples used for thermal recovery of phosphorus. In: A.G. Borrego (Ed.), Organic Petrology Research and applications for the 21st Century Book of Abstracts, p. 35.

Predeanu G., M. Wojtaszek-Kalaitzidi, I. Suarez Ruiz, Bălănescu M.N, A.G. Borrego, M.D. Ghiran, P.C. Hackley, S. Kalaitzidis, J. Kus, M. Mastalerz, M. Misz-Kennan, S. Pusz, S. Rodrigues, G. Siavalas, A. Varma, A. Zdravkov, D. Zivotic. 2024b. Structure and morphology of chars and activated carbons obtained from thermal treatment of coal and biomass origin materials, including their wastes: Results from the ICCP Microscopy of Carbon Materials Working Group. Inter. J. Coal Geol. 288, 104519.

Predeanu, G., Valentim, B., Popescu, L.G., Abagiu, A.T., Anghelescu, L., Guedes, B. A., Bălănescu, M.N., Drăgoescu, M.F., Slăvescu, V., Vasile B.S., Nicoară, A.I., Santos, A. C., Olgun, E.H., Kutlu, Ö., Mousa, E., Ye G., Bontempi, E., Massa, M., Białecka, B., Cempa, M. 2025a. Characterization of the ash samples before and after the microwave thermal extraction targeting products reuse in construction. 2025. Inter. J. Coal Geol. 307, 104808.

Predeanu, G., Bălănescu, M., Drăgoescu M. F., Slăvescu, V., Kutlu, O., Olgun, H. 2025b. Morphology of biochar used as a reducing agent in the process of phosphorus recovery from the P-rich ashes. Annals of the University „Alexandru Ioan Cuza" of Iași (new series) Special Issue, GEO-IAȘI 2025 International Scientific Symposium, OCTOBER 24-26, IAȘI, ROMANIA, 82-86, ISSN 1223-5342. Eds: Dan Stumbea, Daniel Țabără, Ciprian Chelariu.

Valentim, B., Guedes, A., Kuźniarska-Biernacka, I., Dias, J.M., Predeanu, G. 2024. Variation in the composition of municipal solid waste incineration. Minerals 14, 1146.

Design and efficiency assessment of a passive treatment system for acid mine drainage

Ruiwen Yan[1*]

[1]China University of Mining and Technology, Beijing, China

* *Corresponding Author: yanruiwen819@hotmail.com*

Acid mine drainage (AMD) refers to highly acidic, heavy metal-rich effluent generated from mining activities, potentially causing severe environmental contamination. Focusing on the Lujiang alum mine in Anhui Province, this study established a systematic framework for the design and assessment of an integrated passive AMD treatment system using the Phreeqc and AMDTreat software. Based on a comprehensive analysis of the onsite hydrogeochemical characteristics (pH: 2.93–3.06, Fe: 5.98–42.52 mg/L, and Al: 18.87–32.14 mg/L) and physical conditions (flow rate: 50–96 m3/h, available area: about 50000 m2), this study proposed a hybrid passive treatment system comprising a vertical flow wetland and a following aerobic artificial wetland. Finally, this study predicted the performance of the system using a Phreeqc-based hydrogeochemical model. The results indicate that the integrated passive treatment system could effectively increase the effluent pH to approximately 7.6 and yield high removal rates of above 99.0% for Fe and Al and above 97.0% for other heavy metals like Cu. Accordingly, the effluent quality after treatment satisfied the criteria for class III water specified in Chinese standard Environmental Quality Standards for Surface Water (GB 3838−2002). The life-cycle cost analysis performed using AMDTreat indicates that the construction costs and annual operation and maintenance (O&M) costs of the proposed system were approximately 3.68 million yuan and 0.46 million yuan, respectively. Therefore, this system enjoys significant long-term cost advantages over traditional active treatment technologies. The proposed design method that integrates technology selection, efficiency simulation, and economic assessment not only suits the AMD treatment of the Lujiang alum mine but also provides a scientific basis and technical reference for ecological restoration of similar mining areas.

Dispersed organic matter composition and thermal maturity of Upper Ordovician Boas River Formation from Hudson Platform in Northern Ontario, Canada

Julito Reyes[1*], Denis Lavoie[2], Derek Armstrong[2]

[1] Natural Resources Canada-Geological Survey of Canada-Calgary, [2] Natural Resources Canada-Geological Survey of Canada-Quebec, [3]Ontario Geological Survey (Emeritus)

* *Corresponding Author: julito.reyes@nrcan-rncan.gc.ca*

Chitinozoan-rich Upper Ordovician Boas River Formation lime mudstones collected from the Hudson Platform in Northern Ontario, Canada, were analyzed to determine dispersed organic matter (DOM) composition and thermal maturity. Organic petrography was conducted using a reflected confocal microscope equipped with the Hilgers Fossil system for white light and ultraviolet light fluorescence microscopy, as well as vitrinite reflectance (VR) analysis. Reflectance (R in percent) measurements were performed on chitinozoans and vitrinite-like macerals to determine thermal maturity, as true vitrinite was absent in the Ordovician formation. Bulk geochemical analysis was also performed using Rock-Eval6 to determine several key geochemical parameters (e.g., Tmax, TOC, etc.). The result of organic petrography show that DOM is composed mostly of thin bands of dark amorphous organic matter, with a trace amount of yellow to reddish fluorescing liptodetrinite inclusions observed under fluorescent light. It also contains significant amounts of greenish-yellow to yellow fluorescing cyanophytes, acritarchs, and prasinophytes. Chitinozoans, graptolites, conodonts, sponge spicules, and rare radiolaria were also observed in these samples. A thorough analysis of the chitinozoan macerals identifies two distinct genera, categorized as small ornamented and large unornamented (Figs. 1a and b). The average reflectance of vitrinite-like and chitinozoan macerals ranges from 0.60% to 0.69% and 0.76% to 0.85%, respectively. The calculated correlation between these macerals is $R_{vit\text{-}like} = 0.79R_{chi} + 0.013$, which is comparable to the previous correlation analysis by Reyes et al., 2018 on artificially matured Boas River Formation ($R_{vit\ like} = 0.77R_{chi}$) and by Obermajer et al., 1996 on whole rock samples (R_{chi} 20-25% higher than VR) from the same region. The vitrinite-like and the vitrinite reflectance equivalent (VR_{eqv}) of the chitinozoan (0.59% to 0.68%) are higher than the VR_{eqv} (0.40% - 0.51%) of the measured Tmax (421°C-426°C). Overall, geochemical analysis corroborates the organic petrography and VR results, indicating that these samples are organic-rich but mostly immature with TOC values ranging from 3.28 wt.% to 12.84 wt.%. The high hydrogen index (HI = 464-634 mg HC/g TOC) and low oxygen index (OI = 17-32 mg CO_2/g TOC) show that these samples are mostly Type I kerogen with very good to excellent hydrocarbon potential as the high S2 (12.11-71.67 mg HC/g rock) indicates. However, the low S1 (0.91–3.11 mg HC/g rock) confirms that no significant hydrocarbons have been generated, as the samples are thermally immature.

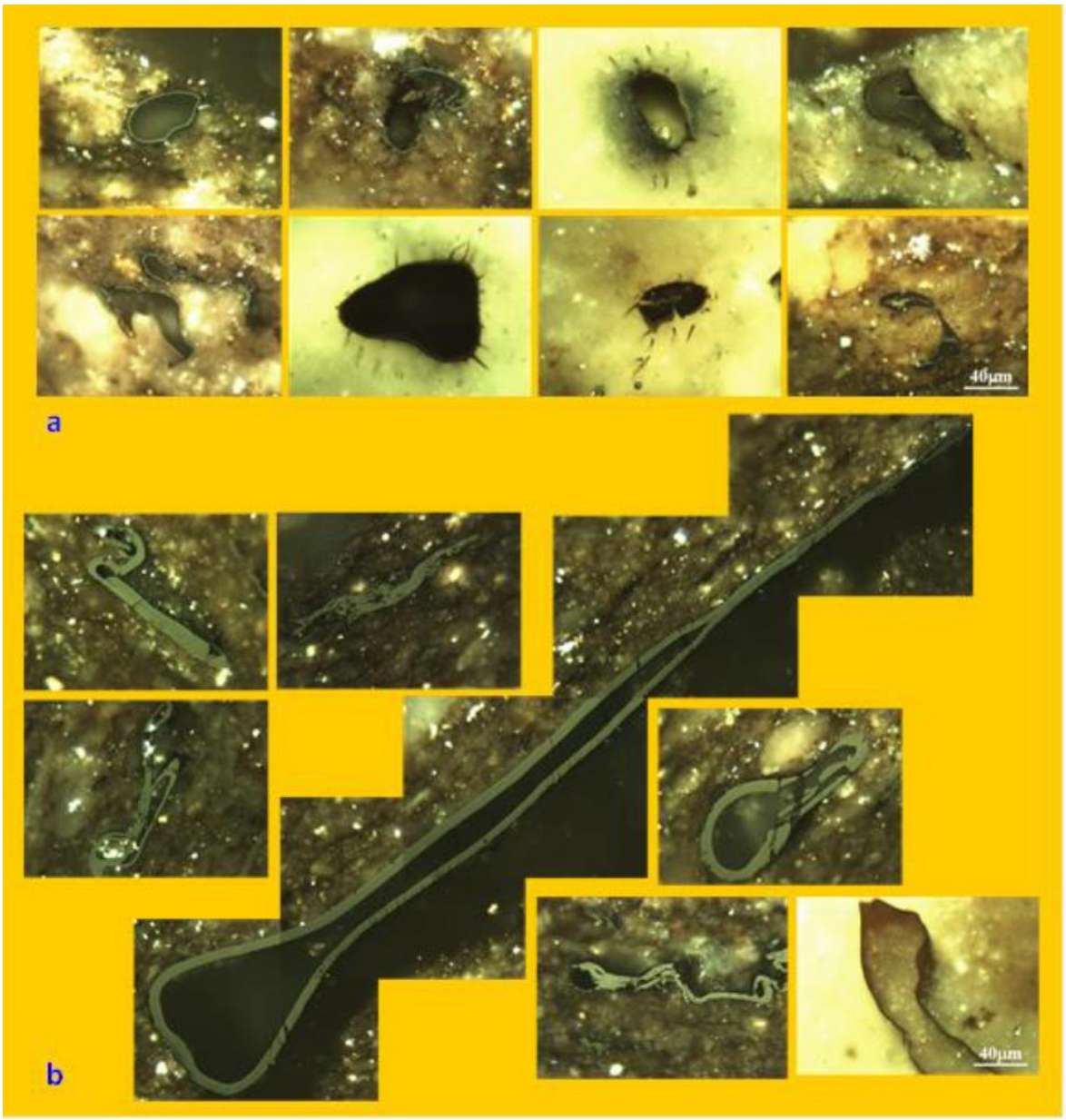

Figure 1. Photomicrographs showing two distinguishable genera of chitinozoan genera from the Boas River Formation. (a) Small, ornamented with simple spinose structures. (b) Large, unornamented, with varying sizes and wall thickness.

References

Obermajer, M., Fowler, M.G., Goodarzi, F., Snowdon, L.R. 1996. Assessing thermal maturity of Paleozoic rocks from reflectance of chitinozoa as constrained by geochemical indicators: an example from southern Ontario, Canada. Mar. Petro. Geol. 13, 907–919.

Reyes, J., Jiang, C., Lavoie, D., Armstrong, D K., Milovic, M., Robinson, R., 2018. Organic petrographic analysis of artificially matured chitinozoan- and graptolite-rich Upper Ordovician shale from Hudson Bay Basin, Canada. Inter. J. Coal Geol. 199, 138–151. (NRCan Contr. # 20180057)

Occurrence and thermal transformation of lithium in Late Permian coal-bearing strata from the Xian'an Coalfield, Guangxi Province, South China

Xiaoyun Yan[1,2*], Zhipeng Wang[1], Jie Sun[2], Yurong Zhu[1]

[1]China University of Mining and Technology, Beijing, China; [2]General Prospecting Institute of China National Administration of Coal Geology, Beijing, China

* *Corresponding Author: xyun.yan@outlook.com; xiaoyunyan@cumtb.edu.cn*

Lithium-enriched coal-bearing strata have recently emerged as a promising unconventional lithium resource because of their considerable resource potential and strategic importance in the global energy transition. However, the occurrence modes of lithium and its behavior during thermal activation remain insufficiently understood, limiting the efficient utilization of these resources.

This study investigates lithium-bearing strata within the Late Permian coal measures of the Xian'an Coalfield, Guangxi Province, South China. Mineralogical, geochemical, and sequential chemical extraction analyses were conducted to determine the occurrence modes of lithium and to evaluate its migration and transformation during calcination. X-ray diffraction (XRD), scanning electron microscopy coupled with energy-dispersive spectroscopy (SEM-EDS), X-ray fluorescence spectroscopy (XRF), and inductively coupled plasma mass spectrometry (ICP-MS) were employed to characterize mineral assemblages and elemental distributions. Sequential chemical extraction was combined with staged calcination experiments (400-900°C) to quantify changes in lithium occurrence states. Lithium concentrations in the investigated samples ranged from 4.69 to 5,083.68 μg/g, the strongest enrichment occurring in the Wanfu mining area on the western side of the coalfield.

The lithium-bearing strata are dominated by clay minerals, including kaolinite, illite-smectite mixed-layer minerals, illite, and cookeite. In uncalcined sample X-4, 91.86% of total lithium occurred in the insoluble aluminosilicate fraction, demonstrating that lithium is predominantly incorporated into clay-mineral lattices through isomorphous substitution. Calcination substantially redistributed lithium among the operationally defined fractions. The insoluble aluminosilicate fraction decreased to a minimum of 12.55% at 700°C in sample X-1 and 9.33% at 800°C in sample X-4; the combined proportion of the four more extractable fractions reached 87.45% and 90.67%, respectively. 700-800°C represents the optimum calcination window for liberating lattice-bound lithium in the investigated samples. At 900°C, the insoluble fraction rebounded to 70.95% in X-1 and 75.43% in X-4, consistent with lithium reincorporation into newly formed refractory aluminosilicate phases.

These findings demonstrate that clay minerals are the principal hosts of lithium in the Xian'an coal-hosted lithium deposit and that thermal activation plays a critical role in modifying lithium occurrence modes. This study provides new insights into lithium enrichment mechanisms in coal-bearing strata and offers a theoretical basis for optimizing lithium extraction from coal hosted lithium resources.

Tracing coal-derived organic matter in Appalachian watersheds using organic petrography

Jennifer Nedzweckas[1*], Matthew Varonka[1], Javin Hatcherian[1], Rebecca Smith[1], Paul Hackley[1]

[1]US Geological Survey, Reston, USA

* *Corresponding Author: jnedzweckas@usgs.gov*

Coal mining can contribute substantial quantities of carbonaceous material to stream sediments, yet the distribution, persistence, and composition of coal-derived organic matter within Appalachian watersheds remain poorly constrained. Organic petrography provides a means to distinguish coal-derived particles from naturally occurring organic matter and may offer a transferable approach for studying environmental contamination in mining-impacted systems.

This study analyzed nine stream sediment samples from three mining district clusters across approximately 1,000 square kilometers in southern West Virginia, covering multiple watersheds impacted by active, mothballed, and closed mines. Sediment samples were processed through acid digestion and heavy liquid separation to produce organic concentrates for petrographic analysis. Reflectance measurements and a 500-point maceral count method were conducted to quantify vitrinite, liptinite, inertinite, pyrite, modern woody material, modern spores, modern inert organic matter, and residual mineral matter. Geographic information system analysis was used to characterize the spatial relationship between sample locations and potential contamination sources.

Preliminary petrographic results indicate that coal-derived organic matter dominates most organic concentrates, with vitrinite typically comprising 67-79% of counted particles and reflectance values ranging from approximately 0.75 to 0.99% R_o. Despite differences in proximity to individual mining operations, many samples exhibit broadly similar coal-derived maceral assemblages, suggesting widespread distribution of coal-related organic matter across the study area. In contrast, one sample associated with the southernmost mining district contains substantially higher mineral matter, abundant woody material, elevated reflectance values (~1.23% R_o), and a markedly reduced coal-derived component, indicating a distinct depositional- or source-related signature.

These results demonstrate the utility of organic petrography for distinguishing coal-derived and modern organic matter in environmental samples and provide the foundation for future integration with bulk geochemical data. The workflow developed in this study may serve as a transferable environmental forensic approach for evaluating legacy and active mining impacts in Appalachian watersheds and other sedimentary systems affected by anthropogenic carbonaceous materials.

Advances on the impact of broad ion beam milling techniques on organic-rich samples

Brett J. Valentine[1*], Paul C. Hackley[1], Jennifer Nedzweckas[1], Javin J. Hatcherian [1], Margaret M. Sanders[1]

[1]U.S. Geological Survey, Reston, VA, USA

** Corresponding Author: bvalentine@usgs.gov*

Broad ion beam (BIB) milling is an advanced preparation method for organic rich geologic materials, but several questions remain regarding reproducibility of surface quality, impact on vitrinite reflectance (R_o), and if BIB could reduce R_o variability. New BIB tests (single gun, 2-8 kV, cooled and non cooled) on a series of seven coals ranging from 0.60–1.74% R_o were performed to evaluate: (1) reproducibility across BIB systems with single versus dual ion guns; (2) whether cooling reduces post milling R_o; and (3) whether BIB decreases R_o standard deviation.

Comparisons between dual gun (Valentine et al., 2019) and single gun systems at 6 kV (3°angle, no cooling, 4 rpm rotation) from lignite to anthracite show similar increases in post milling R_o (single gun avg. R_o increase = 0.25%, avg. std dev 0.057; dual gun avg. R_o increase = 0.23%, avg. std dev 0.050). These results indicate that, regardless of gun configuration, comparable beam conditions (kV, angle, rotation) yield similar relative R_o increases. Lower voltage milling (2-4 kV) still produced elevated R_o values but at half the amount of change (+0.13% avg. R_o increase) compared to 6 kV (+0.26% avg. R_o increase), likely because reduced ion energy causes less surface modification, producing surfaces similar to traditional mechanical polishing.

Cooling the sample surface to -6 °C during milling did not reduce post milling Ro or improve data quality. Of five tested coals, three cooled samples showed higher R_o than their counterparts milled at the same conditions non cooled, and all but one of the cooled samples exhibited higher R_o standard deviations. Sample cooling therefore offers no measurable benefit for reflectance analysis, though it may still be needed for nanoscale analytical applications (e.g., SEM, TEM).

Previous studies (Grobe et al., 2017; Burnaz et al., 2023) suggested that ion milling improves R_o measurement consistency, but our results show that BIB alone does not reliably reduce Ro variability. Changes in standard deviation ranged from -0.048 to +0.046 (avg. +0.005; n = 25). Using modified mechanical polishing techniques to achieve an improved surface prior to BIB may improve consistency, but interlaboratory reproducibility remains uncertain, and the influence of milling artifacts on R_o requires further investigation.

Overall, any deviation from standard polishing protocols affects reflectance outcomes. While BIB milling may not improve R_o analysis, its ability to prepare nanometer scale surfaces makes it valuable for advanced analytical investigations beyond thermal maturity assessment.

References

Burnaz, L., Zieger, L., Schmatz, J., Botero, A.E., Amberg, S., Thüns, N., Littke, R., 2023. Preparation techniques for microscopic observation of dispersed organic matter and their effect on vitrinite reflectance. Int. J. Coal Geol. 272, 104249.

Grobe, A., Schmatz, J., Littke, R., Klaver, J., Urai, J.L., 2017. Enhanced surface flatness of vitrinite particles by broad ion beam polishing and implications for reflectance measurements. Int. J. Coal Geol. 180, 113-121.

Valentine, B.J., Hackley, P.C., Hatcherian, J.J., Yu, J.-J., 2019. Reflectance changes from broad beam ion milling of coals and organic-rich shales due to increased surface flatness: Int. J. Coal Geol. 201, 86-101.

How feedstock and pyrolysis conditions influence biochar soil phytotoxicity

J.N.G.V. Canedo[1], C. Garcia Neto[2*], L. Coelho[1,3], P. Souza Alonso[4], P. Mourão[1,5], R. Castillo Corrêa[1], A. Silva Trindade[1], D. Flores[2†], F. Silva[6], L. Tarelho[6], S. Prats[1,7]

[1]MED – Mediterranean Institute for Agriculture, Environment and Development & CHANGE – Global Change and Sustainability Institute, Instituto de Investigação e Formação Avançada, Universidade de Évora, Évora, Portugal; [2]Institute of Earth Sciences and Departamento de Geociências, Ambiente e Ordenamento do Território, Faculdade de Ciências, Universidade do Porto, Porto, Portugal; [3]GreenCoLab – Associação Oceano Verde, Universidade do Algarve, Faro, Portugal; [4]Department of Soil Science and Agricultural Chemistry, Higher Polytechnic Engineering School, University of Santiago de Compostela, Lugo, Spain; [5]Department of Chemistry and Biochemistry, School of Science and Technology, University of Évora, Évora, Portugal; [6]CESAM, Centre for Environmental and Marine Studies, Department of Environment and Planning, University of Aveiro, Aveiro, Portugal; [7]Misión Biológica de Galicia – National Spanish Research Council (MBG-CSIC), Pontevedra, Spain.

* *Corresponding Author: cgarcia@fc.up.pt*

Understanding ecological trade-offs is essential for the safe application of biochar in soil restoration, particularly regarding how feedstock and production conditions influence phytotoxicity. This study evaluates thirteen biochars derived from: vineyard prunings and stalks in different proportions (4), *Acacia sp.* shredded wood (2), olive pomace (5), and açaí waste (2). Biochars were produced under varying pyrolysis temperatures (450–800 °C) and residence times (15 min to 12.5 h), with or without hydrothermal activation and macronutrient enrichment (N, P and K). Physicochemical characterization – pH, electrical conductivity (EC), organic matter (OM), water holding capacity (WHC), carbon, nitrogen contents, Mehlich-3 extractable nutrients, polycyclic aromatic hydrocarbons (PAHs), FTIR spectroscopy, thermogravimetric analysis and inertinite content – were combined with phytotoxicity assessment using Lactuca sativa germination and root elongation assays across two different soils.

Feedstock type was the main driver of phytotoxicity. *Acacia sp.* wood biochars, with high OM (~93.8%) and low EC (0.5–0.6 dS m^{-1}) and PAHs (<0.2 mg kg^{-1}), showed the lowest toxicity. Vineyard pruning biochar, despite similarly high OM (~93.5%) and low EC (~0.3 dS m^{-1}), exhibited slightly higher toxicity, likely due to its higher PAH content (~2.52 mg kg^{-1}). In contrast, olive pomace and vineyard stalk biochars showed greater toxicity, mainly associated with high EC (9.4-11.4 dS m^{-1}) and elevated PAHs (up to 10.6 mg kg^{-1}), respectively. Hydrothermal activation of olive pomace biochars reduced PAHs (1.14 to 0.08 mg kg^{-1}) but increased salinity-driven toxicity, while macronutrient enrichment of açaí biochar slightly increased OM (65-71%) and EC (0.8-1 dS m^{-1}) without affecting phytotoxicity. Variations in pyrolysis temperature and residence time had comparatively minor effects on both biochar properties and soil phytotoxicity as compared to feedstock type.

Overall, wood-derived biochars (*Acacia sp*. or vineyard pruning) applied at 3-5% are the most suitable for soil restoration, enhancing Lactuca sativa germination and root growth. Biochar application at 3-5% optimized soil conditions, particularly in acidic and low organic matter soils, by promoting pH neutralization and increasing water retention. However, biochars from agricultural residues require pre-application screening, particularly for salinity and PAHs, which remain key factors controlling environmental safety.

Acknowledgments

This work was funded by National Funds through FCT under the Project SOLVO (https://doi.org/10.54499/2022.06004.PTDC) and the MED - Mediterranean Institute for Agriculture, Environment and Development (https://doi.org/10.54499/UIDB/05183/2020) and CHANGE – Global Change and Sustainability Institute (https://doi.org/10.54499/LA/P/0121/2020) for their support. Sergio Prats was supported by the Portuguese Science Foundation (FCT) through research contract CEECIND/01473/2020 and the Spanish Ministry of Science, Innovation and Universities

through research contract RYC2022-035489-I. C. Garcia Neto acknowledge the financial support provided to the Institute of Earth Sciences (ICT) through the multi-annual funding contract with the Foundation for Science and Technology (FCT), under project UID/04683/2025 with the DOI https://doi.org/10.54499/UID/04683/2025.

Subsurface CO_2 storage potential in Romania: mineralogical, geochemical and organic petrography evaluation of primary reservoir and unmieneable coal frontiers

Izabela Mariș[1,2*], Doina Maria Ghiran[1], Stefania Gheorghe[1], Roxana Pirnea[3], Georgeta Predeanu[4], Mihai-Emilian Popa[5]

[1] OMV Petrom SA, Core and Cuttings Technologies Laboratory, Câmpina, Romania; [2]University of Bucharest, Faculty of Geology and Geophysics, Department of Mineralogy, Bucharest, Romania; [3]Independent researcher, Timișoara, Romania; [4]University Politehnica of Bucharest, Faculty of Applied Chemistry and Materials Science, Research Center for Environmental Protection and Eco-friendly Technologies, Bucharest, Romania; [5]University of Bucharest, Faculty of Geology and Geophysics, Doctoral School of Geology, Bucharest, Romania.

** Corresponding Author: izabela@contentlogic.ro*

The permanent geological storage of carbon dioxide (CO_2) in subsurface formations is a critical mechanism for mitigating industrial emissions, requiring a comprehensive understanding of complex rock-fluid interactions. This study delivers a multidisciplinary petrophysical, mineralogical, geochemical and organic petrography evaluation of prospective siliciclastic and carbonate formations across important Romanian stratigraphic intervals – including the Badenian, Oligocene and Middle Jurassic, within Getic Depression. This research establishes the first systematic inventory of primary structural reservoirs alongside a strategic evaluation of unmineable coal seams as a secondary frontier for adsorption-based CO_2 storage.

Using core samples, a focused workflow was deployed to assess structural traps and distinct coal matrices. Thin-section petrography and cathodoluminescence (CL) microscopy identified primary reservoir textures and diagenetic features. Mineralogical vulnerabilities were quantified via XRD, XRF, and high-resolution SEM-EDS to predict CO_2-brine reactions, specifically mapping nanoscale carbonate dissolution and permeability-blocking mineral precipitation. The coal seams were evaluated with organic petrography analysis.

The study evaluates Romania's diverse sites with organic rock deposits to anticipate gas adsorption capacities and matrix-swelling dynamics for potential CO_2-Enhanced Coalbed Methane pathways. The analytical workflow differentiates between distinct coal frontiers, from the deeply buried Middle Jurassic sequences characterized by vitrinite rich matrices optimized for high volume adsorption, to younger Oligocene coals rich in humic and terrestrial organic matter, and Badenian coals which feature lower nano-porosity and higher liptinite content (Table 1).

By integrating these diverse datasets, this project provides a robust predictive framework for long-term containment security and porosity-permeability evolution. Ultimately, these results serve as a foundational asset for Romania's national subsurface screening initiatives, de-risking site selection, reducing future emission liabilities, and accelerating scalable carbon management infrastructure in East-Central Europe.

Table 1

Age	TOC (%)	Tmax (ºC)	VR (%)	Kerogen	Macerals
Badenian	<1,82	409 - 443	0.41 - 0.55	III	Terrigenous macerals (vitrinite, liptinite as, resinite, cutinite, sporinite, and inertinite) associated with marine liptinite macerals (telalginite and lamalginite)
Oligocene	0.55 – 5.71	415 - 435	0.32 – 0.53	II -III and III	Humic and terrestrial organic matter, as well as sapropelic, marine, algal matter, represented by telalginite and lamalginite
Dogger	0.87 – 7.22	426 - 484	0.65 -0.90	III and IV	Vitrinite, liptinite, inertinite

Oil-source rock correlation in the Ediacaran of Pakistan tested through hydrous pyrolysis

Paul C. Hackley[1*], Michael Lewan[2]

[1] U.S. Geological Survey, Reston, USA; [2]Lewan GeoConsulting Corporation, Golden, USA

* *Corresponding Author: phackley@usgs.gov*

Neoproterozoic petroleum systems of Asia are widespread and well-documented in Oman, Siberia, China, India, and Pakistan. However, stacked source rock intervals are present in most basins and oil-source rock correlations remain largely untested, underscoring the value of delineating the geochemical fingerprints of petroleum generated from individual potential source rocks. Here we used hydrous pyrolysis to generate petroleum from oil shale in the Ediacaran Salt Range Formation (SRF), a potential source rock for oils produced from the Kohat and Potwar basins of northern Pakistan, and from the Bikaner-Nagaur Basin of northern India. Two experiments used 30 and 96 g, respectively, of a SRF oil shale sample with total organic carbon (TOC) and hydrogen index values of 38–40 wt.% and 674–709 mg/g, respectively, treated at 355°C for 72 h for maximum oil yield. The experiments generated light crude oil with an API gravity of 31.2. Oil yields ranged 161–269 mg/g TOC, with the lower value attributed to poor recovery. Generated gases in decreasing order of abundance included CH_4, CO_2, C_2H_6, H, C_3H_8, H_2S, and minor C_4H_{10}, with gas dryness values (C_1/C_{1+}) ranging 0.92–1.19. Fractionation of the generated oil yielded a low saturate-to-aromatic ratio (1.23) with 14.9% polar compounds and 4.9% asphaltene compounds. Pristane/Phytane (Pr/Ph) ratios ranged 1.34–1.45 and Pr/*n*-C_{17} and Ph/*n*-C_{18} ratios ranged 0.34–0.42 and 0.29–0.39, respectively. Terrestrial-to-aquatic ratios of normal alkanes [(C_{27} +C_{28} +C_{29})/(C_{15} +C_{17} +C_{19})] were intuitively low (0.04–0.08) due to the global absence of higher plants in Ediacaran. Carbon isotopic compositions of the whole oil and fractions were highly depleted with $\delta^{13}C$ (‰) values of -35.04 to -36.09. The whole oil contained high proportions of C_{29} monoaromatic steroids and sterane compounds. Generated oils share geochemical signatures similar to those of Neoproterozoic oils from Oman, Siberia, China, India, and from elsewhere in Pakistan, particularly with respect to the highly depleted $\delta^{13}C$ signature and $C_{29} > C_{28}$ and C_{27} steranes and monoaromatic steroids. However, we note that Ediacaran SRF oil shale samples present a diverse range in geochemical composition (Hackley et al., 2026) with the expectation that future hydrous pyrolysis experimentation using other SRF samples could yield oils of increasingly diverse character. This study provides direct experimental evidence of petroleum which could be sourced from Ediacaran source rocks and may improve understanding of the regional petroleum systems in Pakistan and India.

References

Hackley, P.C., McAleer, R.J., Thompson, J.M., Valentine, B.J., Khan, I., 2026. Data to determine new age constraints on the Ediacaran Salt Range Formation of Pakistan: U.S. Geological Survey data release, https://doi.org/10.5066/P1WRBPG6.

Catalytic graphitisation of wood-derived biochar using manganese ore

Malgorzata Wojtaszek-Kalaitzidi[1*], Aneta Michałek[1], Anna Rodź[1], Bartosz Mertas[1], Rui Rocha[2]

[1]Institute of Energy and Fuel Processing Technology, Zabrze, Poland; [2]Materials Center of the University of Porto, Porto, Portugal.

* *Corresponding Author: mwojtaszek@itpe.pl*

Replacing fossil carbon materials with renewable biogenic carbon requires a detailed understanding of the structural transformations that biochar may undergo under high-temperature industrial conditions. Among these transformations, catalytic graphitisation is of particular importance because it may significantly increase the structural ordering of biochar and promote the development of semi-graphitic or graphite-like carbon phases. This study presents experimental investigations of catalytic graphitisation of wood-derived biochar in the presence of manganese ore.

The starting material was a wood-derived biochar characterised by a mean reflectance of 4.7%, indicating a relatively high degree of thermal maturity. Graphitisation experiments were performed in closed crucibles made of temperature-resistant silicon carbide. The manganese ore was mixed with biochar in a 50:50 weight ratio. The tests were carried out in a high-temperature furnace at 1500°C under conditions of limited access to air in order to promote carbon structural transformation while restricting extensive oxidation or uncontrolled reduction reactions. The process was maintained for 5 hours and followed by rapid furnace cooling. After the experiment, representative material was collected and used to prepare polished pellets for microscopic and spectroscopic examination.

The reaction products were investigated using reflected-light microscopy with an AxioImager M1m microscope, scanning electron microscopy coupled with energy-dispersive X-ray spectroscopy using an FEI Quanta 400 SEM-EDS system, and Raman spectroscopy with an InVia Raman micro-spectrometer.

Petrographic observations revealed that catalytic graphitisation led to the transformation of the original amorphous and isotropic biochar structure into an anisotropic, flake-like texture (Fig. 1). Two main types of graphitic material were distinguished. The first type represents ex-situ precipitated graphite, formed from droplets of separated metal-rich phases. This material developed as relatively thick layers showing typical graphite lamination. The second type consists of graphitised biochar particles, in which structural reorganisation occurred within the original biochar framework without substantial modification of particle morphology. This indicates that biochar may undergo in-situ transformation into a more ordered carbon phase while largely preserving its inherited cellular or particle structure.

SEM images and EDS-supported observations confirmed the platy morphology and anisotropic character of the graphitised biochar. Raman spectra further demonstrated the development of an ordered graphite-like structure. The semi-graphitic biochar and precipitated graphite showed comparable degrees of ordering, although both retained significant structural defects. These results indicate that manganese ore strongly promotes catalytic graphitisation of biochar under high-temperature, oxygen-limited conditions, relevant to sustainable metallurgical carbon production.

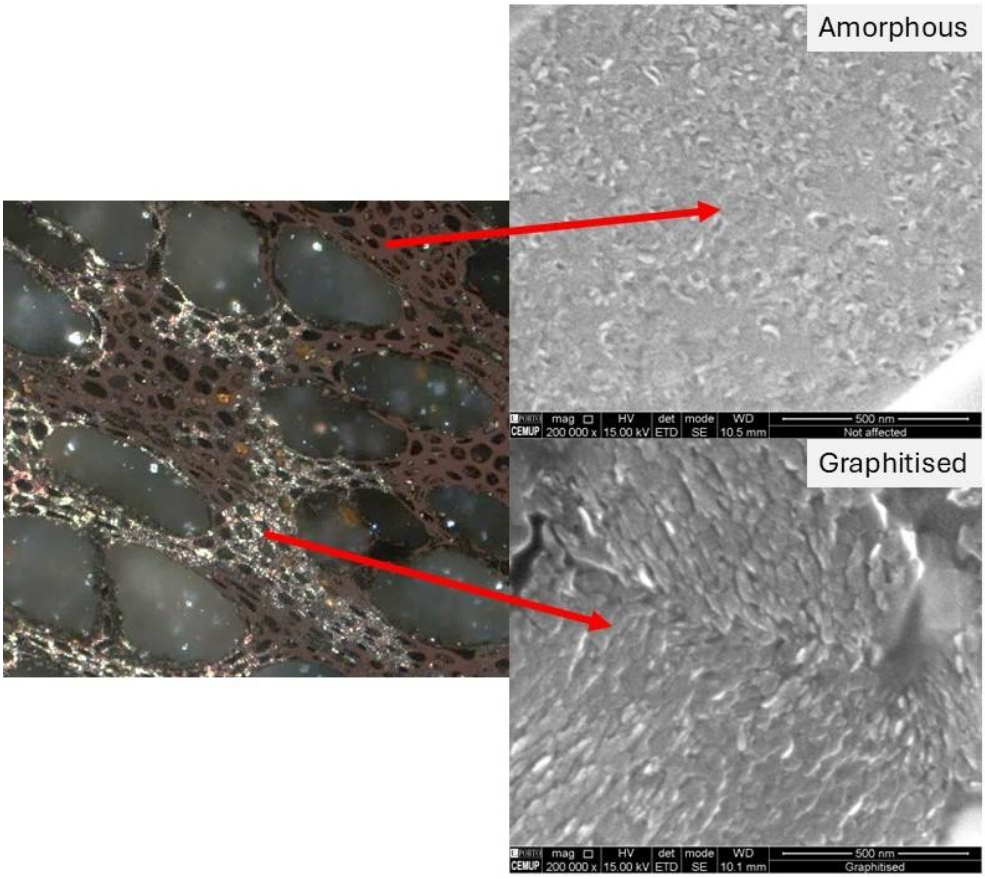

Figure 1. Comparison of unaffected amorphous biochar and anisotropic graphitised biochar. Left: incident-light photomicrograph obtained under polarised light with a lambda plate, 500× magnification, oil immersion. Right: SEM images showing the corresponding textural features

Study on the coupling mechanism of sulfur migration and carbon structure evolution during coal heating

Tang Yuegang[1*], Xue Liping[1], Bai Xiangfei[2], Gao Shuo[3]

[1]College of Geoscience and Surveying Engineering, China University of Mining & Technology, Beijing, China; [2]Research Institute of Coal Chemistry, China Coal Research Institute, Beijing, China; [3]College of Geosciences, China University of Petroleum, Beijing, China

** Corresponding Author: tyg@cumtb.edu.cn*

In this study, coal samples with varying organic sulfur contents were investigated using gold-tube thermal simulation and autoclave direct liquefaction experiments, combined with multiple analytical techniques including GC-MS, FTIR, XPS, XRD, and HRTEM. The systematic investigation focused on the migration patterns of sulfur, the evolution characteristics of carbon structures, and their coupling mechanisms during coal heating. The results show that H_2S yield is controlled by the initial total sulfur content and increases with temperature. During liquefaction, Fourier transform ion cyclotron resonance mass spectrometry (FT-ICR MS) analysis revealed that S_1 class compounds in the tetrahydrofuran extracts of raw coal had carbon numbers distributed between 10 and 43 and double bond equivalents (DBE) ranging from 0 to 26. After liquefaction, S_1 compounds shifted toward higher DBE and carbon numbers, with carbon numbers concentrated between 13 and 24, while aliphatic sulfur compounds essentially disappeared. In terms of carbon structure evolution, both the aromaticity index I and the degree of condensation index DOC showed nonlinear increases with increasing coalification during thermal simulation. The aromaticity index I of low-organic-sulfur coal remained consistently higher than that of high-organic-sulfur coal, indicating that organic sulfur content reduces the degree of coal aromatization. The aliphatic hydrogen content H_{al}/H decreased with increasing coalification, suggesting continuous cleavage of aliphatic structures. After liquefaction, the average interlayer spacing d_{002} of the residues decreased significantly compared to raw coal, while crystallite sizes L_a and L_c, the average number of aromatic layers N_{ave}, and the coalification degree ρ all increased substantially. Meanwhile, the L_a/L_c ratio decreased notably, indicating that crystallite growth was dominated by vertical stacking. HRTEM observations revealed that onion-like fullerene structures were widely developed in low-organic-sulfur coal but were rare in high-organic-sulfur coal, suggesting that organic sulfur may inhibit the development of ordered carbon structures. The coupling between sulfur migration and carbon structure evolution exhibited distinct stage-dependent characteristics: low-evolution stage (300–400 °C), medium-evolution stage (400–500 °C), high-evolution stage (500–600 °C). This study reveals a three-stage coupling mechanism under the dominance of organic sulfur: at the low-evolution stage, sulfur drives carbon decomposition; at the medium-evolution stage, sulfur and carbon constrain each other; and at the high-evolution stage, the progressively condensed carbon structure restricts further sulfur release. This mechanism provides a theoretical basis for the targeted regulation of sulfur and the optimization of carbon structures during coal thermal conversion.

Acknowledgements
This research was supported by the National Natural Science Foundation of China (42030807).

Organic petrographical and geochemical reappraisal of the Mesozoic sedimentary formations in Kurdistan Region, Northern Iraq

Maria Elli Damoulianou[1], Polla Khanaqa[2], Ibrahim M.J. Mohialdeen[3], Kamal Y. Kolo[4], Stavros Kalaitzidis[1*]

[1]Department of Geology, University of Patras, Rio-Patras, Greece; [2] Kurdistan Institution for Strategic Studies and Scientific Research, Sulaimani, Kurdistan, Iraq; [3] Department of Earth Sciences and Petroleum, College of Science, University of Sulaimani, Sulaimani, Kurdistan, Iraq; [4] Department of Petroleum Geoscience, Soran University, Soran, Kurdistan, Iraq

* *Corresponding Author: skalait@upatras.gr*

The present study focuses on nine Mesozoic oil- and gas-prone sedimentary formations outcropping in Kurdistan Region, Iraq, while covering a wide chronostratigraphic range, from Late Triassic to Early Cretaceous. These well-known Formations, from the oldest to the younger, include Butmah Fm. (Upper-Triassic-Lower Jurassic), Adaiyah Fm. (Lower Jurassic), Mus and Alan Fms. (Lower Jurassic), Sargelu Fm. (Middle Jurassic), Naokelekan Fm. (Middle-Upper Jurassic; Damoulianou et al., 2020), Chia Gara Fm. (Upper Jurassic; Damoulianou et al., 2022), as well as Sarmord and Balambo Fms. (Lower Cretaceous; Sarraj et al., 2019). The aim of the study is to evaluate the oil and gas generation potential for each of the nine Mesozoic Formations, in terms of organic matter type and thermal maturity, parameters being both crucial for the amount and kind of the hydrocarbons produced. Furthermore, elucidating any trend between the source rock features of the Formations and their age is a secondary scope of this study. The objectives refer to organic petrographical examination, including organic matter identification and random vitrinite reflectance measurements, as well as Rock-Eval analyses, providing kerogen type, PI and T_{max} data, while GC-MS data are evaluated in the case of Naokelekan Formation.

Regarding the oldest five Formations, from the Upper Triassic - Lower Jurassic Butmah Fm. to Middle Jurassic Sargelu Fm., the Rock-Eval analysis has revealed the predominance of the gas-prone kerogen type III and poor/fair generation potential. The organic petrography revealed the predominance of overmature solid bitumens. Lower Adaiyah Fm., is exceptional, being characterized by mixed II/III types that show marginally good PI. Naokelekan Fm., has been studied in four outcrops, generally showing predominance of solid bitumens and mixed II/III kerogen types. The maturity of the Fm., based on petrographical and various geochemical parameters, increases from NW towards SE, coinciding to the established general maturation trend for all the Fms, and in accordance with the development of the main depocenter in Northern Iraq. Upper Jurassic Chia Gara Fm. is bitumen/bituminite rich and falls within the main oil generation window. Finally, both the Lower Cretaceous Sarmord and Balambo Fms. are rich in solid bitumens and poor in primary macerals, with the older Sarmord Fm. falling within the main oil generation window according to modified infrared spectrometry data, and the later Balambo Fm. reaching the beginning of the oil generation according to petrographic data. Overall, according to the organic petrographical and geochemical proxies of nine Mesozoic Formations in Kurdistan Region, all the Fms. show similar qualitative petrographic features, with predominance of solid bitumens and subordinate occurrence of primary macerals.

References

Damoulianou, M.E. Kolo, K.Y., Borrego, A.G., Kalaitzidis, S.P., 2020. Organic petrological and geochemical appraisal of the Upper Jurassic Naokelekan Formation, Kurdistan, Iraq. Int. J. Coal Geol. 232, 103637.

Damoulianou, M.E., Perleros, K., Mohialdeen, I.M.J., Khanaqa, P., Araujo, C.V., Kalaitzidis, S., 2022. Characterization of the bituminite-rich Chia Gara Formation in M-2 well Miran Field, Kurdistan Region, NE Iraq. Int. J. Coal Geol. 263, 104115.

Sarraj, R.H.A., Mohialdeen, I.M.J., Kalaitzidis, S., 2021. Organic petrographical features and thermal maturity assessment of the Cretaceous Balambo Formation from Zagros Fold-Thrust Belt, Kurdistan Region, Northern Iraq. Arab. J. Geosci. 14, 21.

Organic matter characterization across the Upper Triassic–Lower Jurassic succession of the Lusitanian Basin (Portugal)

Paula Alexandra Gonçalves[1,2*], Augusto Silva[2], Dariusz Więcław[3], João Graciano Mendonça Filho[4], Deolinda Flores[1,2†]

[1]Instituto Ciências da Terra - Pólo da Faculdade de Ciências da Universidade do Porto, Portugal; [2]Departamento de Geociências, Ambiente e Ordenamento do Território, Faculdade de Ciências, Universidade do Porto, Portugal; [3] Faculty of Geology, Geophysics and Environmental Protection, AGH University of Krakow, Poland; [4]Laboratory of Palynofacies and Organic Facies (LAFO), Federal University of Rio de Janeiro, Rio de Janeiro, Brazil. † Deceased

* *Corresponding Author: paula.goncalves@fc.up.pt*

Despite significant advances in the understanding of the Upper Triassic-Lower Jurassic succession of the Lusitanian Basin in Portugal, particularly from the Sinemurian-Toarcian interval, the composition and preservation of the organic matter (OM), as well as the HC potential of the source-rocks across the Triassic-Jurassic transition remain poorly constrained. To address this gap, a multi-proxy approach combining total organic carbon (TOC), Rock-Eval 7S pyrolysis and organic petrology was applied in a set of cuttings from the Alcobaça-1 well, which provides a continuous Upper Triassic-Lower Jurassic record comprising siliciclastic, evaporitic and carbonate deposits.

The Triassic-Hettangian interval is characterized by low TOC and S2 values, varying from 0.12 to 0.78 wt.% and from 0.06 to 0.54 mg HC/g, respectively, indicating a poor HC potential. Significant variations in total pyrite sulfur (Tot Fe S) (0–0.25 wt. %) and total sulfur (TS) contents (0.01–7.94 wt.%) indicate variable depositional conditions. High TS values are associated with evaporitic layers. Low total organic sulfur (TOS) up to 0.01 wt. % and sulfur index (SI) values up to 2 mg S/g TOC indicate presence of low-S kerogen. Microscopic analysis revealed that inertinite is predominant maceral throughout the interval, accompanied by liptinite (bituminite and sporinite) and solid bitumen. Vitrinite is rare and occurs only as very small particles. Conversely, the Sinemurian- Pliensbachian interval exhibits higher TOC values (0.17–2.91 wt.%), S2 yields from 0.12 to 8.04 mg HC/g, HI values up to 319 mg HC/g TOC, T_{max} values between 435 and 446°C, and vitrinite reflectance (VR_o) values of 0.50 – 0.70%. These parameters indicate an early-mature stage of thermal evolution and predominantly Type II kerogen. The low-S kerogen presence is supported by SI values below 5 mg S/g TOC. Organic petrography confirms the predominance of liptinite macerals, mainly bituminite, over vitrinite and inertinite, consistent with pyrolysis data.

Overall, the Upper Triassic-Hettangian succession is characterized by poor OM preservation and limited hydrocarbon generation potential. The wide range of sulfur values reflects a predominantly terrestrial depositional environment influenced by episodic marine incursions, resulting in restricted conditions conducive to sulfur enrichment and localized reducing environments. In contrast, the Sinemurian-Pliensbachian succession records improved OM preservation under more reducing marine conditions. Higher TOC, S2, and HI values, together with the predominance of liptinite and Type II kerogen, indicate a fair to good source-rock potential. Maturity indicators suggest that these rocks are at the early peak stage of the oil window.

Acknowledgments
P.A. Gonçalves acknowledge the financial support provided to the Institute of Earth Sciences (ICT) through the multi-annual funding contract with the Foundation for Science and Technology (FCT), under project UID/04683/2025 with the DOI https://doi.org/10.54499/UID/04683/2025. The Rock-Eval 7S analyses were funded by the subsidy granted to the AGH University of Krakow by the Ministry of Science and Higher Education.

Petrographic and mineralogical study of the Pliocene Ptolemais Lignite sequence of the Southern Field, Ptolemais Basin, NW Greece

Y. Dimitriou[1], K. Christanis[1], G. Iliopoulos[1], A. Patra[2], S. Kalaitzidis[1*]

[1] Department of Geology, University of Patras, Patras, Greece; [2] Public Power Corporation S.A., Western Macedonia Lignite Center, Ptolemais, Greece

** Corresponding Author: skalait@upatras.gr*

The 52.14-m-thick Pliocene lignite-bearing succession of the Southern Field, Ptolemais Basin, is studied by means of organic-petrography and mineralogical techniques in order to reconstruct the peat-forming environment and to assess the relationship among organic matter composition, mineral matter distribution and the coalification degree.

The ash yield of the lignite samples ranges from 7.17 to 49.01 wt.%, indicating a significant mineral matter influx but without a systematic vertical trend. Mineralogical data reveal the predominance of mixed-layer clay minerals (illite-montmorillonite), accompanied by chlorite, kaolinite and locally dickite, whereas other silicate minerals like quartz, muscovite, biotite, orthoclase, and albite, also occur in moderate proportions. Carbonate minerals (calcite, aragonite, dolomite) become more abundant in the lower and middle parts of the sequence. Sulphates (gypsum, anhydrite, bassanite), pyrite and iron oxides remain minor constituents throughout the succession.

Maceral analysis reveals that the organic matter is dominated by huminite (>75 vol.%) throughout the succession, whereas liptinite and inertinite groups occur in lower proportions (<10 vol.%), displaying limited vertical variations. This trend reflects minor changes in vegetation input, water-table fluctuations and oxidation during peat accumulation.

Huminite reflectance measurements indicate a very low degree of coalification, with eu-ulminite reflectance values ranging between 0.25 and 0.35% and corpohuminite between 0.18 and 0.26%; these values confirm the low coal rank.

Overall, the petrographic and mineralogical data indicate that the peat was accumulating in topogenous mires, by the growth of mostly herbaceous plants. Periodic water-table fluctuations resulted in moderate to significant influxes of detrital minerals, resulting in increased ash yields. These findings improve our understanding of the palaeoenvironmental evolution of the Southern Field lignite deposit in Ptolemais Basin and highlight the role of short-term hydro(geo)logical changes in controlling mineral matter distribution during peat accumulation.

Acknowledgments

Y. Dimitriou gratefully acknowledges the ‘’Hellenic Foundation for Research and Innovation (ELIDEK)” for providing a scholarship (Grand number: 99757), which supported her studies.

Organic record of the Coimbra Formation: from restricted to open-marine conditions during the Sinemurian of the Lusitanian Basin (Portugal)

C. Fonseca[1,2*], D. Marques-Lima[3], S. Gomes[3], N. Franco[3], J.G. Mendonça Filho[3], L.V. Duarte[4], D. Flores[2,5]

[1]University of Minho, Braga, Portugal; [2]Institute of Earth Sciences (ICT), Portugal; [3]Laboratory of Palynofacies and Organic Facies (LAFO), Federal University of Rio de Janeiro, Rio de Janeiro, Brazil; [4]University of Coimbra, MARE – Marine and Environmental Sciences Centre, Coimbra, Portugal; [5]Universidade do Porto, Porto, Portugal

** Corresponding Author: cmfonseca@dct.uminho.pt*

The Coimbra Formation (Sinemurian, Lower Jurassic), exposed at São Pedro de Moel (Lusitanian Basin, Portugal), provides an exceptional record of the palaeoenvironmental evolution of the western Iberian margin during the early stages of the opening of the North Atlantic Ocean. Although its sedimentological and stratigraphic framework is well established, the evolution of its organic facies remains poorly constrained. This study integrates organic geochemistry (total organic carbon, insoluble residue and molecular composition) with organic petrography (palynofacies) to reconstruct the depositional environments and organic matter sources throughout the eight lithostratigraphic subunits (UA–UH).

Subunit UA comprises dolomitic and limestone facies interbedded with marly intervals enriched in amorphous organic matter (AOM) of terrestrial origin (TOC 3.5%; IR 81%), together with a bimodal n-alkane distribution, indicating restricted depositional conditions. Sterane distributions are similar in all analyzed samples, with the dominance of C_{29} and occurrence of C_{30} indicating marine conditions, although highly restricted at the base of the section. Carbonate beds contain abundant phytoclasts and sporomorphs (TOC 0.5%; IR 12%), with only minor marine influence, as evidenced by the occurrence of acritarchs. Subunit UB is dominated by stromatolites and microbial facies. Limestone intervals contain freshwater microplankton-derived AOM (TOC 0.9%; IR 29%), suggesting a stratified water column, whereas stromatolitic facies are characterized by low TOC and IR (0.2% and 1%, respectively). This subunit reflects highly restricted, low-energy environments under strong biogenic control, typical of peritidal to lagoonal settings.

Subunit UC was not sampled in this study. Subunit UD displays pronounced variability, where alternating terrestrial and bacterial organic assemblages, together with elevated TOC values (up to 6.4 wt.%), indicate fluctuating redox conditions associated with a regressive phase. The overlying UE records renewed transgression, expressed by a transition from a facies of membranes and sporomophs (clusters) to bacterial AOM (short-chain *n*-alkanes) and terrestrial-derived AOM (bimodal *n*-alkane distribution). Organic matter preservation reaches its maximum in UF (TOC up to 8.7 wt.%), where bacterial and terrestrial AOM dominate under strongly reducing depositional conditions. Subunit UG is composed predominantly of limestones containing terrestrial AOM at its base, marking a regressive trend. In contrast, subunit UH records the establishment of open-marine conditions with normal salinity conditions, as indicated by the occurrence of foraminiferal test-linings, marine microplankton-derived AOM and gammacerane, with the establishment of a third-order maximum flooding surface.

Overall, the Coimbra Formation was deposited on a shallow carbonate ramp and records an overall transgressive trend superimposed on a second-order transgressive-regressive cycle.

Acknowledgments
C. Fonseca acknowledge the financial support provided to the Institute of Earth Sciences (ICT) through the multi-annual funding contract with the Foundation for Science and Technology (FCT), under project UID/04683/2025 with the DOI https://doi.org/10.54499/UID/04683/2025.

A library of North American metallurgical coal samples

Paul Hackley[1], Jennifer Nedzweckas[1], Joe Marquez[2]

[1]U.S. Geological Survey, Reston, USA; [2]CoalTech Petrographic Associates, Inc., Murrysville, USA

* *Corresponding Author: phackley@usgs.gov*

The U.S. Geological Survey (USGS) has participated continuously since 2005 in a quarterly interlaboratory study (ILS) which measures the reflectance and petrographic composition of samples of currently mined North American metallurgical coal. The ILS is convened by a commercial coal testing laboratory CoalTech Petrographic Associates (CPA), Inc. Approximately one-half kilogram of bituminous metallurgical coal is sent by CPA each quarter to participating laboratories in North America and Australia which perform petrographic tests per ASTM test methods D2798 (reflectance) and D2799 (maceral composition) to ensure comparability of technically equivalent measurement values independent of the analysis source. Similar to International Committee for Coal and Organic Petrology accreditation programs, the test results of individual laboratories are compared to the group mean result as a means of process control. The USGS curates the metallurgical coal samples used in the interlaboratory study (currently 85+ samples, with mean vitrinite reflectance values ranging 0.6-1.8%) as a physical library for specialized research requiring bituminous coal of specific petrographic composition and rank. Samples from the metallurgical coal library have been utilized by USGS staff to test broad ion beam milling as a petrographic polishing tool; to investigate properties of specific individual macerals, e.g., micrinite; to illustrate online resources for education, classification, communication, and research; and to illustrate reference works, e.g., the encyclopedia of petroleum geology. Examples of the availability of specific petrographic compositions in the metallurgical coal library include samples with 40–93 vol.% vitrinite, 7–53 vol.% inertinite, and 0–12 vol.% liptinite. Proposed work is underway to centralize these results into a planned, publicly accessible database structure that could include petrographic information for all samples and chemical, rheological, and location information for select samples. Samples from the USGS metallurgical coal library are available to interested parties in small quantities (grams) for collaborative research which requires metallurgical coals of specific composition and rank. This physical library and planned database document the quality of U.S. metallurgical coal, a resource which was recently designated as a critical mineral fundamentally underpinning U.S. economic and national security interests due to its pivotal role in steel production.

Organic petrography of lithium deposits in Thacker Pass, NV, USA

Javin J. Hatcherian[1*], Randal Burns[2], Christopher D. Henry[3], Paul C. Hackley[1]

[1]U.S. Geological Survey, Reston, United States; [2]Lithium Americas Corp., Reno, United States; [3]Nevada Bureau of Mines and Geology, Reno, United States

** Corresponding Author: jhatcherian@usgs.gov*

This paper discusses the utilization of organic petrography methods on lithium (Li) clay deposit samples to explore new applications for organic petrography. The largest deposit of Li in the United States is in the McDermitt caldera in Nevada (Bradley et al., 2017). Within this caldera, the greatest concentrations of Li are in the southern section, in Thacker Pass. There is uncertainty as to whether the enrichment of Li in Thacker Pass is due to diagenetic alteration and mobilization from Li-rich tuffaceous sediments or from hydrothermal input. Here, we attempt to reduce that uncertainty by applying organic petrography techniques to evaluate trends in the vitrinite reflectance of the samples to provide supporting evidence for the presence or absence of hydrothermal activity.

Forty-one samples were evaluated from fourteen exploration boreholes drilled in Thacker Pass. Depths of samples ranged from 11 m to 256 m, along a W-E cross-section of approximately 5.6 km. The western-most wells (WLC-205, WLC-207, and WLC-196) tended to have *Tasmanites*-like alginite and algal mats in the samples at shallow intervals and more amorphous organic matter (AOM) at deeper intervals. In the eastern-most well (LNC-148), we observed repeating cycles of largely intact *Tasmanites*-like algae and lamellar algal material followed by samples largely consisting of AOM with some intact alginite. Total organic carbon (TOC) values range from <1 to 5.2 wt.%. Excluding 11 samples with TOC <1 wt.%, hydrogen index values ranging from 525–853 mg/g confirm that the organic matter (OM) is Type I, as indicated by abundant liptinite materials.

Most samples show no evidence of hydrothermal activity, despite their proximity to faulting (boreholes WLC-205 and WLC-207 are more than 100m from mapped faults), which is largely considered to be the primary source of hydrothermal input in the region (Henry et al., 2017). Preliminary vitrinite reflectance (R_o) measurements (n=8) range between 0.34 and 0.57% R_o. These R_o values are indicative of maximum temperatures from geologic burial below ~60°C. A single sample from 88.2 m in borehole WLC-205 contains solid bitumen with high reflectance values (~1.0%) and associated vein mineralization, suggesting limited hydrothermal influence at this location. Apart from the single sample in borehole WLC-205, petrographic observations show no evidence of proximal hydrothermal activity, e.g., oxidation rims, fracturing of OM, or vein mineralization. The lack of significant Ro shifts or other widespread evidence for OM alteration, combined with preliminary illite crystallinity XRD data and Raman spectroscopy, may suggest that proximal hydrothermal activity was unlikely to be the primary source of Li enrichment in Thacker Pass.

References

Bradley, D.C., Stillings, L.L., Jaskula, B.W., Munk, LeeAnn, McCauley, A.D., 2017. Lithium, chap. K of Schulz, K.J., DeYoung, J.H., Jr., Seal, R.R., II, and Bradley, D.C. (Eds.), Critical mineral resources of the United States – Economic and environmental geology and prospects for future supply: U.S. Geological Survey Professional Paper 1802, p. K1– K21.

Henry, C.D., Castor, S.B., Starkel, W.A., Ellis, B.S., Wolff, J.A., Laravie, J.A., McIntosh, W.C., and Heizler, M.T., 2017. Geology and evolution of the McDermitt caldera, northern Nevada and southeastern Oregon, western USA: Geosphere 13 (4), 1066–1112.

Pilot study on the feasibility of geopolymers development using mining wastes from São Pedro da Cova Coal Mine (Northern Portugal) - Preliminary results

J. Paranhos[1], J. Espinha Marques[1], P. Santos[1*], D. Arduin[2], A. Santos[2], S. Andrejkovičová[2], H. Sant'Ovaia[1], F. Rocha[2]

[1]ICT- Instituto de Ciências da Terra, Departamento de Geociências, Ambiente e Ordenamento do Território, Faculdade de Ciências da Universidade do Porto, Rua do Campo Alegre, Porto, Portugal; [2]GeoBioTec – GeoBioCiências, GeoTecnologias e GeoEngenharias, Departamento de Geociências, Universidade de Aveiro, Campus Universitário de Santiago, Aveiro, Portugal.

** Corresponding Author: patricia.santos@fc.up.pt*

The São Pedro da Cova mine was once the most important coal extraction site in Portugal. Following its closure in 1972, a vast environmental liability remained on the surface, consisting of abandoned buildings and a massive coal waste covering more than 28 000m^2. In 2005, following a fire, the coal-rich mining residues ignited and have been self-combusting ever since. This area has been a matter of deep social and environmental concern, given its proximity to the population and water and soil resources.

The present work aims to provide a preliminary approach to evaluating the feasibility of valorizing this mine waste by incorporating it into geopolymers, in line with the principles of the circular economy.

The waste piles are dominated by Technosols developed from coal mining wastes. Over several decades, these anthropogenic soils underwent natural pedogenic development, with vegetation colonization leading to the formation of organic (O) and surface mineral (A) horizons. However, the self-combustion of the waste pile disrupted pedogenesis by destroying organic matter and creating a highly heterogeneous soil profile with three new subsurface horizons (C1, C2, and C3). Although these soils exhibit hydrophilic behavior, they show marked variability in hydraulic conductivity and significant mineralogical transformations, resulting in unique properties (Fig. 1; Espinha Marques et al., 2021).

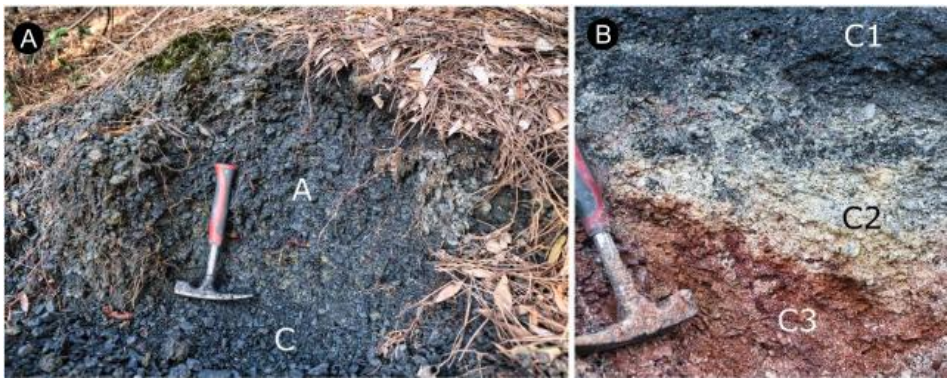

Figure 1. Soil profiles in the São Pedro da Cova waste pile: (A) on the left, a Technosol undergoing normal pedogenesis, showing A and C horizons; (B) on the right, a Technosol affected by self-combustion, with differentiation into C1, C2, and C3 horizons due to the strong thermal gradient (adapted from Espinha Marques et al., 2021).

Soil sampling was conducted in three sectors of the São Pedro da Cova mine waste dump, including one self-combusted area and two non-combusted areas. Composite soil samples from different horizons

were collected and subjected to air-drying, sieving, grinding, and particle-size separation following standardized protocols to ensure sample representativeness and analytical quality. Physicochemical characterization included pH and electrical conductivity measurements, while the mineralogical and geochemical composition was determined using X-ray diffraction (XRD), X-ray fluorescence (XRF), inductively coupled plasma optical emission spectrometry (ICP-OES), and instrumental neutron activation analysis (INAA).

The self-burning acted as an *in-situ* calcination process, reaching temperatures of approximately 1000ºC. This severe thermal exposure promoted the formation of reactive amorphous (glassy) phases, providing the burnt materials with the ideal stability and reactivity to act as precursors in geopolymers, ruling out the direct use of the unburnt waste.

As a preliminary approach, the geopolymers were synthesized by alkaline activation (NaOH + Na_2SiO_3) of burnt mine waste collected from two horizons of the burnt pile (C2 and C3; Fig. 1), in combination with metakaolin (MK) at different incorporation rates. To evaluate the influence of mine waste content on geopolymer performance, seven formulations were developed incorporating mine waste at 30, 50, 70, and 100 wt.%. The formulations were designed to produce geopolymeric materials for civil construction applications while maximizing the incorporation of mine waste. The geopolymers were cast in silicone molds (20mm side) and cured at room temperature (22°C, 53% RH). Structural and mechanical characterization confirmed the successful formation and consolidation of the geopolymeric matrix after 14 days. The characterization was performed using attenuated total reflectance Fourier-transform infrared spectroscopy (ATR-FTIR), XRD, XRF, and scanning electron microscopy coupled with energy-dispersive X-ray spectroscopy (SEM-EDS), and their mechanical performance was evaluated by compressive strength testing. This integrated methodology enabled assessment of the mineralogical, chemical, microstructural, and mechanical properties of the geopolymers, supporting the evaluation of mine waste valorization as a sustainable construction material. The results revealed that the exclusive geopolymerization of the mine waste (100 wt.% C3) is insufficient, yielding only 6.62 MPa. However, the mixtures exceeded expectations at 14 days of curing: the optimum point for the C3 waste was reached at a ratio of 50 wt.% mine waste to 50% metakaolin (50MK50C3), achieving 20.76 MPa. Even more efficiently for the circular economy, the C2 waste achieved an equivalent performance (20.07 MPa) with the 30MK70C2 formulation, allowing the incorporation of mining waste to be maximized to 70 wt.%. Microstructural analyses (ATR-FTIR and SEM-EDS) validated these observations, evidencing the densification of the three-dimensional network (N-A-S-H gel) and the stabilization of unreacted mineral phases, such as hematite, confirming the potential technical viability of these composites for construction applications, such as masonry blocks or paving.

The study comprises a preliminary assessment of the potential to reuse coal mine residues for the synthesis of new sustainable construction materials, showing potential for future applications that may transform and rehabilitate this environmental liability while mitigating the contamination and leaching risks associated with this mining legacy in Northern Portugal.

Acknowledgement
This study was developed in the scope of RESTAURA project – NORTE 2030 – FEDER-02704900, financed by Programa Regional do Norte 2021-2027 (Norte 2030) and was framed within the ICT activities (UID/04683/2025; DOI https://doi.org/10.54499/UID/04683/2025). Also, this work was supported by the GeoBioTec research unit (UID/04035/2025; DOI: https://doi.org/10.54499/UID/04035/2025).

References
Espinha Marques, J., Martins, V., Santos, P., Ribeiro, J., Mansilha, C., Melo, A., Rocha, F., & Flores, D. (2021). Changes induced by self-burning in Technosols from a coal mine waste pile: A hydropedological approach. Geosciences, 11(5), 195.

Author Index

A

Agra, A.A. · 48
Álvarez, P. · 60
Anand, A. · 11
Andrejkovičová, S. · 88
Arduin, D. · 88
Armstrong, D. · 67

B

Bălănescu, M. · 64
Barski, M. · 18
Bauersachs, T. · 28
Biswas, S. · 2, 4
Blinkenberg, K.H. · 11
Blumenberg, M. · 37, 44
Boluk, P. · 64
Borghi, L. · 54
Borrego, A.G. · 48, 55
Bueno-Tokunaga, A. · 58
Bueno-Yamamoto, Y. · 58, 62
Burns, R. · 87

C

Camacho-Ortegón, L.F. · 58
Canedo, J.N.G.V. · 72
Castillo Corrêa, R. · 72
Christanis, K. · 83
Coelho, L. · 72
Concheso, A. · 60
Costa, M. · 52
Cygan, A. · 7
Cyran, W. · 9

D

Damoulianou, M.E. · 80
Dash, N. · 50
De La Rosa-Rodríguez, G. · 58, 62
Dimitriou, Y. · 83
Dimitrov, D. · 45
Drăgoescu, M.F. · 64
Drozd, A. · 22
Duarte, L.V. · 84
Duran, N. · 64

E

Eble, C.F. · 27, 28
Enciso-Cárdenas, J.J. · 58, 62
Espinha Marques, J. · 88

F

Fabiańska, M. · 30, 44
Feng, J. · 33
Firdaus, M. · 25
Flores, B.D. · 48
Flores, D. · 52, 72, 82, 84
Fonseca, C. · 84
Franco, N. · 84

G

Gao, T. · 33
Garcia Neto, C. · 72
García, C.C. · 55
García-Calvillo, I.D. · 58
Garza-Cavazos, D.M. · 58, 62
Georgaki, M. · 7
Gheorghe, S. · 74
Ghiran, D.M. · 57, 74
Gomes, S. · 84
Gonçalves, P.A. · 82
González-Partida, E. · 62
Granda, M. · 60
Guedes, A. · 12, 50, 64
Guzman, M.G. · 55

H

Hackley, P.C. · 16, 70, 71, 76, 86, 87
Hao, L. · 14
Hatcherian, J.J. · 16, 70, 71, 87
Henriques, M.H. · 40
Henry, C.D. · 87
Hung, K.T. · 9

I

Iliopoulos, G. · 83

J

Jakobsen, R. · 11
Jelonek, I. · 6, 47
Jelonek, Z. · 6, 47
Jubb, A.M. · 16

K

Kabadiyski, V. · 45
Kalaitzidis, S. · 7, 80, 83
Kaushal, P. · 11
Kędzior, S. · 22
Khanaqa, P. · 80
Khomenko, D. · 6
Kolo, K.Y. · 80
Kościelny, M. · 30
Kulas, M.I. · 64
Kuo, L. · 14
Kus, J. · 37, 44
Kutlu, O. · 64

L

Lavoie, D. · 67
Lemos de Sousa, M.J. · 58, 62
Lewan, M. · 76
Liping, X. · 79
Littke, R. · 28
Liu, C. · 24
Liu, Y. · 33

M

Machado, D. · 20
Machado, G. · 20
Maciejewska, A. · 18
Majake, M.L. · 4
Mariș, I. · 57, 74
Marques-Lima, D. · 84
Marquez, J. · 86
McAleer, R.J. · 16
Mendonça Filho, J.G. · 44, 54, 82, 84
Mendonça, J.O. · 54
Mertas, B. · 77
Michałek, A. · 77
Michels, F. · 40
Misch, D. · 45
Misz-Kennan, M. · 30
Mohialdeen, I.M.J. · 80
Moreira, P.F. · 58
Mourão, P. · 72

N

Nayak, B. · 50
Nedzweckas, J. · 70, 71, 86
Niembro, C. · 55
Núñez-Useche, F. · 62

O

Oliveira, A.D. · 54
Olmo, J.M. · 55
Opluštil, S. · 28
Osório, E. · 48

P

Paranhos, J. · 88
Patra, A. · 83
Pereira, S. · 12, 50
Petersen, H.I. · 11
Pinto de Jesus, A. · 52
Pirnea, R. · 57, 74
Popa, M.E. · 57
Popa, M.-E. · 74
Prats, S. · 72
Predeanu, G. · 57, 64, 74
Prusty, S. · 50

Q

Qu, J. · 16

R

Reyes, J. · 67
Ribeiro, J. · 40
Rocha, F. · 88
Rocha, R. · 77
Rodrigues, C.A. · 58, 62
Rodź, A. · 77
Romanowska-Duda, Z. · 47
Rudra, A. · 11

S

Sachsenhofer, R.F. · 45
Sadd, I. · 25
Salva, O. · 28
Sanches, A. · 20
Sanders, M.M · 71
Sanei, H. · 11
Sang, P.N. · 9

Sant'Ovaia, H. · 88
Santos, A. · 88
Santos, P. · 88
Scheeder, G. · 37
Shuo, G. · 79
Sierra, U. · 60
Silva Trindade, A. · 72
Silva, A. · 82
Silva, E.F. · 52
Silva, F. · 72
Silva, G.L.R. · 48
Slăvescu, V. · 64
Słoczyński, T. · 22
Smith, G. · 25
Smith, R. · 70
Souza Alonso, P. · 72
Souza, J.T. · 54
Stoyanov, S. · 45
Sun, B. · 24
Sun, J. · 69
Sun, Q. · 32
Sýkorová, I. · 28
Szram, E.A. · 44

T

Tarelho, L. · 72

V

Valentim, B. · 12, 50, 64
Valentine, B.J. · 16, 71
Varonka, M. · 70
Vasile, B.S. · 64
Vigil, A. · 60
Vilela, A.C.F. · 48

W

Wagner, N.J. · 2, 4
Waliczek, M. · 9, 18
Wang, K. · 32
Wang, Z. · 69
Weitz, J. · 45
Więcław, D. · 9, 82
Wojtaszek-Kalaitzidi, M. · 7, 12, 77
Woźniak, C. · 47

X

Xiangfei, B. · 79
Xiaoyu, D. · 14
Xu, N. · 39

Y

Yan, R. · 66
Yan, X. · 69
Yuegang, T. · 79

Z

Zdravkov, A. · 45, 46
Zhang, Y. · 16
Zhao, Z. · 34
Zhou, K. · 35
Zhu, Y. · 69
Zielińska, M. · 44
Ziemianin, K. · 42
Zlatkov, B. · 45